Aus dem Pathologischen Institut der Ludwig-Maximilians-Universität München

Direktor: Prof. Dr. med. Thomas Kirchner

Significance of heterogeneous WNT and MAPK signaling in colorectal cancer

Dissertation zum Erwerb des Doktorgrades der Naturwissenschaften

an der Medizinischen Fakultät der Ludwig-Maximilians-Universität München

vorgelegt von

Cristina Blaj

aus Timișoara

2016

Gedruckt mit Genehmigung der Medizinischen Fakultät der Ludwig-Maximilians-Universität München

Betreuer: Prof. Dr. rer. nat. Andreas Jung

Zweitgutachter: Prof. Dr. Olivier Gires

Dekan: Prof. Dr. med. dent. Reinhard Hickel

Tag der mündlichen Prüfung: 16.05.2017

Eidesstattliche Versicherung

Cristina Blaj

Ich erkläre hiermit an Eides statt, dass ich die vorliegende Dissertation mit dem Thema

„Significance of heterogeneous WNT and MAPK signaling in colorectal cancer“

selbständig verfasst, mich auβer der angegebenen keiner weiteren Hilfsmittel bedient und alle Erkenntnisse, die aus dem Schrifttum ganz oder annähernd übernommen sind, als solche kenntlich gemacht und nach ihrer Herkunft unter Bezeichnung der Fundstelle einzeln nachgewiesen habe.

Ich erkläre des Weiteren, dass die hier vorgelegte Dissertation nicht in gleicher oder in ähnlicher Form bei einer anderen Stelle zur Erlangung eines akademischen Grades eingereicht wurde.

Ort, Datum: Unterschrift:

Meinen Eltern

Table of contents

1. Introduction

1.1. Colorectal cancer

Cancers figure beside diseases of the circulatory system as the leading cause of death worldwide. With about 14.1 million new cancer cases and 8.2 million deaths worldwide in 2012, cancers represent a massive societal burden affecting both developed and developing countries. While the genetic component and, in some tumor types, inherited genetic susceptibility play a major role in tumor initiation, environmental risk factors like tobacco use, alcoholism, obesity and some chronic infections have a great contribution to the high incidence of cancer (Torre et al., 2015).

Cancer is the result of a multistep process transforming normal tissue cells into malignant tumor cells. Most solid human tumors require two to eight sequential genetic alterations to develop over a timeframe of 20 to 30 years (Vogelstein et al., 2013). During malignant transformation, tumor cells acquire several specific capabilities, which have been defined as the hallmarks of cancer. These include malignant traits like proliferation, replicative immortality, angiogenesis, invasion, metastasis, reprogramming energy metabolism and the eschewal of growth suppressors, cell death and immune surveillance (Hanahan & Weinberg, 2011).

Among cancers, colorectal cancer (CRC) is a major cause of cancer morbidity and mortality, ranking third in cancer incidence among men and women (Jemal et al., 2009). CRC is associated with good survival rates of about 90% if the cancer is diagnosed early, but the chances of survival decrease to 12% if distant metastases are present. Poor survival rates are associated with the deregulation of crucial signaling pathways, such as WNT, NOTCH and Hedgehog, the presence of distant metastases and the acquired resistance to targeted therapies. (Cheruku et al., 2015; Van Emburgh, Sartore-Bianchi, Di Nicolantonio, Siena, & Bardelli, 2014). Diagnosis of CRC is traditionally based on histologic characteristics, tumor stage and increasingly assessment of individual mutations (Linnekamp, Wang, Medema, & Vermeulen, 2015). Furthermore, over the past decade whole exome sequencing revealed the genomic landscapes of CRC and provided further insights into the pathways involved in tumorigenesis (The Cancer Genome Atlas Network, 2012).

Colorectal cancers derived from normal colonic mucosa by accumulation of mutations that transform colonic epithelial cells into malignant tumor cells. Most CRCs are initiated by mutations in APC or β-catenin that lead to over activation of the WNT signaling pathway in these tumors (The Cancer Genome Atlas Network, 2012). This first mutation confers a selective growth advantage to affected intestinal epithelial cells over surrounding cells, and is therefore called a "driver" mutation (Vogelstein et al., 2013). Aside from mutations in genes associated with the WNT pathway, activating mutations in codons 12 or 13 of *KRAS* are present in about 40 % of these tumors, causing an over activation of MAPK signaling. These occur early within the malignant transformation process and contribute to the clonal expansion of adenomas (Vaughn et al, 2011) (Figure 1).

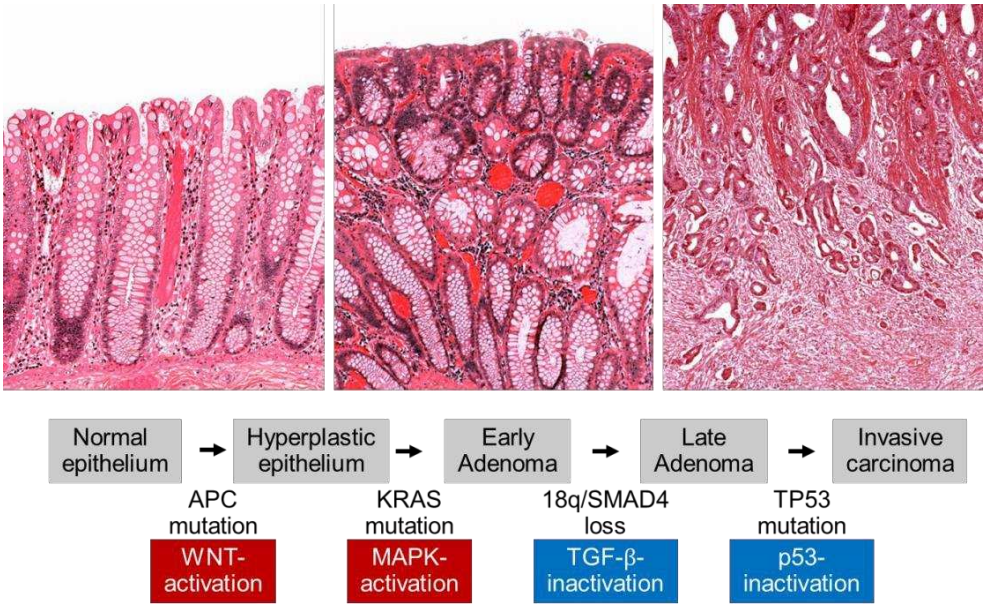

Figure 1. Multistage transformation process from normal colon epithelium to carcinoma. Upper panel: H&E staining of normal colon epithelium (left), adenoma (middle) and carcinoma (right). Lower panel: Deregulation of crucial signaling pathways accompanying the adenoma–carcinoma sequence.

Further common genetic alterations in colorectal cancer lead to deregulation of PI3K, TGF-β or P53 signaling pathways. The frequency of genetic mutations in CRC is variable and about 16% of CRC have very high mutation frequencies due to an impaired DNA mismatch repair mechanism (The Cancer Genome Atlas Network, 2012).

Mutations in driver genes and the resulting deregulation of key signaling pathways cause a selective growth advantage by influencing on core cellular processes, like cell fate

determination, cell survival and genome maintenance (Vogelstein et al., 2013). A better understanding of these pathways and their underlying mechanisms has broad implications for cancer therapy. Since the discovery of activating mutations in driver genes, a series of potential therapeutic targets, like EGFR or BRAF, have been identified. The limited success of therapies, that selectively target signaling pathways in CRC, has been related to acquired drug resistance based on genetic intratumoral heterogeneity (Misale et al., 2012; Snuderl et al., 2011).

1.2. The tumor microenvironment

The tumor microenvironment describes the complex mixture of non-transformed cell types present in the tumor and the proteins secreted by these cells. Angiogenic vascular cells, fibroblasts, cancer associated fibroblasts, infiltrating immune cells, the extracellular matrix and secreted factors constitute the topography of the tumor surroundings. The relationship between cancer cells and the associated stroma can influence tumor initiation and progression, metastatic colonization, but also therapeutic response and resistance to therapy. Immune cells can have both pro- and anti-tumor roles, dependent on their activation status and their localization (Junttila & de Sauvage, 2013). The perivascular niche within tumors has the potential to harbor cancer stem cells (Calabrese et al., 2007) and soluble factors secreted by endothelial cells can promote the cancer stem cell phenotype (Krishnamurthy et al., 2011; Lu et al., 2013).

The tumor microenvironment is considered to have a great contribution to the tumor formation in the colon, as many colorectal cancers are associated with inflammation (Quante, Varga, Wang, & Greten, 2013). TNF-α and IL-6 are two of the main drivers of cancer inflammation, that activate proliferation and survival pathways in epithelial cells. Cancer associated fibroblasts at the invasive tumor edge release pro-invasive factors like TGF-β, EGF, HGF and PDGF supporting signaling crosstalk with tumor cells and the dissemination of cancer cells in the course of metastasis. In this context, elevated TGF-β activity in advanced stages of CRC is responsible for promoting disease progression and is linked to poor prognosis. Finally, the complex and variable microenvironments can contribute to the inter- and intratumoral heterogeneity and play a critical role in the clinical outcome (Junttila & de Sauvage, 2013; Quail & Joyce, 2013; Tauriello & Batlle, 2016).

1.3. Intratumoral heterogeneity

Intratumoral heterogeneity is defined as the coexistence of tumor cell subpopulations with distinct biological or phenotypic characteristics within the same tumor. This heterogeneity may be associated with distinct genetic profiles but also occurs within the same core genetic background of a tumor. Most human tumors exhibit substantial heterogeneity with regard to cellular morphology, gene expression, metabolism, as well as the proliferative, angiogenic and metastatic potential (Marusyk & Polyak, 2013; Snuderl et al., 2011) .

Heterogeneity within tumors can be observed at different levels: genetic, epigenetic and functional (Welch, 2016). Genomic instability can lead to clonal differences if it is an early event in tumor evolution, or to subclonal expansion, reflecting later events. Intrinsic differences can be also caused by epigenetic changes (Baylin & Jones, 2011). Selective pressure, like stress, nutrition or therapies, can modulate the tumor evolution in a time dependent manner. Positional heterogeneity is influenced by the exposure of tumor cells to external stimuli like growth factors, hypoxia or signals from other tumor cells (McGranahan & Swanton, 2015; Welch, 2016). Genetically identical cancer cells can also display heterogeneous phenotypes. The differentiation of cells with extensive self-renewal potential, also known as cancer stem cells, into fully differentiated cancer cells, which lost the capacity to fuel tumor growth, can account for a tumor heterogeneity, that can't be explained by clonal evolution or environmental differences (Kreso & Dick, 2014).

Tumor heterogeneity, on both genetic and functional level, can have profound implications on therapy efficiency. The presence of *KRAS* or *EGFR* mutations in small subpopulations within a cancer is associated with higher relapse rates after anti-EGFR therapy. The selective therapeutic the pressure allows the expansion of these cells and to the repopulation of the tumor (Diaz et al., 2012; Misale et al., 2014). Another observed mechanism of therapy resistance in CRC is the clonal cooperation, where cetuximab resistant *KRAS* mutant subclones support the survival of drug-sensitive *KRAS* wildtype cells (Hobor et al., 2014). Recent studies found that individual colorectal cancer cells with identical genetic background show a functional heterogeneity regarding the capacity of long-term clonal propagation and response to therapy. Actively proliferating cells can be eliminated by chemotherapy with oxaliplatin while their non-proliferating counterparts are nonresponsive and are able to reinitiate the tumor after therapy (Kreso et al., 2013). Others show that a transient drug

tolerance appears to reflect an epigenetic heterogeneity within a cancer cell population (Sharma et al., 2010).

These studies highlight the clinical implications of intratumoral heterogeneity. In order to improve the efficiency of personalized therapy, the functional heterogeneity of cancer cells has to be taken into account for future drug development strategies.

1.4. Intestinal stem cells and colon cancer stem cells

In healthy intestinal epithelia small populations of adult stem cells are responsible for the maintenance of the tissue homeostasis (Barker, 2014). The human colon is composed of millions of crypts and each crypt contains distinct functional compartments. The stem cells are located in the niche at the base of the crypt, the proliferating transit amplifying zone constitutes the mid of the crypt and the differentiated cells (goblet cells, enterocytes, enteroendocrine cells and tuft cells) expand towards the crypt apex (Cernat et al., 2014; Humphries & Wright, 2008). Cheng and Leblond proposed a model, by which all different intestinal cell types are derived from a single crypt base columnar (CBC) cell (Cheng & Leblond, 1974). Direct evidence for this stem cell model was provided in 2007 by Barker and colleagues, who identified the Lgr5 gene, a WNT target gene, as the genuine stem cell marker of the small intestine and of the colon (Figure 2).

They performed in vivo lineage tracing from Lgr5 positive intestinal stem cells using a Lgr5-EGFP-ires-CreERT2/Rosa26lacZ mouse model. Lineage tracing is a molecular tool used for the identification of all progeny of a single cell. Labeling the cells without changing their features provides insight into their behavior in the context of the intact tissue over a long period of time (Kretzschmar & Watt, 2012). In this mouse model, a GFP and CreERT2 expressing cassette was inserted into the genomic locus of LGR5. Additionally, these mice contain a LoxP flanked STOP cassette in front of a LacZ reporter gene within the Rosa26 locus. After tamoxifen induction, recombination and thus LacZ expression occurs specifically in LGR5 expressing cells at the intestinal crypt bases of the small intestine and colon. Over time whole LacZ expressing crypts derive from these cells, demonstrating LGR5 to be an intestinal stem cell marker (Barker et al., 2007).

Further animal studies revealed, that the expression of additional CBC marker, like *Bmi1*, *Tert, Hopx, Smoc2, Sox9, Prom1* and *Lrig1* partially overlaps and that CBC and +4 intestinal stem cells can interconvert, adding to the complexity of the stem cell concept (Itzkovitz et al., 2012; Muñoz et al., 2012; Louis Vermeulen & Snippert, 2014).

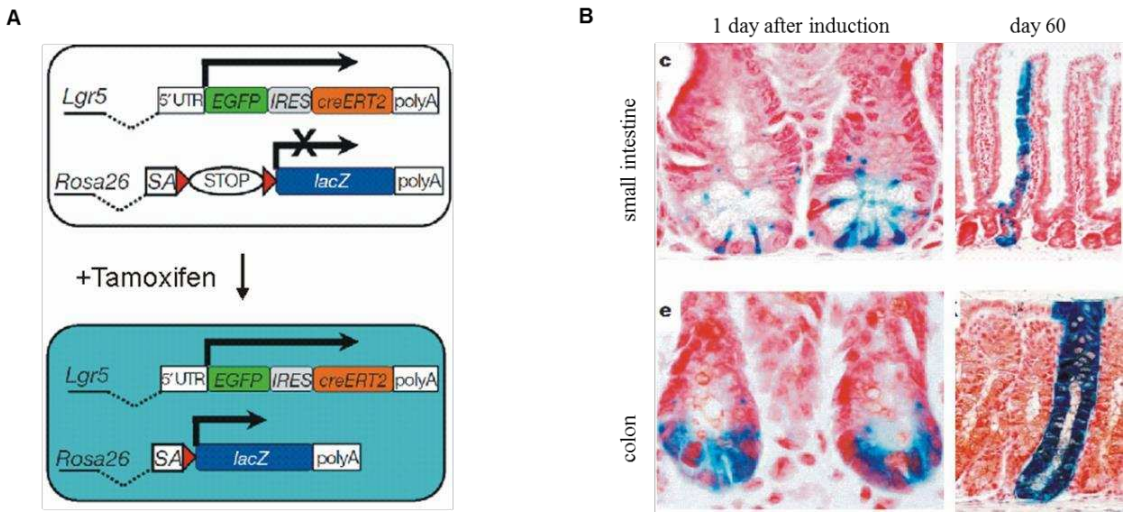

Figure 2. Lineage tracing of stem cells in the small intestine and colon. (A) Generation of the Lgr5-EGFP-ires-CreERT2/Rosa26lacZ mouse model. (B) Histological analysis of LacZ activity one day and 60 days after tamoxifen induction. Figure modified after (Barker et al., 2007)

Many cancers retain features of normal tissue organization (Cernat et al., 2014; L Vermeulen, Sprick, Kemper, Stassi, & Medema, 2008), where cancer stem cells (CSCs) are responsible for fueling tumor growth. Cancer stem cells can be defined by their self-renewal potential and by their ability to generate heterogeneous tumors comprised of tumorigenic and non-tumorigenic progenies (Vermeulen et al., 2008). The cancer stem cell model has generated considerable interest because of the relevance of CSCs in drug resistance, metastasis and tumor recurrence (Chen, Huang, & Chen, 2013; Cojoc, Mäbert, Muders, & Dubrovska, 2015). Initially the cancer stem cell model was described in AML and breast cancer (Al-Haji et al., 2003; Bonnet & Dick, 1997). These publications were followed by the identification of CSCs in tumors of various organs, like brain (Singh et al., 2004), colon (Ricci-Vitiani et al., 2007), head and neck (Prince et al., 2007), pancreas (Li et al., 2007) and others. However, not all cancers follow the cancer stem cell model. In some tumors, like acute myeloid leukemia

(AML), CSCs represent a small population of less than 1%, while other malignancies, like acute lymphoblastic leukemia, have CSC frequencies of up to 82% (Cojoc et al., 2015).

In colon cancer, cell-surface-markers such as CD133, CD166 and CD44 have been validated in the identification of CSCs (Dalerba et al., 2007; O'Brien, Gallinger, Pollett, & Dick, 2007; Ricci-Vitiani et al., 2007). *In vivo* limiting dilution transplantation assays have been the gold standard for the estimation of CSC frequencies. However, conflicting results about the right marker combination and the right xenograft models point to the limitations of current methods used in cancer stem cell research (O'Brien, Kreso, & Jamieson, 2010). In CRC the $EpCAM^{high}$/CD44 combination provides a more robust marker profile than CD133, which is expressed only in subsets of colorectal tumors (Dalerba et al., 2007). Another disadvantage of limiting dilution assays is the necessity to dissociate the tumor cells from their environment before transplantation, which might change their behavior and lead to a misrepresentation of CSC frequencies. Finally, CSC abundance can be underestimated when less immunodeficient mice are used for serial transplantations (Quintana et al., 2008). The application of a lineage tracing system to resolve individual cell fate within tumors might overcome some limitations of transplantation assays and facilitate the efforts to characterize CSC.

Identifying the pathways that regulate CSC self-renewal decisions will lead to a better understanding of the mechanisms driving tumor growth. The activation of pathways like WNT, NOTCH, Hedgehog, and others have been reported to fuel CSC initiation and propagation (Hoey et al., 2009; Varnat et al., 2009; Louis Vermeulen et al., 2010). Interactions between cancer cells and surrounding stroma cells have been hypothesized to sustain these pathways by mediating signals emitted from the tumor microenvironment. Keeping the different levels of intratumoral heterogeneity in mind, different outcomes can be postulated with regard to the self-renewal capacity: some CSC may have the ability to regulate the necessary pathway and remain independent of the surrounding microenvironment, while others may need the niche support, but many cancer cells probably lose this capacity, regardless of the stromal support they receive (O'Brien, Kreso, & Jamieson, 2010) (Figure 3).

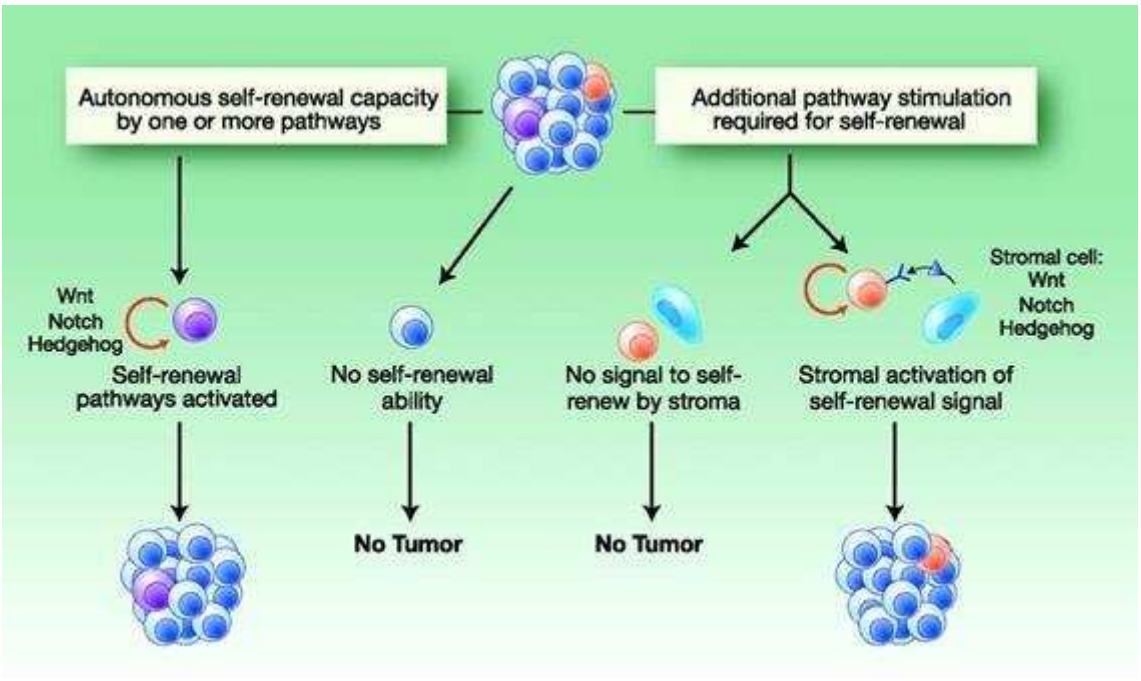

Figure 3. Cancer stem cell self-renewal capacities in the context of the tumor microenvironment. Several pathways, including WNT, NOTCH and Hedgehog are involved in the regulation of CSC self-renewal decisions. Figure from (O'Brien et al., 2010).

CSCs have been also linked to therapy resistance and recurrence. Beside the activation of developmental pathways and the microenvironmental stimuli, they use a variety of mechanisms for chemo- and radiotherapy resistance, like drug efflux by ABC transporters (Golebiewska et al. 2011), aldehyde dehydrogenase activity (Marcato et al. 2011), enhanced DNA damage response and reactive oxygen species (ROS) scavenging (Peitzsch et al. 2013) as well as autophagy (Rausch et al. 2012).

The properties of drug resistance are reflected in particular in the context of metastasis. Recent studies provided evidence, that CSCs have the ability to initiate metastasis and are responsible for relapse after chemotherapy (Todaro et al., 2014). The metastatic process includes the dissemination of cancer cells from the primary tumor and their ability to give rise to macroscopic tumors in foreign tissues. There is growing evidence that only a subset of CSC harbor a metastasis-forming potential (Dieter et al., 2011). In colon cancer CD26 positive CSC show an enriched metastatic capacity, enhanced invasiveness and chemoresistance compared to their CD26 negative counterparts (Pang et al., 2010). It has also been suggested that tumor cells can gain metastatic capacities during epithelial-mesenchymal transition

(Kalluri & Weinberg, 2009; Mani et al., 2008), but the exact relationship between these processes has yet to be elucidated.

1.5. Epithelial-mesenchymal transition

The epithelial-mesenchymal transition (EMT) is an evolutionarily conserved process, during which cells lose their epithelial features and become more migratory. Epithelial tissues are characterized by the loss of migratory freedom, with cells establishing an apico-basal axis of polarity through the expression of adherens junctions, desmosomes, and tight junctions (Thiery, Acloque, Huang, & Nieto, 2009). EMT governs the embryonic development, tissue regeneration, but also plays a major role in organ fibrosis and cancer metastasis. During morphogenesis, EMT and the reverse process, mesenchymal-epithelial transition (MET), are associated with gastrulation, neural crest delamination and heart formation (Lim & Thiery, 2012).

Loss of CDH1 (E-cadherin) expression is considered a central event during EMT. Several transcription factors, like SNAI1, ZEB, E47, KLF8, TWIST, E2.2, FoxC2, TCF and LEF, have been described to repress CDH1 either directly, by binding to its promoter, or indirectly, by interacting with miRNAs (Gonzalez & Medici, 2014; Thiery et al., 2009). The traditional assessment of the EMT phenotype is the decreased expression of selected markers, like E-cadherin, occludins and cytokeratins and the increase in N-cadherin, LAMC2 or Vimentin. But recent studies indicate a higher complexity, with intermediate epithelial and mesenchymal phenotypes reflecting the capacity of cells to induce or reverse the EMT process (Nieto, Huang, Jackson, & Thiery, 2016) (Figure 4). Interactions between epigenetic and transcription regulators are also thought to regulate the transitional states during EMT/MET (Tam & Weinberg, 2013).

The role of EMT in cancer progression is still controversial. In some cancer types EMT might not be prerequisite for metastasis (Zheng et al., 2016), yet there is a vast body of evidence that links the EMT program to malignant traits (Thiery et al., 2009).

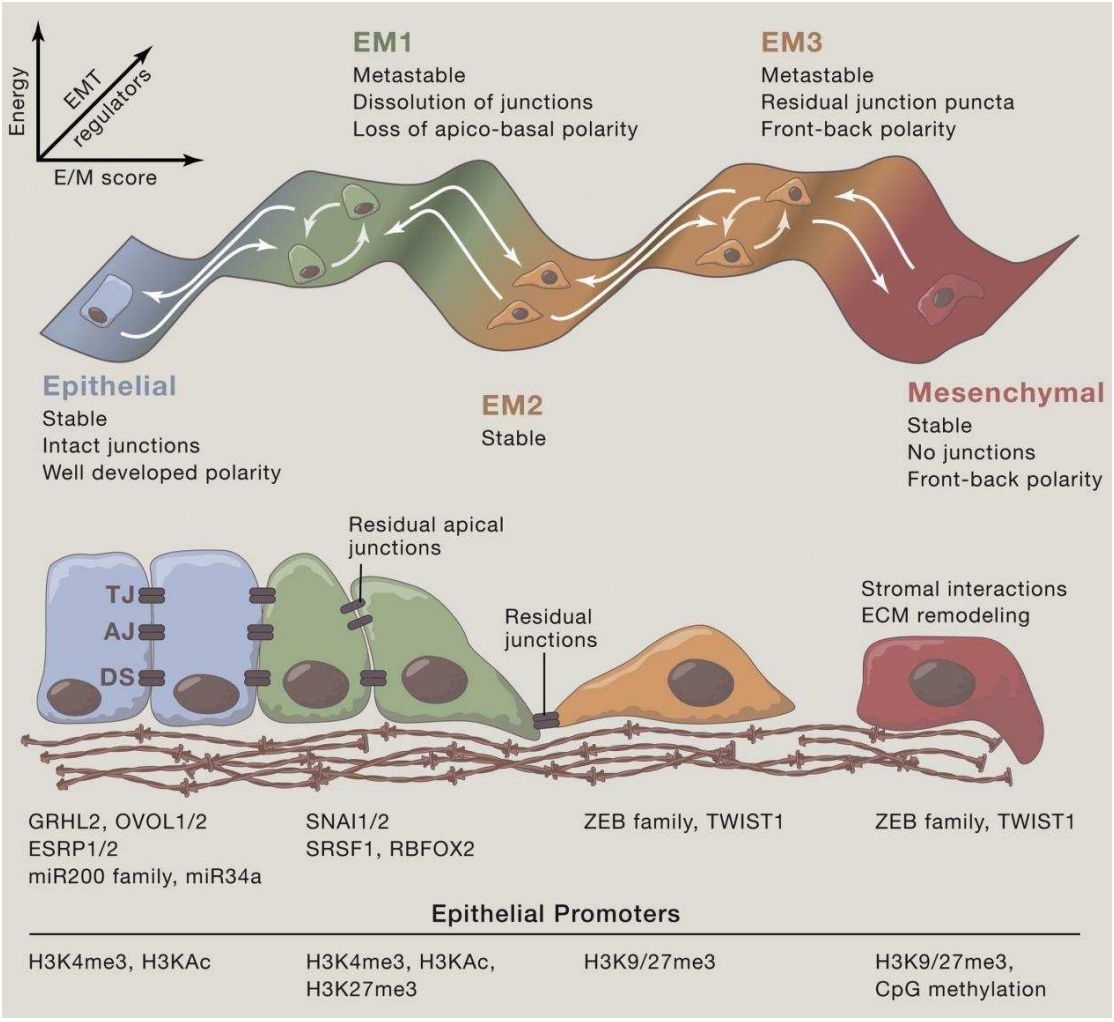

Figure 4. A dynamic phase transition between epithelial and mesenchymal phenotypes. Extracellular signals, epigenetic and transcription regulators interact to govern the epithelial-mesenchymal plasticity. Figure from (Nieto et al., 2016)

In colorectal cancers EMT seems to play a central role in the formation of metastasis. CRC exhibit an intratumoral EMT gradient, where the tumor center shows a differentiated, epithelial pattern while at the invasive front tumor cells gain a more mesenchymal phenotype. At the interface between the tumor and its microenvironment EMT processes enable cellular detachment, the first step in the process of metastasis. These disseminating cells display an accumulation of nuclear β-catenin, which is indicative of an active WNT pathway. (Brabletz, Jung, Spaderna, Hlubek, & Kirchner, 2005; Thiery et al., 2009).

The crosstalk between WNT and other pathways, such as TGF-β, BMP, RTK, NOTCH, Hedgehog and hypoxia signaling regulates the expression and function of EMT-inducing transcription factors (Gonzalez & Medici, 2014). Given the involvement of EMT in various

processes, it is not surprising, that it is governed by many overlapping pathways and can be influenced by a wide array of extracellular signals. Understanding the relationship between these different pathways and their role in promoting EMT may provide crucial insights into the fundamental mechanisms of metastasis and to the improvement of therapeutic strategies.

1.6. The wingless-related integration site pathway

WNTs are secreted cysteine rich proteins that activate a highly conserved signaling pathway. During embryonic development WNT signaling regulates cell fate determination, polarity, migration and organogenesis and in adults it plays a crucial role in homeostasis and stem cell maintenance (Clevers, 2006; Clevers & Nusse, 2012).

The combination between the human WNTs encoded by 19 genes and the more than 15 different WNT receptors and co-receptors results in a highly complex downstream signaling, activating β-catenin dependent (canonical) or independent (non-canonical) pathways (Miller, 2001).

Deregulated canonical WNT signaling activity is implicated in hereditary diseases, neurological disorders and various cancers (Clevers & Nusse, 2012; De Ferrari & Moon, 2006; Nishisho et al., 1991). The canonical pathway is activated by the interaction of WNT with a Frizzled protein and LRP5/6. Subsequently it was supposed that the "destruction complex", a large multiprotein assembly responsible for the proteolysis of β-catenin, dissociates and causes the stabilization of β-catenin. But recent studies show that upon receptor activation, Dishevelled undergoes a conformational switch, facilitating its binding to AXIN1, which is recruited to the phosphorylated tail of LRP. The ubiquitination of β-catenin is inhibited, leading to the saturation of the destruction complex with phosphorylated β-catenin. The newly synthesized, nonphosphorylated β-catenin can accumulate and translocate into the nucleus. There it displaces Groucho from TCF/LEF and activates WNT target genes (Clevers, 2006; V. S. W. Li et al., 2012; Gammons et al., 2016) (Figure 5).

In the absence of WNT ligands the destruction complex is responsible for the phosphorylation of β-catenin by the serine/threonine kinases CK1 and GSK3α/β, followed by ubiquitination through the βTrCP ubiquitin ligase, and subsequent degradation by the proteasome. Further core components of the destruction complex are the scaffold protein AXIN1, which is the

rate-limiting factor of the destruction complex and adenomatous polyposis coli (APC), a crucial negative regulator of the WNT pathway (Heppner Goss & Groden, 2000; Lee, Salic, Krüger, Heinrich, & Kirschner, 2003; V. S. W. Li et al., 2012) .

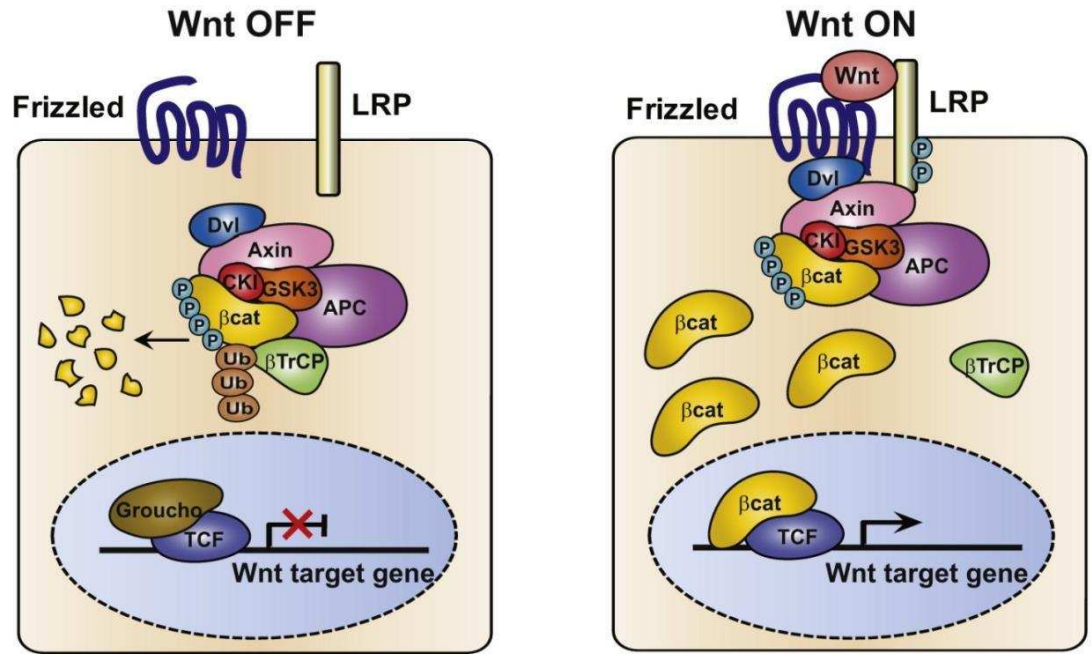

Figure 5. Regulatory model of WNT/β-catenin signaling. In the absence of the WNT signal, the destruction complex binds to the cytosolic β-catenin which is subsequently degraded by the proteasome. The binding of WNT to its receptors leads to the stabilization and translocation of β-catenin to the nucleus, where it displaces Groucho from TCF/LEF and activates WNT target genes Figure from (Li et al., 2012).

Despite the mutational activation, WNT signaling in CRC remains regulated on high levels, resulting in distinct tumor cell subpopulations with relatively low or high WNT activity (Horst et al., 2012a). Colon cancer cell subpopulations with high WNT levels were attributed certain characteristics such as more mesenchymal phenotypes and putative cancer stem cell traits, express markers that are linked to tumor invasion, and therefore are thought to be crucial drivers of colon cancer progression (Brabletz et al., 2005). These tumor cells are typically located at the infiltrative tumor edge where they invade the surrounding tissue, while those with lower WNT levels are frequently more central within the tumor and appear phenotypically more differentiated (Cernat et al., 2014; Kirchner & Brabletz, 2000). Due to these findings, high WNT signaling activity is assumed to be a driving force of colon cancer invasion and progression, making it an attractive potential target for therapeutic intervention. However, since WNT signaling is required for various physiological processes including adult

tissue and stem cell homeostasis, efforts in targeting this central pathway in clinical settings is complicated, and serious side effects may be anticipated (Kahn, 2014).

1.7. The mitogen-activated protein kinase pathway

Mitogen-activated protein kinase (MAPK) signaling cascades are evolutionarily conserved signal transduction pathways involved in the regulation of gene expression, proliferation, survival and differentiation of normal cells. Mammalian cells possess at least four well characterized MAPKs, extracellular signal-related kinases (ERK)-1/2, p38 proteins (p38α/β/γ/δ), Jun amino-terminal kinases (JNK1/2/3) and ERK5, that function downstream of cell surface receptors in response to stress, growth factor or cytokine stimulation (Roberts & Der, 2007) (Figure 6).

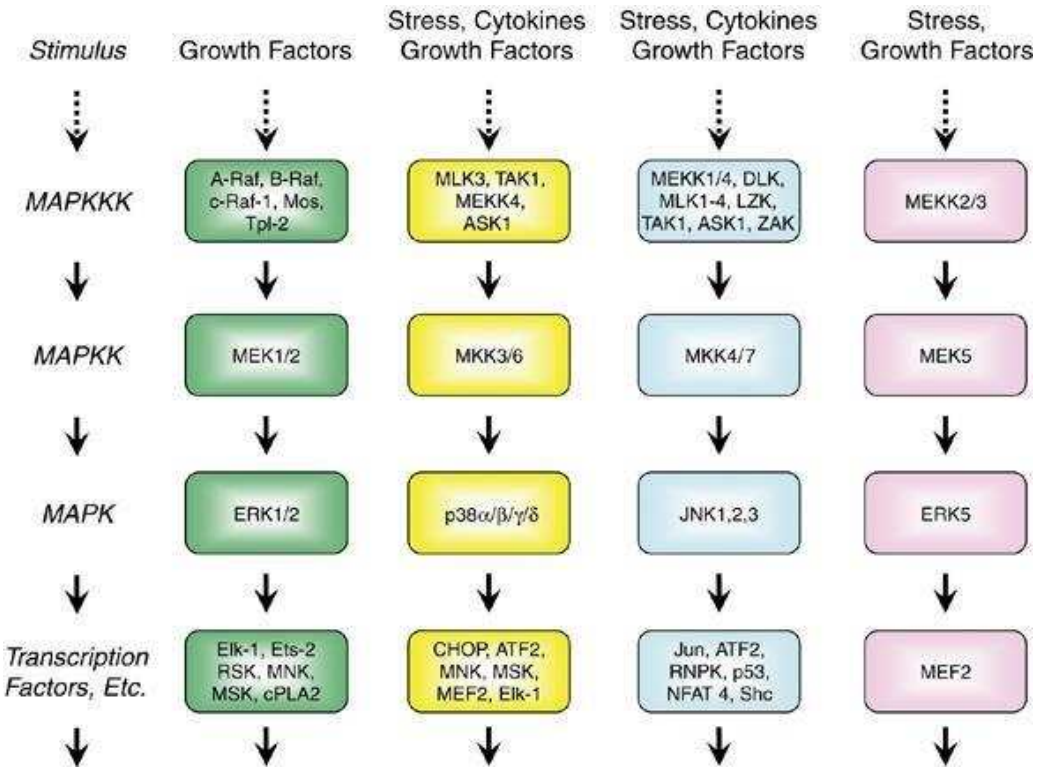

Figure 6. The four major mammalian MAPK cascades: stimuli and substrates. The ERK pathway is usually activated by growth factors, while the JNK, p38 and ERK5 can be activated by stress, cytokines and growth factors. Figure from (Roberts & Der, 2007)

Deregulation of the RAS–RAF–MEK–ERK signaling pathway can be observed in nearly 50 % of human malignancies (Herrero et al., 2015) (Figure 7).

The GTPase KRAS is a component of mitogen-activated protein kinase (MAPK) signaling that communicates signals from growth factor receptors into the cell nucleus (Schubbert, Shannon, & Bollag, 2007). In *KRAS* wild-type tumor cells, binding of epidermal growth factor (EGF) to its receptor (EGFR) causes GTP-loading of KRAS which activates RAF to phosphorylate MAPK/ERK-activating kinase (MEK), which in turn phosphorylates extracellular signal-regulated kinase (ERK). Phosphorylated ERK (p-ERK) then causes expression of MAPK target genes through ELK1 and AP1 transcription factors that promote malignant traits of tumor progression including invasion and metastasis (Urosevic et al., 2014; Yordy & Muise-helmericks, 2000). However, in contrast to wild-type KRAS, mutated KRAS binds GTP permanently and independently of EGFR stimulation (Scheffzek et al., 1997). MAPK signaling therefore is thought to be constitutively activated in *KRAS* mutated CRC, promoting tumor progression independently of external EGFR stimulation (Hatzivassiliou et al., 2013; Khambata-Ford et al., 2007). This translates into clinical application, since in contrast to wild-type cases, *KRAS* mutated CRC lacks significant treatment response to upstream MAPK inhibition when targeting the EGFR with antibody drugs, such as cetuximab (Lievre et al., 2008).

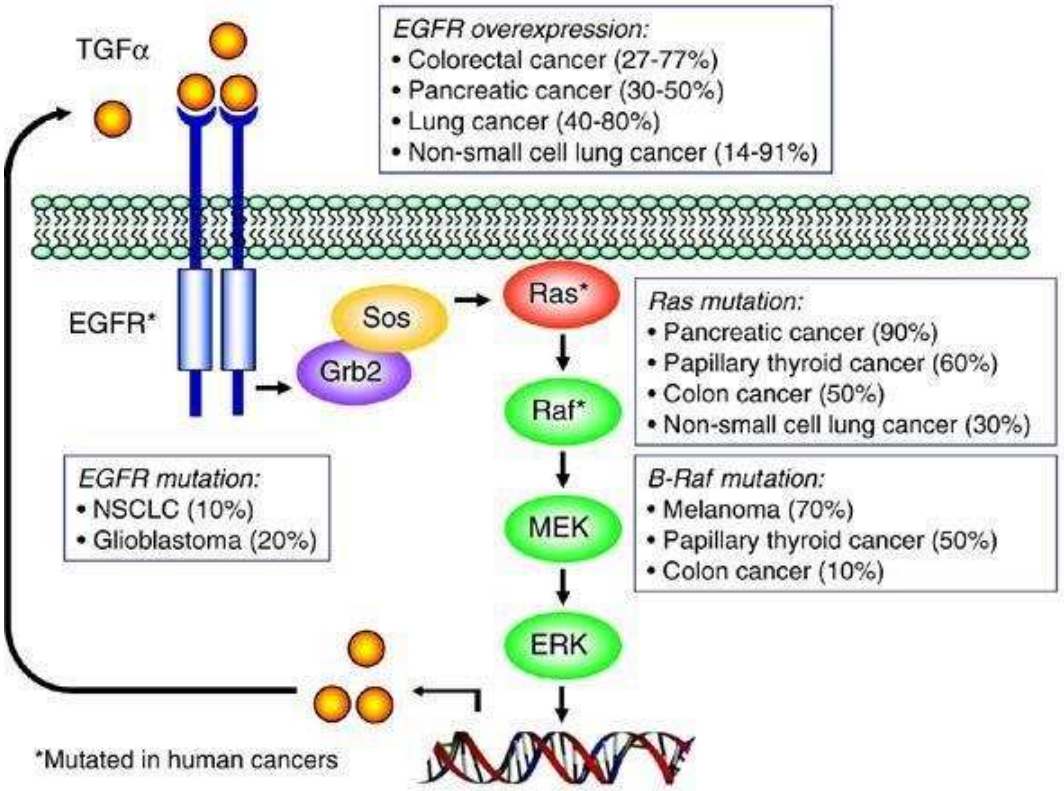

Figure 7. Mutational activation of the RAS–RAF–MEK–ERK signaling pathway in various types of cancers. Mutations of the EGFR and the Ras small guanosine triphosphatases (GTPases) lead to a constitutive activation of downstream effectors, which promote tumor progression and metastasis. Figure from (Roberts & Der, 2007)

Previous studies demonstrated that MAPK signaling regulates WNT signaling, and suggested a contribution of MAPK signaling to phenotypic tumor cell heterogeneity in CRC (Horst et al., 2012b). However, the extent of differential MAPK activity and its significance in KRAS wild-type and mutant CRC has remained largely unknown.

1.6. Activity-dependent neuroprotector homeobox

The differential regulation of signaling pathways like WNT and MAPK, leads also to a heterogeneous expression of target genes within tumors. Many of these target genes control critical cellular processes such as proliferation, survival, and invasion. Exploring their functional relevance may lead to the identification of new prognostic markers and therapeutic targets. In this work we identified activity-dependent neuroprotector homeobox (ADNP) as a pharmacologically inducible repressor of WNT signaling in colon cancer.

ADNP was initially discovered in brain tissue and encodes a ubiquitously expressed zinc finger homeobox protein with transcription factor activity (Bassan et al., 1999; Zamostiano et al., 2001). Most knowledge on ADNP function is related to the central nervous system where it is required for brain formation and cranial neural tube closure (Pinhasov et al., 2003). It also assumes protective roles against cognitive defects in neurodegenerative disease (Vulih-Shultzman et al., 2007). Moreover, ADNP has been shown to reduce the expression of genes involved in regulation of transcription, organogenesis and neurogenesis, and is suggested to interact with chromatin remodeling complexes that are associated with cellular differentiation (Mandel & Gozes, 2007). In regard to cancer, a previous report demonstrated overexpression of ADNP in proliferative tissues and several different malignancies, including colon cancer, and since ADNP depletion reduced the viability of certain cancer cells suggested a possible association with tumorigenesis and cell survival (Zamostiano et al., 2001). However, the contribution of ADNP to human cancer and its functional role in malignancies is still poorly understood.

Objectives

The deregulation of WNT and MAPK signaling plays a key part in colorectal cancer development. Despite mutational activation these signaling pathways can remain regulated in CRC and contribute to distinct phenotypes of tumor cell subpopulations.

The first objective of this work was to investigate the intratumoral signaling heterogeneity in colorectal cancer and exploit its functional relevance. Focusing on transcription factors linked to WNT signaling, the second aim was to translate the findings from the studies on tumor cell heterogeneity into diagnostic and clinically applicable markers.

2. Material

2.1 Chemicals and reagents

Chemicals	Supplier
4-Hydroxytamoxifen ≥70% Z isomer	Sigma-Aldrich, St.Louis, MO, USA
4x Laemmli Sample Buffer	Bio-Rad, Munich, Germany
Agarose Biozym LE	Biozym Scientific, Hessisch Oldenforf, Germany
All-purpose Hi-Lo DNA Marker	Bionexus, Netanya, Israel
Ammonium peroxodisulfate	Carl Roth GmbH, Karlsruhe, Germany
Ampicillin sodium salt	Sigma-Aldrich, St.Louis, MO, USA
Antibody diluent	Dako, Carpinteria, CA, USA
beta-Mercaptoethanol	Carl Roth GmbH, Karlsruhe, Germany
Biofreeze Einfriermedium	Biochrom, Berlin, Germany
Blasticidin	Carl Roth GmbH, Karlsruhe, Germany
BSA (Albumin Faktor V)	Carl Roth GmbH, Karlsruhe, Germany
Cetuximab	Merck Serono, Darmstadt, Germany
Chloroform	Sigma-Aldrich, St. Louis, MO, USA
Collagen	Santa Cruz Biotechnology, Santa Cruz, CA, USA
cOmplete, Mini Protease Inhibitor Cocktail Tablets	Roche Diagnostics GmbH, Penzberg, Germany
Crystal violet	Carl Roth GmbH, Karlsruhe, Germany
DAPI	Carl Roth GmbH, Karlsruhe, Germany
Dimethylsulfoxide	Sigma-Aldrich, St.Louis, MO, USA
DMEM	Invitrogen GmbH, Karlsruhe, Germany
dNTP Mix	Fermentas GmbH, St. Leon-Rot, Germany
Doxycycline	Sigma-Aldrich, St.Louis, MO, USA
EGF Recombinant Human	Invitrogen GmbH, Karlsruhe, Germany
Ethidiumbromide 1%	Carl Roth GmbH, Karlsruhe, Germany
Epitope Retrieval Solution	Leica Biosystems, Nussloch, Germany

Chemicals	Supplier
Fast SYBR Green Mix	QIAGEN GmbH, Hilden, Germany
Fast-Media Amp Agar	InvivoGen, San Diego, CA, USA
FCS	Invitrogen GmbH, Karlsruhe, Germany
FGF-Basic (AA 10-155) Recombinant Human Protein	Invitrogen GmbH, Karlsruhe, Germany
Fugene 6	Promega GmbH, Mannheim, Germany
HiPerFect Transfection Reagent	QIAGEN GmbH, Hilden, Germany
Immedge Pen	Biozym Scientific, Hessisch Oldenforf, German
Immobilon Western Chemiluminescent HRP Substrate	Merck Millipore, Billerica, MA, USA
Ketamine	Ratiopharm, Ulm, Germany
LB Media	Carl Roth GmbH, Karlsruhe, Germany
Lenti-X Concentrator	Clontech, Mauntain View, Ca, USA
LipoD293	Tebu-Bio, Le Perray-en-Yvelines, France
LiCl	Sigma-Aldrich, St.Louis, MO, USA
Matrigel	Corning, New York, NY, USA
NP40 Substitute	Sigma-Aldrich, St.Louis, MO, USA
Oleoyl-L-alpha-lysophosphatidic acid	Santa Cruz Biotechnology, Santa Cruz, CA, USA
Opti-MEM	Thermo Fisher Scientific Inc., Waltham, MA, USA
Page Ruler Plus Prestained	Fermentas GmbH, St. Leon-Rot, Germany
Paraformaldehyde	Carl Roth GmbH, Karlsruhe, Germany
Penicillin/Streptomycin	Biochrom, Berlin, Germany
PhosSTOP	Roche Diagnostics GmbH, Mannheim, Germany
Polybrene	Sigma-Aldrich, St.Louis, MO, USA
ProLong Gold Antifade Reagent	Invitrogen GmbH, Karlsruhe, Germany
Protein Block	Dako, Carpinteria, CA, USA
Puromycin, dihydrochlorid	Merck Millipore, Billerica, MA, USA
Rotiphorese Gel 30 (37,5:1)	Carl Roth GmbH, Karlsruhe, Germany
Sodium dodecyl sulfate	Carl Roth GmbH, Karlsruhe, Germany
Skim milk powder	Sigma-Aldrich, St.Louis, MO, USA

Chemicals	Supplier
Sunflower oil	Sigma-Aldrich, St.Louis, MO, USA
Tamoxifen free base	Sigma-Aldrich, St.Louis, MO, USA
Target Retrieval solution	Dako, Carpinteria, CA, USA
TEMED	Carl Roth GmbH, Karlsruhe, Germany
TritonX100	Carl Roth GmbH, Karlsruhe, Germany
Trizol Reagent	Invitrogen GmbH, Karlsruhe, Germany
Trypsin/EDTA	Biochrom, Berlin, Germany
TWEEN 20	Sigma-Aldrich, St.Louis, MO, USA
WNT3A	R&D Systems, Minneapolis, MN, USA

2.2. Kits and disposables

Kits and disposables	Supplier
Active Ras Pull-Down and Detection Kit USABio-Rad DC Protein Assay Reagents Package Kit	Thermo Fisher Scientific Inc., Waltham, MA, Bio-Rad, Munich, Germany
Dual-Luciferase Reporter Assay System 10-Pack	Promega GmbH, Mannheim, Germany
Pure Yield Plasmid Midi Prep Kit	Promega GmbH, Mannheim, Germany
Quantitect Reverse Transcription Kit	QIAGEN GmbH, Hilden, Germany
Rapid DNA Ligation Kit	Fermentas GmbH, St. Leon-Rot, Germany
StemPro® hESC SFM KIT	Invitrogen GmbH, Karlsruhe, Germany
Vectastain ABC Kit Universal	Vector Laboratories, Burlingame, CA, USA
Wizard V Gel and PCR Clean-Up System	Promega GmbH, Mannheim, Germany
Chromatography Paper 10 cm x 100 m	GE Healthcare
Immobilon-P Transfer Membrane	Merck Millipore, Billerica, MA, USA
ThinCert cell culture inserts	Greiner Bio-One, Kremsmünster, Austria
Rotilabo Filter .45µm PES	Carl Roth GmbH, Karlsruhe, Germany
E-Plate 16	Omni Life Science, Bremen, Germany

2.3. Enzymes

Enzymes	Supplier
T4 Polynucleotide kinase	Fermentas GmbH, St. Leon-Rot, Germany
Klenow	Fermentas GmbH, St. Leon-Rot, Germany
FastAP Thermosensitive Alkaline Phosphatase	Fermentas GmbH, St. Leon-Rot, Germany
Pfu Polymerase	Fermentas GmbH, St. Leon-Rot, Germany
Restriction endonucleases	Fermentas GmbH, St. Leon-Rot, Germany

2.4. Buffers and solutions

Name	Ingredients
50x TAE Buffer	40 mM Tris Base 20 mM acetic acid 1 mM EDTA pH 8.0
10x PCR Buffer	166 mM NH_4SO_4 670 mM Tris pH 8.8 67 mM $MgCl_2$ 100 mM β-Mercaptoethanol
RIPA Buffer	1% NP40 0.5% sodium deoxycholat 0.1% SDS 150 mM NaCl 50 mM TrisHCl, pH 8.0

Name	Ingredients
10x TBS	20 mM Tris base 150 mM NaCl
1x TBST	TBS 0.1% Tween 20
1x FACS Buffer	1 mM EDTA 0.5% BSA 10 mM HEPES pH 6.5, ad 500ml PBS
10x Running Buffer	1.92 M glycine 250 mM Tris base 1% SDS, pH 8.5
10x Transfer Buffer	1.92 M glycine 250 mM Tris base 1% SDS, pH 8.5 20% Methanol
4x SDS-PAGE Lower Buffer	1.5 M Tris-base 0.4% SDS, pH 8.8
4x SDS-PAGE Upper Buffer	500 mM Tris-base 0.4% SDS, pH 6.8

2.5. Laboratory equipment

Device	Supplier
Axioplan 2	Carl Zeiss GmbH, Oberkochen, Germany
Centrifuge 5415R	Eppendorf AG, Hamburg, Germany
FACSAria III	BD Bioscience, Heidelberg, Germany
HERACell 240i Co2 Incubator	Thermo Fisher Scientific, Inc., Waltham, MA, USA
Heraeus Megafuge 40R Centrifuge	Thermo Fisher Scientific, Inc., Waltham, MA, USA
Image Station 440 CF	Kodak, Rochester, New York, USA
Light Cycler 480 II	Roche Diagnostics GmbH, Mannheim, Germany
Mini-PROTEAN Tetra System	Bio-Rad, Munich, Germany
MultiImage Light Cabinet	Alpha InnoTec, Kasendorf, Germany
ND-100 Spectrophotometer	NanoDrop products, Wilmington, DE, USA
Orion II Micropate Luminometer	Berthold Detection Systems, Pforzheim, Germany
PEQPOWER	PEQLAB
PrimoVert	Carl Zeiss GmbH, Oberkochen, Germany
SAFE 2020 T	Thermo Fisher Scientific Inc., Waltham, MA, USA
T100 Thermo Cycler	Bio-Rad, Munich, Germany
Varioscan	Thermo Fisher Scientific Inc., Waltham, MA, USA
xCELLigence RTCA DP	Roche Diagnostics GmbH, Penzberg, Germany

3. Methods

3.1. Clinical samples and statistical analyses

Resection specimens of patients diagnosed with FAP as well as CRC specimens from patients that underwent intentionally curative surgical resection between 1994 and 2006 at the LMU were drawn from the archives of the institute of pathology. For CRC specimens, inclusion criteria were localized colorectal adenocarcinomas with absence of nodal (N0) or distant metastasis (M0) at the time of diagnosis (UICC stage I and II). Follow-up data were recorded prospectively by the Munich Cancer Registry. CRC tissues were assembled into tissue microarrays (TMAs) with representative 1 mm cores, including tumor edges and tumor centers of each case. The final CRC collection consisted of 221 cases of which in 43 cases (19%) patients had died of their tumor within the follow-up period. For tumor specific survival analysis, CRC attributed deaths were defined as clinical endpoints. For analysis of disease free survival, tumor progression after surgical resection was the clinical endpoint, documented as either tumor recurrence or metastasis. Survival was analyzed by the Kaplan-Meier method and groups were compared with the log-rank test. Cox proportional hazards model was used for multivariate analysis. Statistics were calculated using SPSS (IBM).

For *KRAS* mutational testing, tumor tissue was scraped from deparaffinized tissue sections under microscopic control using sterile scalpel blades, and tumor DNA was extracted from the tissue, in a final volume of 20 µl, using Qiagen FFPE Micro Kits. 1 µl of the DNA solution was amplified by PCR using the *KRAS* exon-specific primer pair 5'-NNNGGCCTGCTGAAAATGACTGAA-3' and 5'-Biotin-TTAGCTGTATCGTCAAGGCACTCT-3' and HotStar Taq Polymerase (Qiagen). The PCR was performed with 1 x PCR buffer, 5 mM $MgCl_2$, 200 µM dNTP mix, 400 nM of each primer and 1 unit of Taq polymerase, under the following conditions: 1 x 15 minutes at 95° C, and 50 cycles (30 seconds at 95° C, 30 seconds at 60° C, 30 seconds at 72° C) followed by 2 minutes at 72° C.

KRAS exon 2 then was analyzed by pyrosequencing on a PyroMark Q24 Advanced instrument (Qiagen) with primers 5'-NNNGGCCTGCTGAAAATGACTGAA-3' and 5'-TGTGGTAGTTGGAGCT-3' for sequencing. *KRAS* wild-type and mutated CRCs then were

grade and stage matched, resulting in a final collection of 160 cases, half of which had *KRAS* exon 2 mutations and the other half of which were *KRAS* wild-type (Table 1). Specimens and data were anonymized, and the need for consent was waived by the institutional ethics committee of the Medical Faculty of the LMU.

Table 1. Colorectal cancer case characteristics.

Characteristics	**Total**	***KRAS* mutation status**							
		WT	**G12D**	**G12V**	**G12S**	**G12A**	**G12C**	**G12R**	**G13D**
All patients	160	80	27	25	8	4	3	2	11
Age (y, Median									
≤ 68	72	40	14	10	2	0	1	0	5
≥ 69	88	40	13	15	6	4	2	2	6
Gender									
Male	88	48	16	15	2	2	0	0	5
Female	72	32	11	10	6	2	3	2	6
T-stage (UICC)									
T3	126	63	23	19	6	4	3	2	6
T4	34	17	4	6	2	0	0	0	5
Tumor grade									
low grade	102	51	15	17	4	2	3	1	9
high grade	58	29	12	8	4	2	0	1	2

3.2. Gene expression data sets, TCGA data, and GSEA

Three sets of differentially expressed genes from colon cancer cells with low and high WNT activity were screened for consistently deregulated genes (Horst et al., 2012b; Louis Vermeulen et al., 2010). From The Cancer Genome Atlas (TCGA) database (https://tcga-data.nci.nih.gov/tcga/) RNA-Seq data of 41 normal mucosa samples and 457 colon cancer samples were retrieved. Within the cancer sample data, pearson correlations of *ADNP* expression and expression of 20,531 genes within this data set were calculated and genes were ranked accordingly. GSEA analyses were conducted using this ranked gene list against curated sets of upregulated WNT targets derived from Nusse et al. (web.stanford.edu/group/nusselab/cgi-bin/WNT/target_genes) and (Herbst et al., 2014). Gene sets are listed in Table 2. Heat maps for individual factors were drawn with GENE-E (Broad Institute).

Table 2. WNT target gene sets used for GSEA.

Herbst et al. WNT target gene set				Nusse et al. WNT target gene set
KIAA1199	SLC7A2	SEMA3F	SLC5A6	MYC
NAV2	C12orf24	RNF44	RCL1	MYCN
ASCL2	FGF18	TMEM97	KLHL29	CCND1
EDAR	FGF9	KATNB1	MDN1	HNF1A
ABCB1	GJA3	WFDC9	NHP2L1	TCF7
ADAMTS19	PIK3AP1	HSD11B2	PAICS	LEF1
AXIN2	ADCK3	CR2	DCAF4	PPARD
KCNJ8	ABHD6	LDLRAD3	SORD	JUN
TNFRSF19	ECE2	C5orf13	WDR74	FOSL1
DEPDC7	NPTX2	CDC25A	PTDSS1	PLAUR
SLC4A8	GAS5	AIF1L	NOP2	MMP7
LOC100134361	PPP2R2C	LOC100505644	DDX20	AXIN2
RNF43	BCL11A	RSL1D1	ADCY3	NRCAM
GLS2	SMPDL3B	TMEM80	CD83	TCF4
SLC9B2	MEX3A	QSOX2	SFXN4	GAST
SUSD4	MAOB	TEX10	NME1	CD44
LOC100287482	PDCD2L	TFB2M	MCAM	EPHB2
CTNNB1	PLD6	LOC202181	ADSL	EPHB3
MYC	ACTR3B	GEMIN5	NLE1	BMP4
PXK	TXLNG	KIF9	IMP3	CLDN1
B7H6	NSUN5P1	RFC3		BIRC5
APCDD1	MCOLN2	CCNO		VEGFA
GAD1	RABEPK	SCLY		FGF18
DPYSL3	UBE2CBP	HPCAL4		MET
RORA	POLR3G	KCNJ5		EDN1
TMEM177	C10orf2	LOC100506469		MYC
ISM1	GALNT6	CD44		L1CAM
ZNRF3	SLC16A10	MKI67IP		ID2
VSNL1	SNHG1	SKP2		JAG1
BCL2L15	CSTF3	HAS2		MSL1
LOC100507303	RPIA	MATR3		DKK1
CTDSPL	C7orf40	BCS1L		FGF20
BDNF	C1QTNF9B-AS1	BCL2L11		SOX17
CCNB1IP1	BEGAIN	FXN		SOX9
MIR17HG	SPTLC3	NAV3		TIAM1
SLC2A3	SLC6A16	KIAA1804		LGR5
FKBP7	DKC1	DHX33		WNT

3.3. Bacterial cell culture, transformation and plasmid DNA preparation

The *Escherichia coli* strains DH5α or Stbl3 (Invitrogen) were used for plasmid replication. Bacterial cells were cultured in LB medium at 37’°C for 12-18 hours or on LB agar plates, in order to isolate DNA from single cell clones. 100 µg/ml ampicillin were added to the LB-medium for selection of antibiotic–resistant cells.

For transformation 100 µl bacteria were thawed on ice, 100 ng plasmid or 10 µl of a ligation reaction were added and incubated for 30 minutes on ice, followed by a heat-shock at 42°C for 45 seconds. The transformed bacterial cells were mixed with 500 µl antibiotic-free LB-medium and incubated for 45 minutes at 37°C. The bacterial cells were plated on LB-agar plates containing ampicillin and incubated at 37°C overnight. Single cell clones were used to inoculate ampicillin containing LB medium and incubated for 8-12 hours at 37°C.
For plasmid DNA isolation the mi-Plasmid Miniprep Kit (Metabion) or the Pure Yield Midi Prep Kit (Promega) were used following the manufacturer's instructions.

3.4. DNA cloning and sequencing

Amplification of DNA was performed in a 40 µl master mix containing 50 ng DNA, 4 µl 10 x PCR Buffer, 2 µl specific oligonucleotides (Table 5) , 1 µl dNTPs, 2 µl DMSO and 1 µl *Pfu* polymerase under following PCR cycling conditions: three minutes at 95°C initial denaturation, 36 cycles of 30 seconds denaturation at 95°C, 90 seconds annealing at 55-65°C (depending on the melting temperature of the used oligonucleotides) and 45 seconds per kb of product length extension at 72°C, and for the final extension step 5 minutes at 72°C. The length of the PCR products was analyzed on a 1% agarose gel by electrophoresis. The DNA was purified from excised gel fragments using the Wizard® SV Gel and PCR Clean-Up System (Promega) following the manufacturer's protocol.

Enzymatic digestions were performed at 37°C for 30 minutes using 1 µg DNA, 20 units (U) of restriction enzymes and 3 µl Green Buffer (Fermentas) in a 30 µl master mix. The DNA was 5’-dephosphorylated by adding 10 U Fast AP at 37°C for 15 minutes. For DNA blunting 2 U Klenow Fragment was added for 15 minutes at 37°C to fill-in 5'-overhangs.

For DNA ligation vector and insert DNA was mixed in a molar ratio of approximately 1:3 and incubated with 5 U T4 ligase for 20 minutes at 22°C.
The verification of DNA sequences was executed via Sanger sequencing by GATC Biotech (Konstanz).

3.5. Isolation of RNA and qPCR

Total RNA was isolated from cancer cells using TRIzol (Invitrogen) according to the manufacturer's protocol. 1 µg RNA was reverse transcribed into cDNA using the Quantitect Reverse Transcription Kit (Qiagen) following the manufacturer's instructions. The quantitative real-time PCR protocol consisted of 40 cycles of amplification at 95 °C (15 seconds) and 60
°C (1 minute) and was performed a LightCycler 480 (Roche) with a Fast SYBR Green Master Mix (Applied Biosystems) using primers indicated in Table 3**.** *ACTB* and *GAPDH* served as housekeeping genes. The results were analyzed with the $^{\Delta\Delta}$Cp method (Livak & Schmittgen, 2001) and presented as relative mRNA expression.

Table 3. Primer sequences used for qPCR.

Gene	**Forward 5'->3'**	**Reverse 5'->3'**
ACTB	CCAACCGCGAGAAGATGA	CCAGAGGCGTACAGGGATAG
GAPDH	GAAGGTGAAGGTCGGAGTC	GAAGATGGTGATGGGATTTC
ADNP 1	CCCATCACTTACGAAAAACCA	GGACATTGCGGAAATGACTT
ADNP 2	GGACCACATTGTCAATTCACACC	GGACAAGCGCTGCAGCAGAAAGG
ADNP 3	GTGACATCGCTTCCCATTTTAG	CCACTCAGCATCAAAATCCATC
AXIN2	AGGCCAGTGAGTTGGTTGTC	CATCCTCCCAGATCTCCTCA

3.6. Cell and spheroid culture

SW122 were a gift from the Ludwig Institute for Cancer Research (New York, USA) and primary colon cancer cells (P-Tu) were obtained from the HTCR (Munich, Germany). Other cell lines were from the ATCC. Cell lines were cultured in DMEM containing 10 % FCS, 100

U/ml penicillin, and 0.1 mg/ml streptomycin (Biochrom) at 5% CO2 and 37°C. P-Tu colon cancer cells were grown as spheroids in StemPro hESC SFM medium supplemented with 20 ng/ml EGF and 10 ng/ml bFGF (Life Technologies) in ultra-low attachment flasks (Corning).

Colon cancer cell lines were cryo-preserved in 90 % FCS and 10 % DMSO (Sigma) and tumor spheroids in Biofreeze (Biochrom).

3.7. *In vitro* treatments

For WNT induction or inhibition, cells were treated with 20 ng/ml WNT3A (R&D Systems), 20 mM LiCl, or 10 µM XAV939 (both Sigma-Aldrich), respectively. *In vitro* ketamine treatment was done at concentrations of 200 µM (Ratiopharm).

For *in vitro* MAPK stimulation experiments, cells were starved for 24 hours in serum-free medium, treated with 10 µg/ml cetuximab (Merck Serono) or PBS, and then with 40 ng/ml EGF (Invitrogen) for 10 minutes before protein isolation. For the induction of caMEK, cells were cultivated in serum-free medium and treated at several time points with 1 µg/ml doxycycline before protein isolation. To assess phenotypic effects, tumor spheroids of P-Tu colon cancer cells were mixed with 25 µl rat tail collagen I (Santa Cruz), placed in 8-well culture slides (Falcon), incubated for four days in serum free DMEM with or without 100 nM oleoyl-L-alpha-lysophosphatidic acid (LPA, Santa Cruz), and subjected to immune fluorescence as described below.

3.8. Lentiviral vectors

All template plasmids were obtained through Addgene (www.addgene.org).

For stable *ADNP* knockdown, oligonucleotides containing specific targeting sequences (Table 4) were selected from The RNAi Consortium shRNA Library (Broad Institute) and inserted between BamHI and EcoRI restriction sites of the lentiviral pGreenPuro shRNA vector (System Bioscience).

pLenti SRE-GFP was constructed by replacing the PGK promoter in pLenti PGK-GFP (pRRLSIN.cPPT.PGKGFP.WPRE, a gift from Didier Trono) with a serum response element

optimal promoter cassette (3xSRE), containing synthetic GGATGTCCATATTAGGACATCT binding sites (Hayes, Sengupta, & Cochran, 1988). We then removed the internal ribosomal entry site (IRES) of pBMN-I-GFP (a gift from Garry Nolan) using Not1 and Nco1 restriction enzymes, amplified CreERT2 from pCAG-CreERT2 (Matsuda & Cepko, 2007) by PCR, and inserted both into the SalI sites of pLenti PGK-GFP and pLenti SRE-GFP, yielding pLenti PGK-GFP-CreERT2 and pLenti SRE-GFP-CreERT2. For the Cre sensitive recombination vector pLenti lox-mCh-LacZ, we replaced the GFP cassette of pLenti PGK-GFP with a synthetic sequence containing two lox2272 and loxP sites (Zhang et al., 2010) as well as EcoRV and HpaI restriction sites. PCR amplified H2BmCherry from PGK-H2BmCherry (Kita-Matsuo et al., 2009) and LacZ from LV-Lac (Pfeifer, Brandon, Kootstra, Gage, & Verma, 2001) then were inserted or reversely inserted into EcoRV and HpaI sites, respectively. For construction of pLenti CMVTRE3G-caMEK Puro, we amplified constitutively active MEK1 (caMEK) from pCScherryActMEK (Covassin et al., 2009) by PCR and inserted it between BamHI and XbaI restriction sites of pLenti CMVTRE3G eGFP Puro (a gift from Eric Campeau), replacing eGFP by caMEK. Modified vector elements were verified by restriction analysis and sequencing.

For *in vitro* induction, pLenti CMV rtTA3G Blast (a gift from Dominic Esposito) and pLenti CMVTRE3G-caMEK Puro transduced T84 and P-Tu colon cancer cells were treated with 10 ng/ml doxycycline in PBS or with PBS alone before protein isolation and immunoblotting.

Table 4. shRNA sequences

shRNA	**Sequence**
sh1ADNP	GCCATGATTGGGCACACAAAT
sh2ADNP	GCCCGAGAAGAGAGTAGTATT
shCtrl	GGCTACGTCCAGGAGCGCACC

Table 5. Primer sequences for DNA amplification.

Gene	**Forward 5'->3'**	**Reverse 5'->3'**
CreERT2	ATGTCCAATTTACTGACCGTACACC	TCAAGCTGTGGCAGGGAAACC
mCherry	GCCGCCACCatgCCAGAGCCAGCGAA	CCGCTTTACTTGTACAGCTCGT
LacZ	GCCGCCACCATGAAAGTGTTCCGCAAT	TTATTATTATTTTTGACACCAGACCAACT
caMEK	ATAGGATCCGCCACCATGGATGCCCAAGAA	ATATCTAGATTAGACGCCAGCAGCATGG

3.9. Transient transfections

For transient knockdown, pre-designed siRNAs targeting *CTNNB1*, *ADNP* (Thermo Fisher), *DNMT1*, or *TLN1* (Dharmacon), or scrambled (siCtrl) were transfected into HCT116 or SW1222 cells at 10 nM final concentration using HiPerFect (Qiagen). 48 hours after transfection, cells were harvested for further analysis.

Transient ADNP overexpression was achieved by transfecting HCT116 and SW1222 cells with 1 µg p4.2-hADNP or, as control, empty p4.2 plasmid (a gift from Vivien Bubb), in 6-well plates in the presence of 6 µl FuGENE 6 (Promega).

3.10. Luciferase assays

For luciferase reporter assays, treated cells or cells with stable or transient ADNP knockdown or overexpression were transfected or co-transfected, respectively, in 24-well plates with 10 ng Renilla luciferase control vector and 100 ng TOPflash or FOPflash luciferase reporter constructs carrying either wild-type or mutant TCF-binding sites (The Cancer Genome Atlas Network, 2012). Firefly luciferase activity was measured with dual-luciferase Reporter Assays (Promega) after 24 hours according to manufacturer's instructions with an Orion II luminometer (Berthold), analyzed with the SIMPLICITY software package (DLR) and normalized to Renilla luciferase activity.

3.11. Lentiviral transductions and single cell sorting

For transductions, lentivirus was produced in HEK293 cells by co-transfection with 10 µg lentiviral vector, 10 µg pCMV-dR8.91, and 3 µg pMD2.G, in the presence of 60 µl LipoD293. Virus containing medium was passed through 0.45 µm filters (Millipore), mixed 1:1 with DMEM, and used to infect colon cancer cells in the presence of 8 µg/ml polybrene (Sigma-Aldrich).

Transduced cells were single cell sorted into 96-well plates on a FACSAria III instrument (BD Biosciences) and expanded.

3.12. CRISPR/Cas9 genome editing

Synthetic oligonucleotide pairs of two guide sequences targeting the coding region (Exon 6) of ADNP were selected using the Zhang Laboratory MIT CRISPR Design Tool. Each pair was annealed and inserted into pSpCas9(bb)-2A-GFP (PX458, a gift from Feng Zhang, Addgene plasmid 48138), resulting in two different *ADNP* targeting vectors. Both vectors then were co-transfected into HCT116 and SW1222 colon cancer cells in 24-well plates with FuGENE 6. After 2 days, GFP positive single cells were sorted into 96-well plates on a FACSAria III instrument (BD Biosciences) and expanded. Single cell clones with loss of ADNP expression were selected by immunoblotting.

Table 6. sgRNA sequences.

sgRNA	Forward 5'->3'	Reverse 5'->3'
ADNP Ex6-1	caccgCTACTTGGTGCGCTGGCGTT	aaacAACGCCAGCGCACCAAGTAGc
ADNP Ex6-2	caccgCCTGATAGCCTATACGTTCA	aaacAACGCCAGCGCACCAAGTAGc

3.13. Gene expression analyses

RNA was isolated from cell lines using TRIzol (Invitrogen) according to manufacturer's protocol.

Libraries were constructed using the Encore Complete RNA-Seq library system (NuGEN) according to manufacturer's protocol. In brief, 150 ng of total RNA were used for first-strand cDNA synthesis and fragmented. cDNA was end repaired, ligated with barcoded adaptors, and the strand selected library was amplified with AMPure XP beads (Beckman Coulter). Barcoded libraries then were quantified, pooled at 10 nM concentration, and sequenced in multiplex on a HiSeq 1500 as 100 b single reads. Data then were demultiplexed, adaptor sequences and polyA tails were removed, and mapped to the hg19 human reference genome. Sequence reads for annotated genes were counted and comparative analyses of gene expression were done with the DEseq2 package with a <5 % false discovery rate (FDR). GSEA on fold change ranked gene lists were done and heat maps were drawn as described

above. Significantly upregulated genes were characterized according to signaling pathways using PANTHER version 10.0 (www.pantherdb.org).

Expression data are accessible through GEO (GSE79395).

3.14. Immunoblotting

For Immunoblotting cell were lysed in RIPA buffer supplemented with protease and phosphatase inhibitors (Roche). Sonication was performed for 10 seconds at 85% amplitude with the HTU SONI130 (G. Heinemann Ultraschall- und Labortechnik). Protein concentrations were determined with the DC Protein Assay Reagents Package Kit (Biorad) according to manufacturer's instructions and measured with a Varioskan Flash Multimode Reader using the SkanIt RE 2.4.3 software (Thermo Scientific). 50 µg of the protein samples supplemented with Laemmli buffer were denatured at 95°C for five minutes and separated on 9 % SDS- polyacrylamide gel using the Mini-PROTEAN Tetra System (Biorad) and Tris-glycine-SDS running buffer. Proteins were transferred onto Immobilon-P PVDF Transfer Membranes using the PerfectBlue™ SEDEC blotting system (Peqlab) and transfer buffer with constant electrical current of 100 mA per gel for 45-90 minutes. In order to block unspecific protein binding the membranes were incubated in 5% skim milk/TBST for one hour. The incubation with primary antibodies diluted in TBST was done overnight at 4°C. The detection of proteins was accomplished using secondary antibodies conjugated with horseradish peroxidase (HRP) and a chemiluminescent ECL/HRP substrate (Immobilon) on the CF440 Imager (Kodak). Antibodies are listed in Table 7.

3.15. Mass spectrometry (MS)

For mass spectrometry (MS) proteome analysis, cells were lysed, sonicated, and centrifuged through QIA-Shredder devices (Qiagen). 10 µg of total protein was reduced with 4.5 mM dithiothreitol for 30 minutes, alkylated with 10 mM iodoacetamide for 20 minutes, and incubated overnight at 37 °C with 200 ng porcine trypsin (Promega). For separation an EASY-nLC 1000 chromatography system connected to an Orbitrap XL instrument (Thermo Scientific) was used. 2.5 µg of peptides in 10 µl 0.1 % formic acid were transferred to

PepMap100 C18 trap columns and separated at flow rates of 200 nl/minutes on analytical PepMap RSLC C18 columns (Thermo Scientific) using consecutive linear gradients from 2 % to 25 % solvent B (0.1 % formic acid, 100 % acetonitrile) in 260 minutes and 25 % to 50 % solvent B in 60 minutes. For data acquisition, a top five data dependent collision-induced dissociation method was used at a needle voltage of 1.9 kV. MS raw data files were processed with the Homo sapiens subset of the UniProt database and MaxQuant V1.5.1 with the following parameters: (i) enzyme, trypsin; (ii) mass tolerance precursor, 10 ppm; (iii) mass tolerance MS/MS, 0.8 Da; (iv) fixed modification, carbamidomethylation of cysteine; (v) variable modifications, acetylation of protein N-terminus and oxidized methionine. FDRs at peptide and protein levels were set to 1
%. Missing values for proteins detected in at least three replicates per group were handled by MaxQuant imputation. Proteins with log2 fold changes of ± 0.6 at P values < 0.05 were considered relevant.

3.16. RAS-GTP assays

For detection of active RAS-GTP, 500 μg cell lysates were incubated with GST-Raf1-RBD (Thermo Fisher) for 60 minutes at 4°C, washed 3 times with washing buffer (25mM Tris HCl, pH 7.2, 150 mM NaCl, 5 mM $MgCl_2$, 1 % NP-40 and 5 % glycerol), eluted with SDS sample buffer (25 mM Tris HCl, pH 6.8, 2% glycerol, 4% SDS (w/v) and 0.05% bromophenol blue) and heated for 5 minutes at 95°C. Proteins were separated by SDS-PAGE, transferred onto PVDF membranes (Merck Millipore) and incubated with primary antibodies. Bands were visualized using HRP-conjugated secondary mouse (Promega) or rabbit (Sigma) antibodies and ECL/HRP Substrate (Millipore).

3.17. Immunohistochemistry, immunofluorescence and imaging

For immunohistochemistry, 5 µm tissue sections of CRC samples were deparaffinized, incubated with primary antibodies listed in Table 7 and stained on a Ventana Benchmark XT autostainer with an ultraView Universal DAB detection kit (Ventana Medical Systems).

Scoring of ADNP and β-catenin in colon cancer cases was done in a manner blinded for clinical outcome, and cases were classified semi-quantitatively for overall ADNP and β-catenin expression intensity, ranging from absent or barely detectable to strong overexpression. Staining intensities of ADNP in tumor cells with low or high β-catenin were quantified with ImageJ (NIH).

For immunofluorescence, cultured cells were fixed in 4 % paraformaldehyde for 10 minutes, permeabilized with 0.2 % TritonX100 for 15 minutes, blocked with 3 % BSA in PBS for 30 minutes and then incubated with for 60 minutes at RT with ADNP Ab (1:50), AXIN2 Ab (1:100), or DNMT1 Ab (1:100). Secondary *Alexa Fluor* 488 or 555 conjugated antibodies (Invitrogen) were used for visualization and nuclei were counterstained with DAPI (Vector Laboratories). Confocal fluorescence images were taken on a LSM 700 laser scanning microscope using the ZEN software (Carl Zeiss).

For mutational analyses of tumor cell subpopulations, 1000 positive or negative tumor cells were laser-microdissected from p-ERK stained slides with a PALM system (Zeiss). DNA from these tumor cell subpopulations then was separately isolated and subjected to *KRAS* mutation analysis as described above. For immune fluorescence, sections of CRC cases and xenografts were deparaffinized and antigens were retrieved in Target Retrieval Solution (Dako) or Epitope Retrieval Solution pH8 (Leica) for 20 minutes in a microwave oven. Spheroid cultures were fixed in 4 % paraformaldehyde and 5 % sucrose in PBS for 20 minutes, permeabilized in 1 % Triton X-100 for 10 minutes, and blocked with 3 % BSA in PBS for 30 minutes at RT. Sections or spheroids then were incubated with primary antibodies listed in Table 7. Secondary Alexa Fluor 488 or 555 conjugated antibodies (Invitrogen) were used for visualization and nuclei were counterstained with DAPI (Vector Laboratories). Confocal fluorescence images were taken on a LSM 700 laser scanning microscope using the ZEN software (Zeiss). Co-localization of fluorescence signals was measured using Volocity 6.1.1 software (PerkinElmer) and plotted as percentage values of maximum fluorescence intensity.

Table 7. Antibody details and concentrations for immunoblotting (WB), immune fluorescence (IF) and immunohistochemistry (IHC).

Antibody	Species	Manufacturer	WB	IF	IHC
ADNP	Rabbit	Proteintech	1:1000	1:50	1:100
AXIN2	Rabbit	Cell Signaling	1:1000	1:50	
DNMT1	Rabbit	Santa Cruz	1:1000	1:50	
TLN1	Mouse	Santa Cruz	1:1000		
LEF1	Rabbit	Cell-Signaling	1:1000		
p44/42 MAPK (ERK1/2)	Mouse	Cell Signaling	1:10000		1:100
Phospho p44/42 MAPK (Thr202/Tyr204)	Rabbit	Cell Signaling	1:1000	1:100	
MEK1/2 (L38C12)	Mouse	Cell Signaling	1:10000		
Phospho-MEK1/2 (Ser221) (166F8)	Rabbit	Cell Signaling	1:1000		
EGF Receptor (D38B1)	Rabbit	Cell Signaling	1:1000		
Phospho-EGF Receptor (Tyr1068) (D7A5)	Rabbit	Cell Signaling	1:1000		
H-Ras (sc-520)	Rabbit	Santa Cruz	1:1000		
N-Ras (sc-519)	Rabbit	Santa Cruz	1:1000		
K-Ras (sc-30)	Mouse	Santa Cruz	1:1000		
E-cadherin (24E10)	Rabbit	Cell Signaling	1:1000	1:200	
SNAIL (C15D3)	Rabbit	Cell Signaling	1:1000	1:50	
FRA1 (sc-28310)	Mouse	Santa Cruz	1:1000	1:50	1:100
CD44 (DF1485)	Mouse	Dako	1:1000		
ASCL2	Mouse	US Biological	1:1000		
EPHB2 (clone 3B3)	Mouse	Sigma-Aldrich	1:1000		
Laminin-5-γ2 (clone D4B5)	Mouse	Merck Millipore		1:250	
Fibronectin 1	Rabbit	Sigma-Aldrich		1:50	
Ki67 (8D5)	Mouse	Cell Signaling		1:100	
Active β-catenin (clone 8E7)	Mouse	Merck Millipore	1:1000		
β-Catenin	Mouse	BD Biosciences		1:200	
β-Galactosidase	Rabbit	Thermo Fisher		1:500	1:1000
GFP (4B10)	Mouse	Cell Signaling	1:1000	1:180	1:180
GFP	Rabbit	Cell Signaling		1:180	
Tubulin (DM1A)	Mouse	Sigma-Aldrich	1:50000		
Alexa Fluor 488	Goat	Invitrogen		1:500	
Alexa Fluor 555	Goat	Invitrogen		1:500	

3.18. Proliferation, migration and invasion assays

To assess cell proliferation $5x10^4$ cells per well were seeded in 200 µl cell culture media on conductive microtiter plates (E-Plate 16) and monitored for up to 150 hours using an xCELLigence DP instrument (ACEA Bioscience). For transwell migration and invasion assays 8 µm ThinCert cell culture inserts (Greiner Bio-One) were used, which for invasion were coated with 100 µl of 1 mg/ml growth factor-depleted Matrigel (Corning). $1x10^5$ cells/well were seeded in serum free medium in the upper insert chambers and after 24 h DMEM with 10 % FCS was added to the lower chambers of the inserts. For HCT116 and SW1222 cells, inserts were removed after 1 or 3 days for migration, and 3 or 5 days for invasion, respectively. Cells were fixed with 4 % paraformaldehyde, stained with crystal violet, residual cells from the upper chamber were removed, and photomicrographs were taken. For quantification, staining was dissolved in 250 µl of 30 % acetic acid, and absorbance was measured at 590 nm on a Varioskan instrument (Thermo Scientific).

3.19. Tumor xenografts and *in vivo* treatments

Mouse experiments were reviewed and approved by the Regierung von Oberbayern.

To determine effects of ADNP depletion, $8x10^6$ SW1222 ADNP knockdown or control cells were suspended in 200 µl of a 1:1 mixture of PBS and growth factor-depleted Matrigel and injected subcutaneously into age and gender matched 6-8 week old NOD/SCID mice (NOD.CB17-Prkdcscid, The Jackson Laboratory). Tumor growth was measured over time using calipers. Matched mice carrying ADNP knockdown and control xenografts were sacrificed when knockdown tumors reached volumes of 500-900 mm^3. For *in vivo* treatment studies, subcutaneous xenografts were grown as described above using SW1222, HCT116, or primary colon cancer cells. Mice were randomly assigned to control or treatment groups when tumor volumes reached 100 mm^3. Ketamine (20 mg/kg in PBS) or as control PBS were administered daily intraperitoneally until tumors reached volumes of 1000-1300 mm^3.

Single clone expanded T84 or P-Tu colon cancer cells, either native or carrying the respective lentiviral constructs described above, were suspended in 100 µl of a 1:1 mixture of PBS and growth factor-depleted Matrigel (Corning), and injected subcutaneously into 6-8 week old

NOD/SCID mice for xenograft formation. In pLenti CMV rtTA3G Blast and pLenti CMVTRE3G-caMEK Puro transduced T84 colon cancer cell-derived xenografts, caMEK expression was induced with 1 mg doxycycline (dissolved in aqua ad injectabilia) in *p.o.* For lineage tracing, pLenti lox-mCh- LacZ and pLenti PGK-GFP-CreERT2 or pLenti SRE-GFP-CreERT2 transduced P-Tu colon cancer cell-derived xenografts were treated once with 3 mg tamoxifen (dissolved in 10% ethanol and 90 % sunflower oil) by *i.p.* injection. Treatments were done when tumor diameters reached 7 mm. Non-treated tumors were included as controls. Mice were sacrificed and tumors were removed 4 days after caMEK induction, and 2 or 21 days for short and long term lineage tracing experiments, respectively. All xenograft tumors were formalin fixed and paraffin embedded for further analyses.

4. Results

4.1. Identification of ADNP as a repressor of WNT signaling in colon cancer

The results presented in this section are part of the following publication:

Blaj, C., Bringmann, A., Schmidt, E.M, Urbischek, M., Lamprecht, S., Fröhlich, T., Arnold, G., Krebs, S., Blum, H., Hermeking, H., Jung, A., Kirchner, T., Horst, D. ADNP is a therapeutically inducible repressor of WNT signaling in colorectal cancer. *Clinical Cancer Research*, 2016 Nov 30.

4.1.1. ADNP is overexpressed in colon cancer cells with high WNT signaling activity

To identify transcription factors that are linked to WNT signaling in colon cancer, we comparatively analyzed three previously published gene expression profiles of colon cancer cell subpopulations with low and high WNT activity (Horst et al., 2012a; Louis Vermeulen et al., 2010). Among few genes that were consistently upregulated in tumor cells with high WNT signaling, we identified *ADNP* as the only overexpressed gene encoding a transcription factor (Table 8). Direct comparison confirmed that increased *ADNP* expression coincided with high WNT target gene expression and, conversely, with repression of genes linked to tumor cell differentiation (Figure 8 A). We then analyzed an independent data set of 41 normal mucosa samples and 457 colon cancers from The Cancer Genome Atlas (TCGA) by Gene Set Enrichment Analyses (GSEA), and found that *ADNP* mRNA expression on average was 2.73 fold increased in colon cancer compared to normal mucosa, and that ADNP in colon cancer samples strongly correlated with genes enriched for WNT target gene signatures (Figure 8 B; 2). On the protein level, ADNP was overexpressed at the infiltrative tumor edge of colorectal cancers, where it co-localized with strong nuclear β-catenin expression, a marker for colon cancer cells with high WNT activity (Figure 8 C-E). Moreover, in adenomas of FAP patients (n=23 adenomas), known to carry *APC* gene mutations (Smith et al., 1993), ADNP was overexpressed when compared to normal mucosa (Figure 8 C). In addition, even in normal mucosa, epithelial cells at the crypt base, where WNT activity is increased (Humphries & Wright, 2008), showed slightly increased ADNP expression (Figure 8 F). These findings demonstrated consistent upregulation of ADNP in colorectal cancer cells and precursor lesions with high WNT activity on mRNA and protein levels, and suggested a possible regulation of ADNP by WNT.

Table 8. Fold change (F.C.) of consistently deregulated genes in three gene expression data sets of colon cancer cells with high vs. low WNT activity, and F.C. in differential expression of these genes in TCGA data in colon cancer vs. normal mucosa. P values are t test results**.**

	WNT high vs. low dataset		**TCGA dataset**	
Gene symbol	**F.C.**	***P* value**	**F.C**	***P* value**
INHBB	4.19	0.00005	0.42	0.03477
DPEP1	4.01	0.00039	0.6	0.00344
FN1	3.11	0.00794	0.67	0.19989
ITPR2	2.76	0.00003	1.16	0.43835
DRAM1	2.75	0.0009	1.82	<0.00001
KIF3C	2.48	0.00013	1.32	0.18091
KRT23	2.38	0.00021	0.6	0.00018
PROM1	2.04	0.0002	1.01	0.82154
RGS19	2	0.00064	1.37	0.60719
APOBEC3B	1.95	0.00226	1.5	<0.00001
TCTN1	1.91	0.00284	2.34	<0.00001
ANXA9	1.9	0.00001	1.31	<0.00001
VSNL1	1.86	0.00135	1.14	<0.00001
EML1	1.79	0.04144	0.97	<0.00001
FLNA	1.78	0.00012	0.93	<0.00001
SORBS1	1.77	0.01099	0.87	<0.00001
BCAS3	1.76	0.00219	2.13	0.16157
CEP68	1.71	0.00561	2.35	0.07352
SESN1	1.61	0.00002	1.04	0.00226
SEPT6	1.59	0.00061	1.72	<0.00001
SEZ6L2	1.56	0.00294	1.35	<0.00001
H2AFJ	1.53	0.00221	1.47	0.25736
TTLL5	1.43	0.00167	3.34	0.00099
MSRB2	1.42	0.01328	2.19	0.46093
HYAL2	1.36	0.00463	1.62	<0.00001
CCNF	1.35	0.00203	2.35	<0.00001
CDC45	1.33	0.00322	2.51	<0.00001
SUPT7L	1.29	0.00539	4.2	<0.00001
GINS1	1.29	0.00009	1.75	<0.00001
VPS54	1.24	0.00001	2.91	0.1922
VPS13B	1.22	0.00259	2.3	0.02021
ADNP	1.1	0.0015	2.73	<0.00001
PLCE1	0.7	0.00017	1.61	<0.00001
FA2H	0.67	0.00024	1.79	0.00141
SULT1B1	0.6	0.00004	0.96	<0.00001
RARRES1	0.58	0.00007	0.57	0.01459
SPINK5	0.45	0.01115	0.7	<0.00001
GCNT3	0.43	0.00179	0.71	<0.00001
FCGBP	0.41	0.00084	0.52	<0.00001

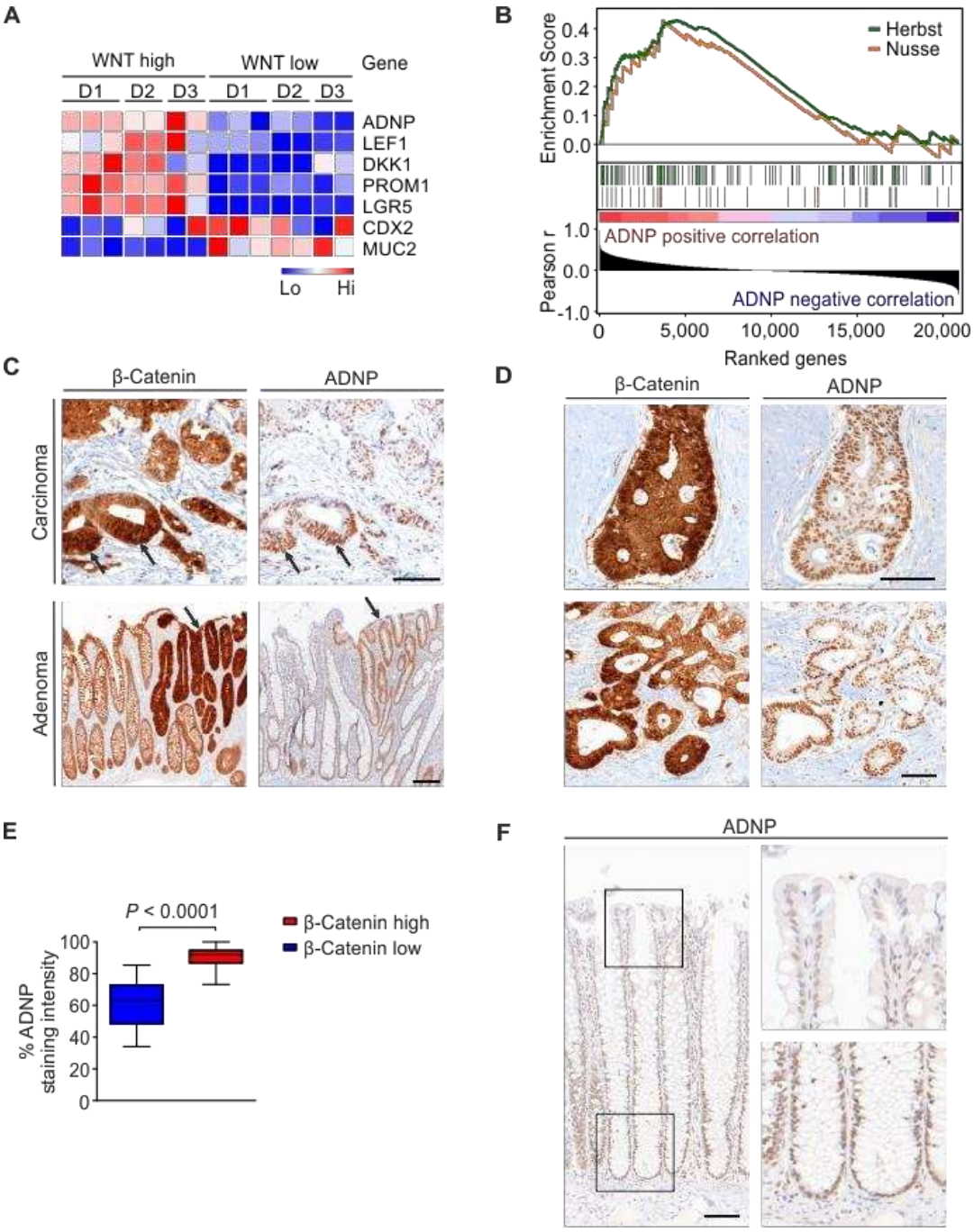

Figure 8. ADNP is overexpressed in colon cancer cells with high WNT activity (A) Heat maps of *ADNP*, selected WNT targets and differentiation factors in these three data sets (D1-D3) of colon cancer cells with high and low WNT activity. (B) GSEA for genes ranked by Pearson correlation (Pearson r) to ADNP expression for two WNT target gene signatures by Herbst et al. (*green curve*: NES = 1.70, $P < 0.001$) and Nusse et al. (*orange curve*: NES = 1.36, $P = 0.09$) in 457 RNA-Seq data sets of colon cancer from TCGA. (C) Immunohistochemistry on serial sections of colon cancer (*upper panels*; scale bar, 100 µm) and a colonic adenoma of an FAP patient (*lower panels*; scale bar, 200 µm) illustrate upregulation of ADNP in areas with increased β-catenin staining (*arrows*). (D) Immunostaining for ADNP and β-catenin on serial sections of two colon cancers. (E) Staining intensities of ADNP in colon cancer cells (n = 500, 5 different tumors) with high or low nuclear β-Catenin

expression. P value is t test result. (C) Immunostaining for ADNP in normal mucosa. Right panels are magnifications of areas boxed in left panel. Scale bars, 100 µm.

In order to test if ADNP expression directly responds to WNT, we stimulated WNT signaling in HEK293 cells by the GSK3β inhibitor lithium chloride (LiCl) or by WNT3A, and then evaluated ADNP mRNA and protein levels. Surprisingly, although TOPflash luciferase assays and overexpression of β-catenin and AXIN2 indicated strong induction of WNT signaling, there were no significant effects on ADNP expression (Figure 9 A-B). Also, suppressing WNT activity by silencing β-catenin in colorectal cancer cell lines had no significant impact on ADNP protein levels (Figure 9 C). Hence, while ADNP expression strongly coincided with WNT signaling activity in colon cancer, it apparently is no direct WNT target gene.

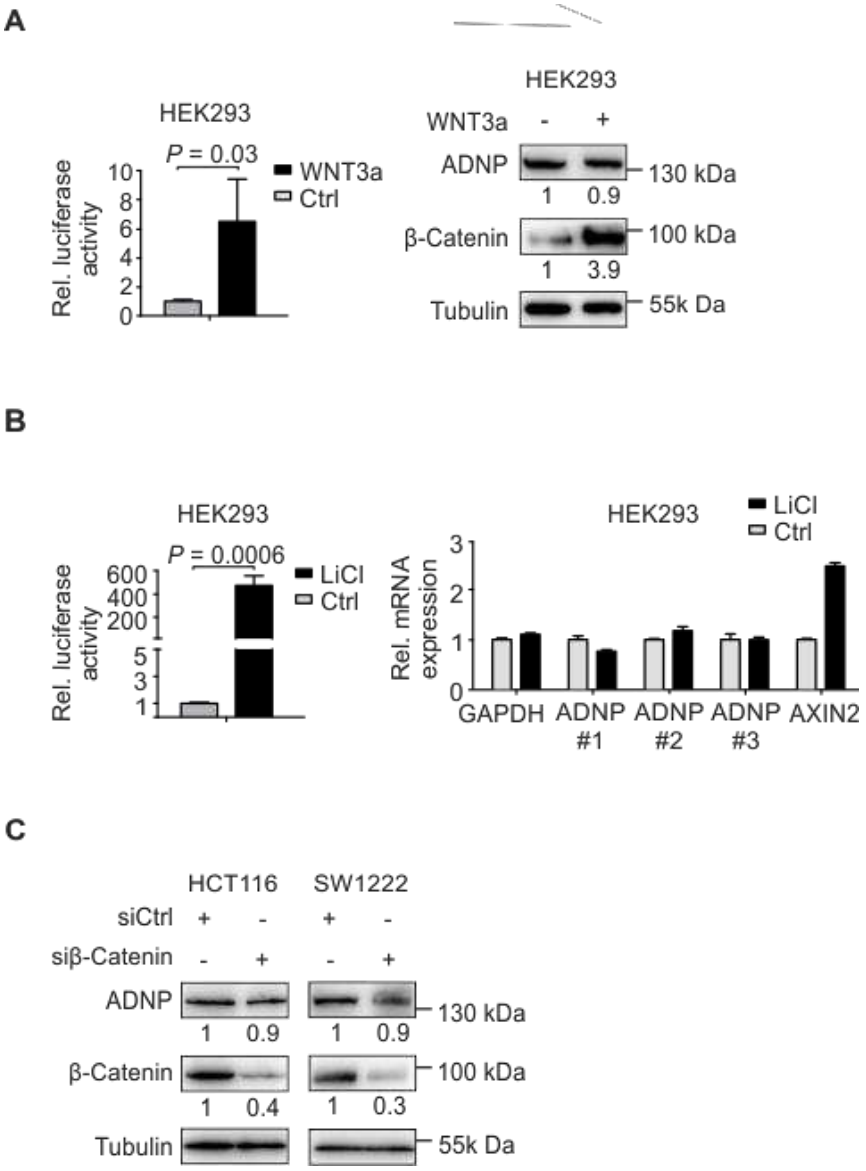

Figure 9. ADNP is not affected by WNT manipulation. (A, B) Dual-luciferase assays with TOPflash reporter constructs, immunoblotting, and qRT-PCR results on indicated proteins or genes after stimulation of HEK293 cells with LiCl (A) or WNT3A (B). P values are t test results, data are mean ± SD, n ≥ 3. (C) Immunoblotting of indicated proteins after transfection of HCT116 and SW1222 colon cancer cells with siRNA against β-Catenin. Numbers below immunoblots indicate fold change by densitometry.

4.1.2. ADNP is a repressor of WNT signaling in colon cancer

To obtain initial insights into ADNP function in colorectal cancer, we next analyzed the effects of ADNP knockdown on gene expression in HCT116 colon cancer cells using RNA-seq. Depletion of ADNP by siRNA caused 1.4 fold or more deregulation of 4.82 % of the transcriptome. Interestingly, upregulated genes were significantly more frequent than downregulated genes (3.69 % vs. 1.13 %, $p<0.0001$), suggesting predominantly repressive functions of ADNP on the transcriptome (Figure 10 A). To identify potential targets of ADNP repression, we therefore focused on genes that were upregulated by ADNP knockdown and screened them for functional and pathway associations using the PANTHER analysis tool. Surprisingly, these analyses revealed that WNT signaling was the pathway most prominently related to genes affected by ADNP depletion (Figure 10 B). We therefore compared our gene expression data set with WNT target gene signatures using GSEA, and found that indeed upregulated WNT target genes were significantly enriched upon ADNP depletion (Figure 10 C), with overexpression of typical WNT targets such as *DNMT1*, *CD44*, *AXIN2* and *TCF7* (Figure 10 D). These findings suggested repression of WNT signaling by ADNP.

Next, to determine effects on the proteome level, we used mass spectrometry analysis and identified deregulated proteins after ADNP silencing. Consistent with our transcriptome data, we found that upregulated proteins were significantly more abundant than downregulated proteins (2.8% vs. 1.43%, $p<0.0001$, Figure 10 E). Furthermore strong correlation between our transcriptome and proteome results among 58 factors that were significantly deregulated in both data sets indicated consistency within these analyses (Pearson $r^2=0.52$, $P=0.001$, data not shown). Among proteins that showed most significant upregulation were the WNT target DNMT1, a known driver of cell proliferation and interaction partner of β-Catenin, as well as Talin-1, a recently identified key node of WNT signaling with roles in cell migration, invasion, and angiogenesis of human cancers (Figure 10 F, Table 9) (Bayerlová et al., 2015; Bostanci et al., 2014).

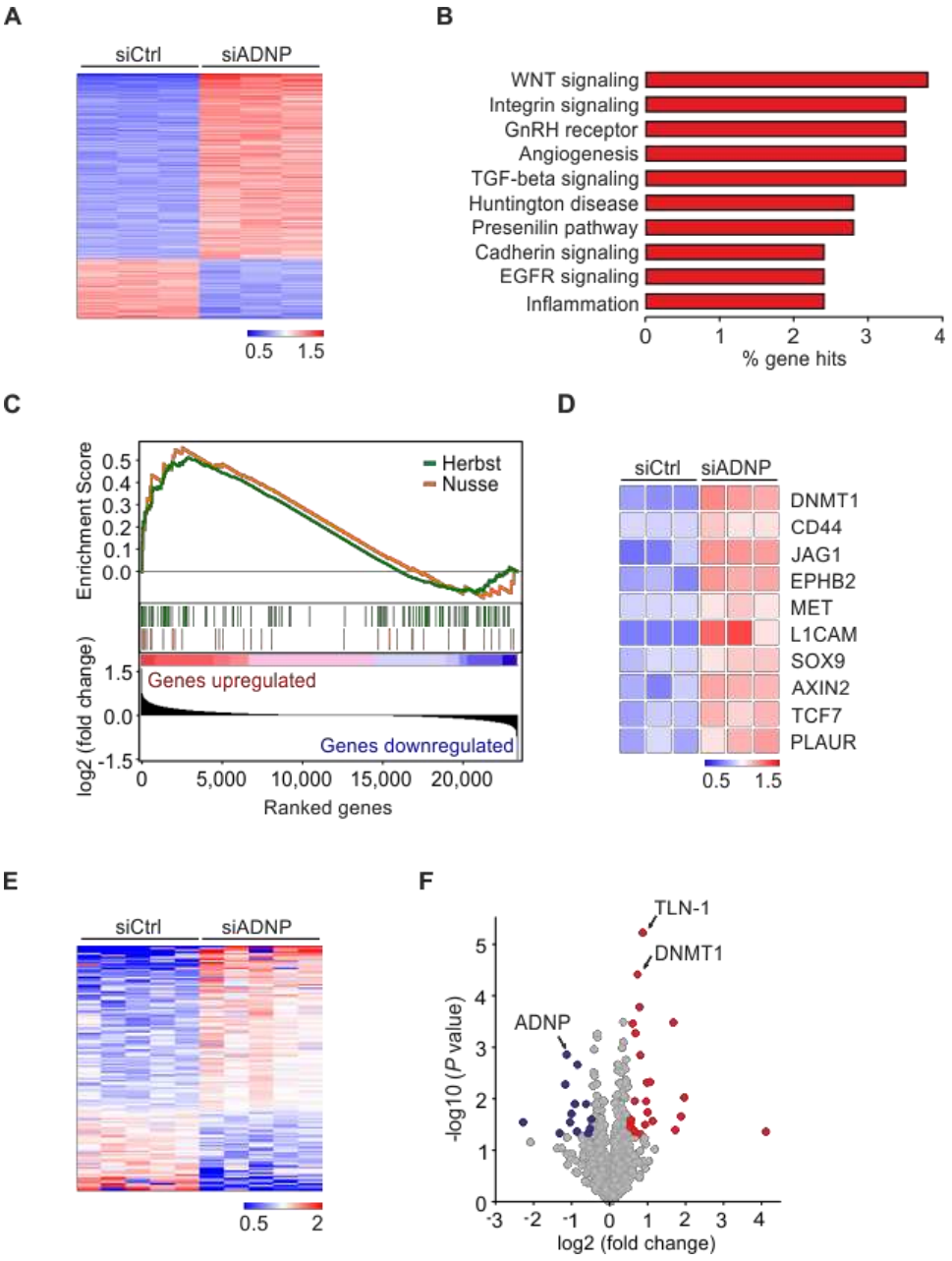

Figure 10. ADNP depletion shows de-repressive effects on transcriptome, proteome and WNT signaling in colon cancer cells. (A-D) Gene expression analyses for ADNP knockdown in HCT116 cells. (A) Heat map results of genes with significantly ($P < 0.05$) differential expression and 1.4 or more fold change. Rows represent gens and columns represent biological replicates. (B) Top ten results of PANTHER analysis showing frequencies of upregulated genes linked to pathways indicated. (C) GSEA with genes ranked by fold change for WNT target gene signatures by Herbst et al. (*green curve*: NES = 1.54, $P < 0.001$) and Nusse et al. (*orange curve*: NES = 1.36, $P = 0.04$). (D) Heat map of selected WNT targets among differentially expressed genes. (E, F) Proteome analyses for ADNP knockdown in HCT116 cells. (E) Heat map results of proteins with significant ($P < 0.05$) differential expression. Rows represent proteins and columns represent biological replicates. (F) Volcano plot of protein expression. *Red* and *blue* dots indicate proteins with significant up- or downregulation ($P < 0.05$; abs. fold change >1.5), respectively. *Arrows* highlight most significantly deregulated proteins. Legends on heat maps indicate fold change

Table 9. Proteome analysis results upon ADNP depletion. Proteins with significant up- or downregulation are listed (P < 0.05; abs. fold change >1.5)

Gene symbol	fold change	*P* value
SCAMP1	17.3	0.04499
RBP1	3.87	0.00969
PFDN1	3.65	0.02272
CBFB	3.29	0.04149
PPP1R14B	3.18	0.00034
ATP5I	2.18	0.02753
IPO11	2.06	0.00486
CLIC4	1.98	0.01883
MOV10	1.95	0.00502
HMGCS1	1.93	0.01151
MSI1	1.89	0.00327
TLN1	1.81	6.1E-06
TBCD	1.75	0.04971
YWHAH	1.73911	0.00148
DSP	1.71421	0.00017
DNMT1	1.65193	0.00004
MTPN	1.59213	0.00055
DCBLD2	1.57902	0.04529
CRABP2	1.56989	0.01137
KIF2A	1.52558	0.04091
ALDH9A1	1.51196	0.00036
GLRX5	0.64654	0.01303
POLR2G	0.55182	0.00224
SMAP	0.54448	0.04437
ASF1B	0.52641	0.01293
HINT2	0.49374	0.02004
DYNC1I2	0.48191	0.02935
ADNP	0.45216	0.00144
UBQLN4	0.44124	0.00544
NAPRT1	0.39740	0.04786
THRAP3	0.20366	0.02930

We further addressed the effects of ADNP on WNT signaling in HCT116 and SW1222 colon cancer cells *in vitro*. In both cell lines ADNP silencing increased expression of active-β-catenin and the WNT target genes DNMT1, AXIN2 and LEF1 (Figure 4A). Immune fluorescence of HCT116 cells confirmed these results with cytoplasmic and membranous, or nuclear increase of AXIN2 and DNMT1, respectively (Figure 4B). In addition, upon ADNP

silencing, both cell lines showed elevated WNT activity when assessed by TOPflash luciferase reporter assays (Figure 11 C). In contrast, overexpression of ADNP reduced β-catenin and LEF1 (Figure 11 D), and repressed WNT signaling in TOPflash assays (Figure 11 E). These results further corroborated the hypothesis, that ADNP negatively regulates WNT signaling in colorectal cancer with repression of factors related to cell proliferation and other malignant traits of colorectal cancer cells.

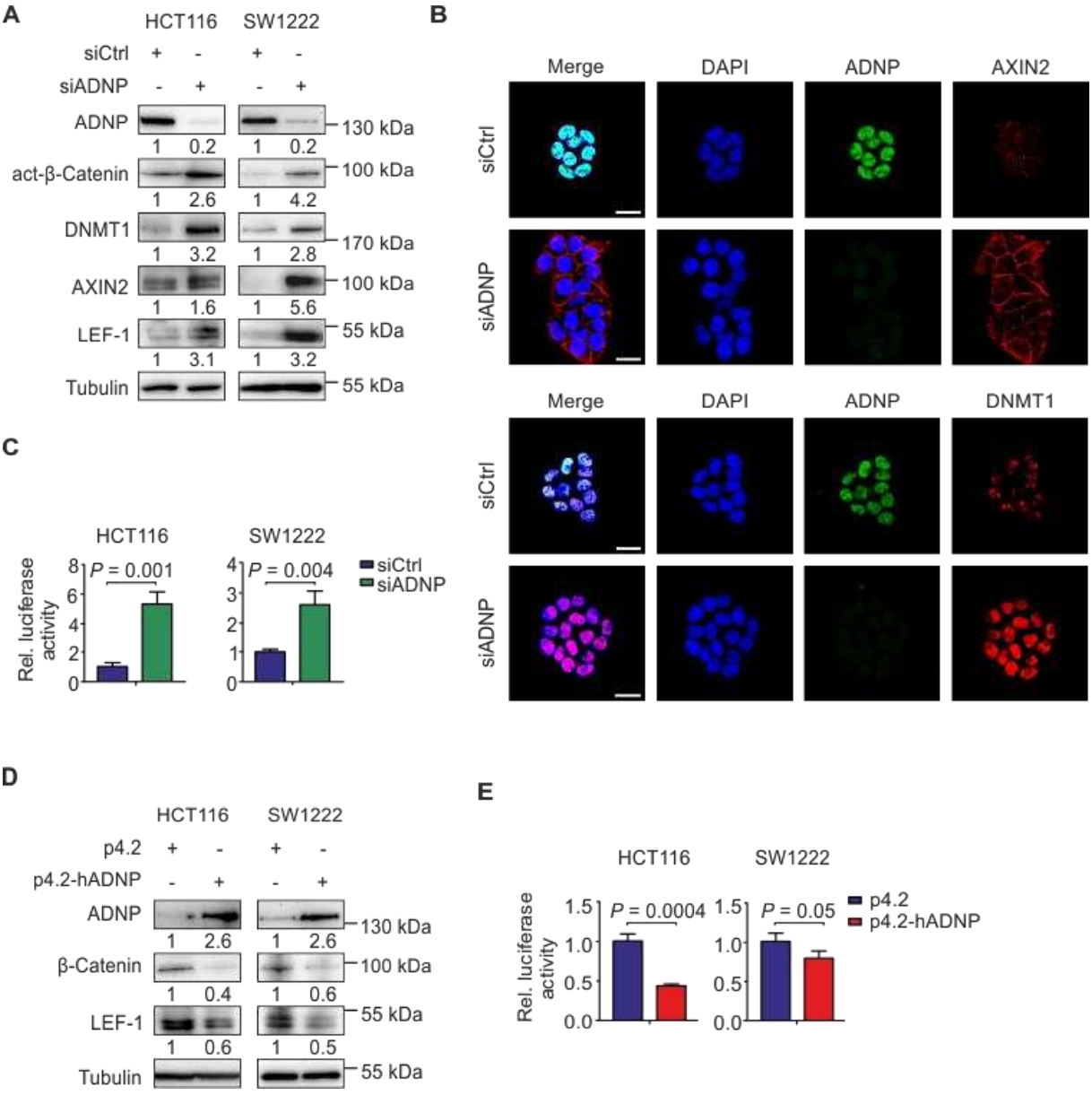

Figure 11. ADNP represses WNT signaling in colon cancer *in vitro*. (A-C) Effects of ADNP or control (Ctrl) knockdown by siRNA on HCT116 and SW1222 colon cancer cells, harvested 48 h after transfection. (A) Immunoblotting of indicated proteins on whole cell lysates. (B) Representative confocal immunofluorescence

images of HCT116 cells for indicated proteins and DAPI as nuclear counterstain. Scale bars, 20 µm. (C) Dual-luciferase assays for HCT116 and SW1222 colon cancer cells, simultaneously transfected with indicated siRNAs and TOPflash reporter constructs. (D, E) Effects of transient ADNP overexpression by transfection of HCT116 and SW122 with p4.2-hADNP compared to empty p4.2 vector for 24 h. (D) Immunoblotting of indicated proteins on whole cell lysates. (E) Dual-luciferase assays for HCT116 and SW1222 colon cancer cells, simultaneously transfected with p4.2-hADNP or p4.2 and TOPflash reporter constructs. Numbers below immunoblots indicate fold change by densitometry. *P* values are t test results, data are mean ± SD, $n \geq 3$.

4.1.3. ADNP represses malignant traits and tumor growth of colon cancer

Because WNT and its associated factors DNMT1 and Talin-1 are known to regulate proliferation, migration and invasion of colorectal cancer (Bayerlová et al., 2015; Bostanci et al., 2014), we tested the functional relevance of ADNP loss for these malignant traits in HCT116 and SW1222 colon cancer cells. We depleted ADNP by two different shRNAs, and also generated ADNP knockout cells by CRISPR/Cas9 genome editing (Figure 12 A, Figure 13 A). Importantly, ADNP depletion or knockout caused dramatic increases in transwell cell migration and invasion of both colon cancer cell lines as determined by Boyden chamber assays (Figure 12 B-C, Figure 13 C). Of note these effects could be counteracted in ADNP knockout cells by concomitant depletion of β-Catenin, DNMT1, or Talin-1 (Figure 13 B- D).

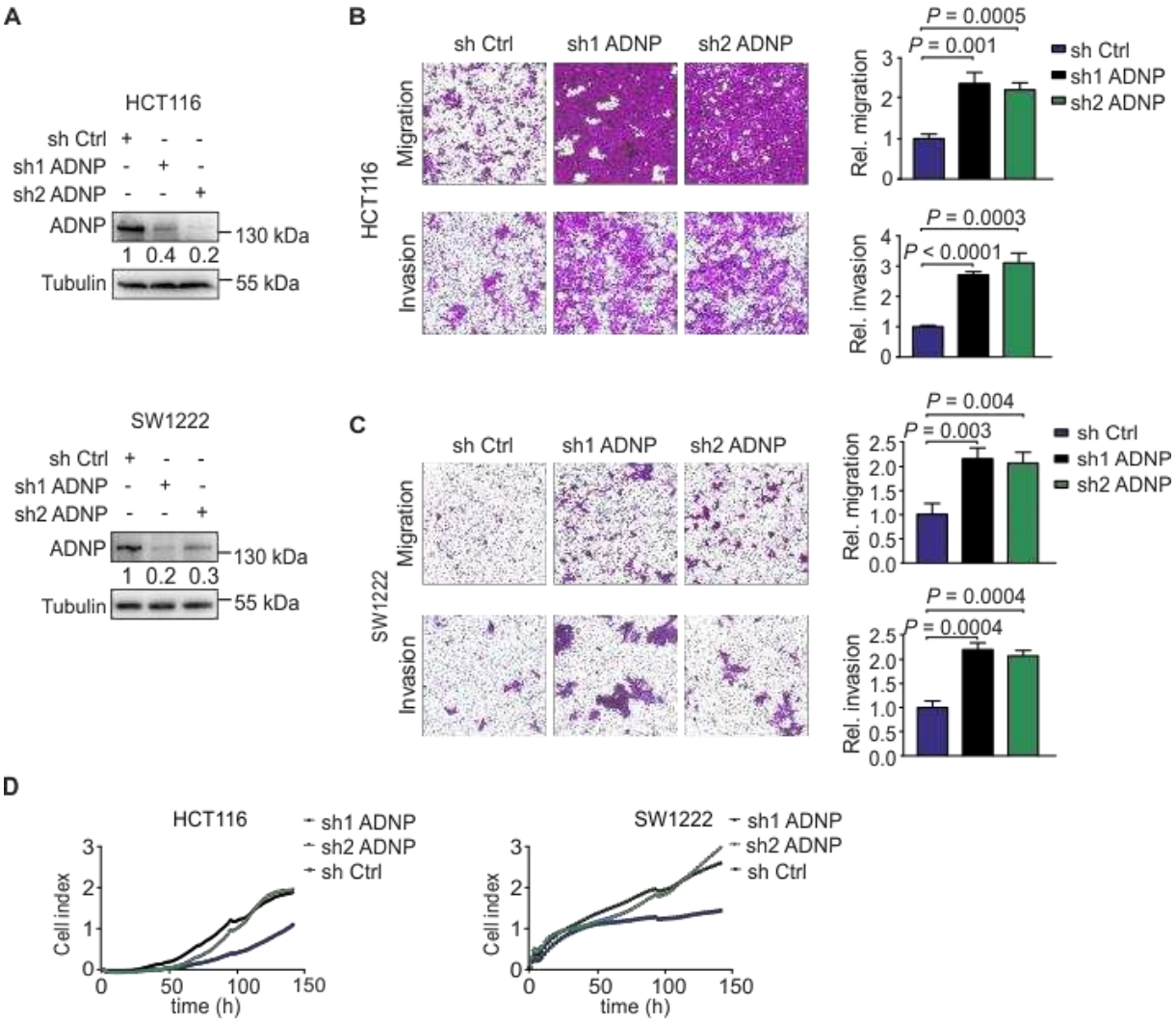

Figure 12. ADNP depletion increases migration, invasion and proliferation of colon cancers cells *in vitro*. (A-D) Effects of stable ADNP depletion by two different shRNAs against ADNP (sh1/2 ADNP) versus unspecific control shRNA (sh Ctrl) on HCT116 and SW1222 colon cancer cells. (A) Immoblotting for indicated proteins. Numbers below immunoblots indicate fold change by densitometry. (B, C) Representative micrographs (*left panels*) and quantification (*right panels*) of migrated or invaded tumor cells in transwell assays for indicated cell lines. (D) Representative proliferation kinetics based on cell quantification by impedance measurements. Data are mean, n ≥ 3, *P* values are t test results.

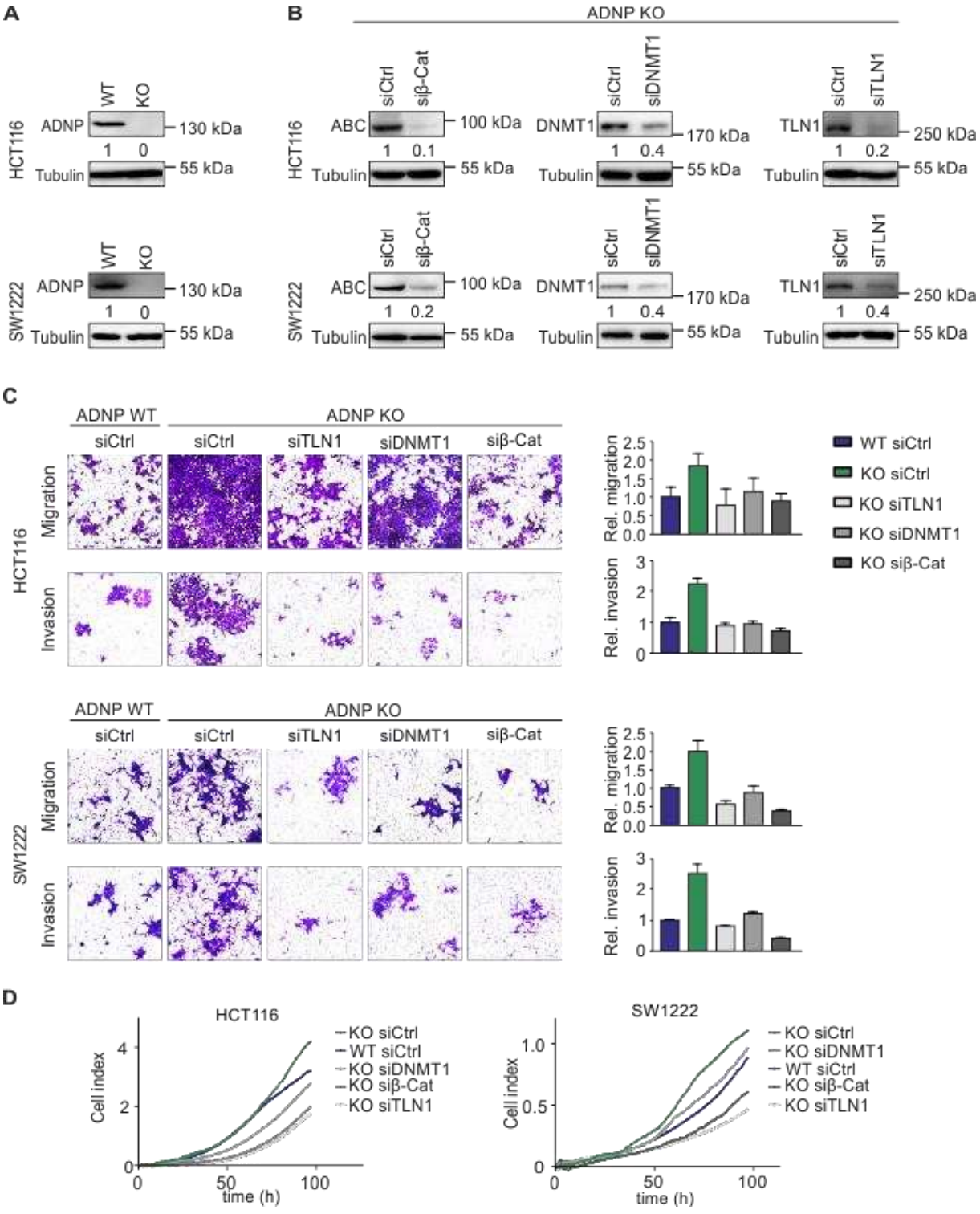

Figure 13. Depletion of β-Catenin, DNMT1, or TLN-1 conteracts the effects of the ADNP kockout. (A-B) Immunoblotting of indicated proteins on whole cell lysates in ADNP wild-type (WT) or knockout (KO) cell lines. Numbers below immunoblots indicate fold change by densitometry. (C) Representative micrographs (left panels) and quantification (right panels) of migrated or invaded tumor cells in transwell assays for indicated ADNP WT and KO cell lines, treated with indicated siRNAs or control siRNA (siCtrl). (D) Representative proliferation kinetics based on cell quantification by impedance measurements. Data are mean, n ≥ 3. β-Cat = β-catenin.

In addition, ADNP depletion or knockout significantly increased cell proliferation of both cell lines as determined by impedance measurements (Figure 12 D, Figure 13 D). Moreover, ADNP overexpression showed opposite effects on invasion and migration (Figure 14).

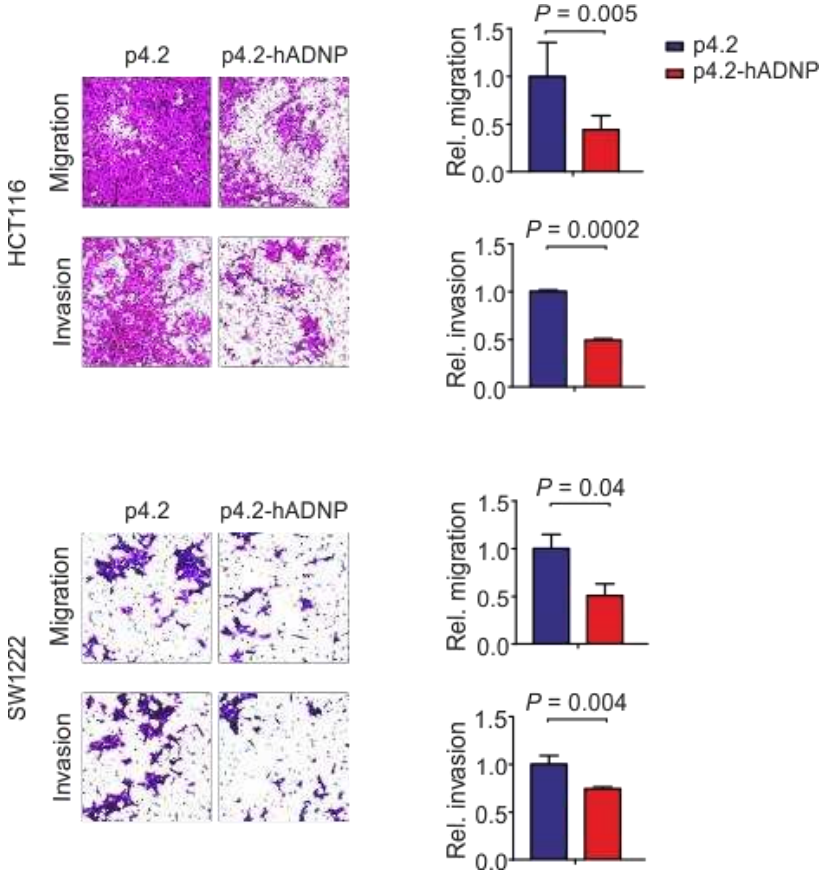

Figure 14. ADNP overexpression inhibits migration and invasion *in vitro*. Representative micrographs (left panels) and quantification (right panels) of migrated or invaded HCT116 or SW1222 tumor cells with transient ADNP overexpression by transfection with p4.2-hADNP compared to empty p4.2 vector for 24 h in transwell assays.

To further assess effects *in vivo*, we then injected $8x10^6$ SW1222 cells with and without stable ADNP knockdown subcutaneously into flanks of NOD/SCID mice and measured tumor growth over time. In line with our *in vitro* data, tumor xenografts derived from SW1222 cells with ADNP knockdown grew significantly faster, yielding larger tumors, with darker color due to increased intratumoral hemorrhage, when compared to tumor xenografts with normal ADNP levels (Figure 15 A). Immunohistochemical staining of these tumors for Ki67 revealed that proliferation was increased upon ADNP knockdown *in vivo*, explaining these observed differences in tumor growth and size (Figure 15 B). Taken together, these data showed strong effects of ADNP depletion on migration, invasion and proliferation of colon cancer cells *in*

vitro as well as tumor growth *in vivo*, and suggested a tumor suppressor function of ADNP through repression of WNT signaling in colorectal cancer.

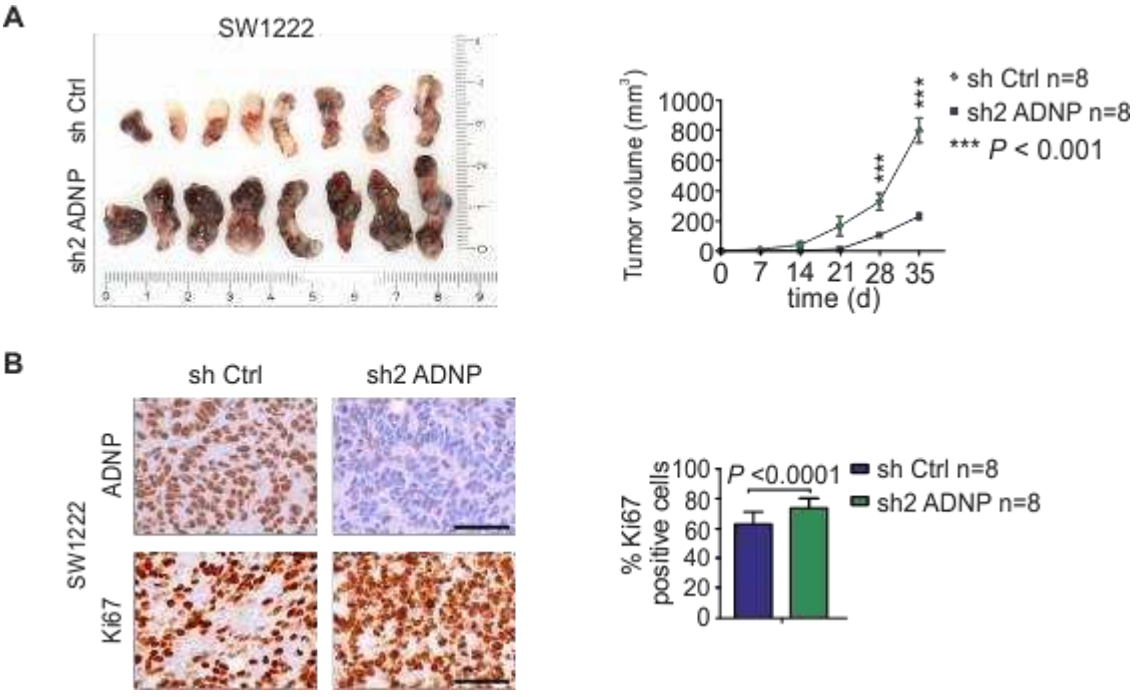

Figure 15. ADNP depletion increases *in vivo* tumor growth of colon cancers. (A, B) Effects of stable ADNP depletion (sh2 ADNP, n = 8) compared to control transduction (sh Ctrl, n = 8) of SW1222 colon cancer cells on xenograft tumor growth *in vivo*. (A) Photograph and growth curves of SW1222 colon cancer xenografts transduced with indicated shRNA constructs. *P* values are t test results, data are mean ± SE. (B) Immunohistochemistry for ADNP and the proliferation marker Ki67, and quantification of Ki67 in xenograft tumors. Data are mean ± SD, *P* values are t test results, n = 8. Scale bars, 50 µm.

4.1.4. Induction of ADNP by sub-narcotic ketamine suppresses tumor growth *in vivo*

Previous studies indicated that ADNP expression can be pharmacologically induced by sub-narcotic doses of ketamine in cortical neurons (Brown et al., 2015; Turner et al., 2012). Exploiting this potential, we treated colon cancer cell lines and primary colon cancer cells, which had high endogenous WNT activity (Figure 16 A-B), with low dose ketamine and observed slight but steady increases of ADNP protein levels by immunoblotting (Figure 16 C). To determine the effects of ketamine-induced ADNP induction on WNT signaling, we then subjected these cell lines and primary colon cancer cells to TOPflash luciferase assays

and indeed observed significant reductions in WNT activity under ketamine treatment (Figure 16 D).

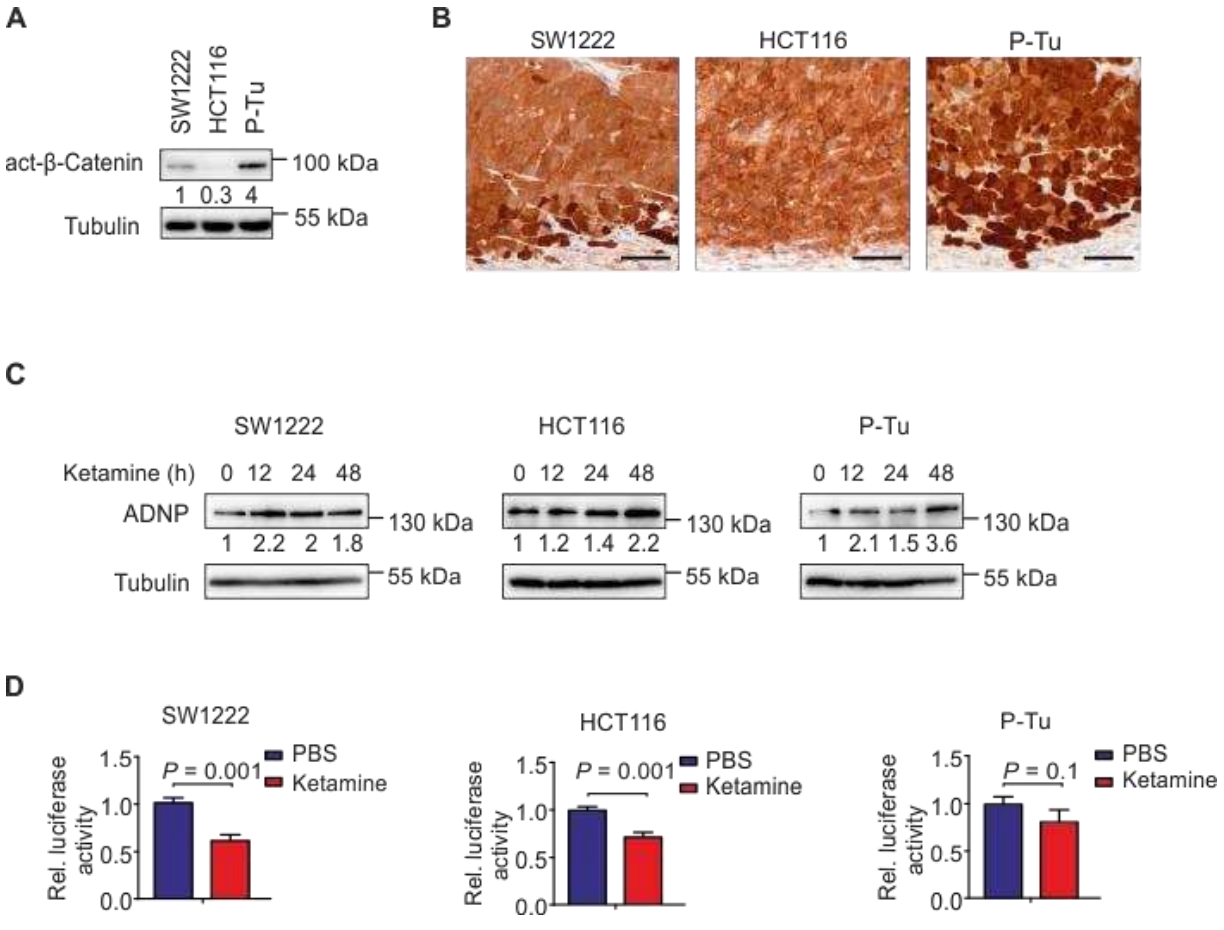

Figure 16. Low dose ketamine induces ADNP and represses WNT activity (A) Immunoblotting of indicated proteins on whole cell lysates of SW1222, HCT116 cell lines and primary colon cancer (P-Tu) cells. Numbers below immunoblots indicate fold change by densitometry. (B) Immunostaining of SW1222, HCT116 and primary colon cancer (P-Tu) xenografts for β-Catenin. Scale bars, 50 µm. (C, D) Effects of *in vitro* treatment of SW122, HCT116, and primary colon cancer cells (P-Tu) with 100 µM ketamine. (C) Immunoblotting for indicated proteins on indicated time points after addition of ketamine to culture media. Numbers below immunoblots indicate fold change by densitometry. (D) Dual-luciferase assays for indicated colon cancer cells transfected with TOPflash reporter constructs under treatment with ketamine or PBS as control. Data are mean ± SD, *P* values are t test results, $n \geq 3$.

Importantly, these relative repressive effects of ketamine on WNT activity were decreased in ADNP knockout cell lines, while the effects of a direct WNT inhibitor (XAV939) remained unchanged, suggesting that WNT repression by ketamine in part depended on ADNP induction (Figure 17 A-B).

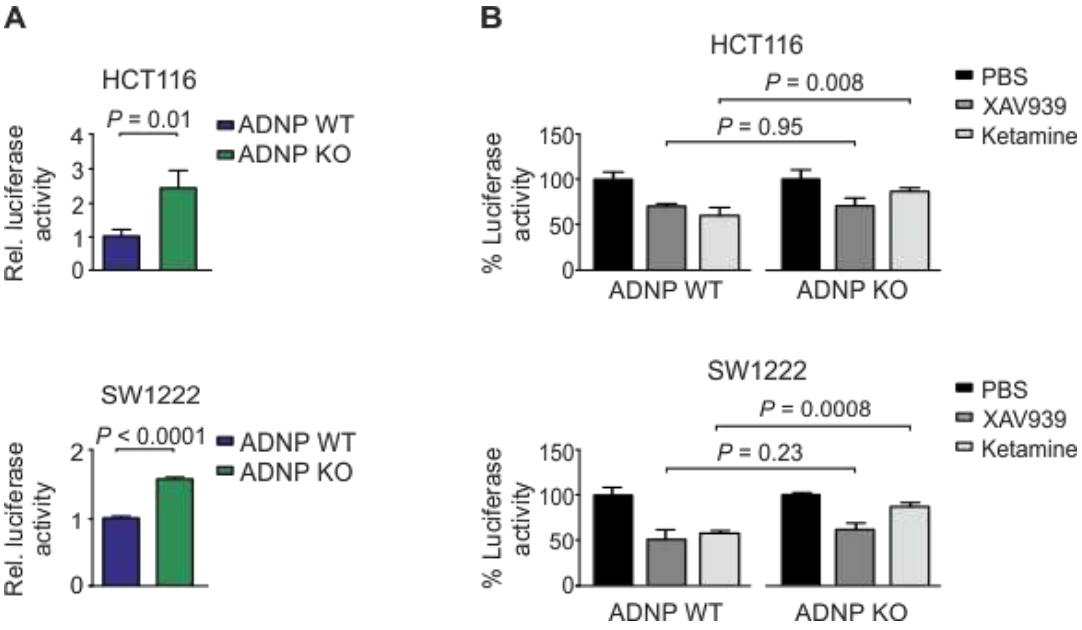

Figure 17. WNT repression by ketamine partially depends on ADNP induction (A-B) Dual-luciferase assays for indicated ADNP wild-type (WT) or knockout (KO) colon cancer cells transfected with TOPflash reporter constructs. Treatments with PBS, ketamine or the WNT inhibitor IWP-2, as indicated.

Additionally, similar to the effects of ADNP overexpression, ketamine reduced migration and invasion of colon cancer cells (Figure 18).

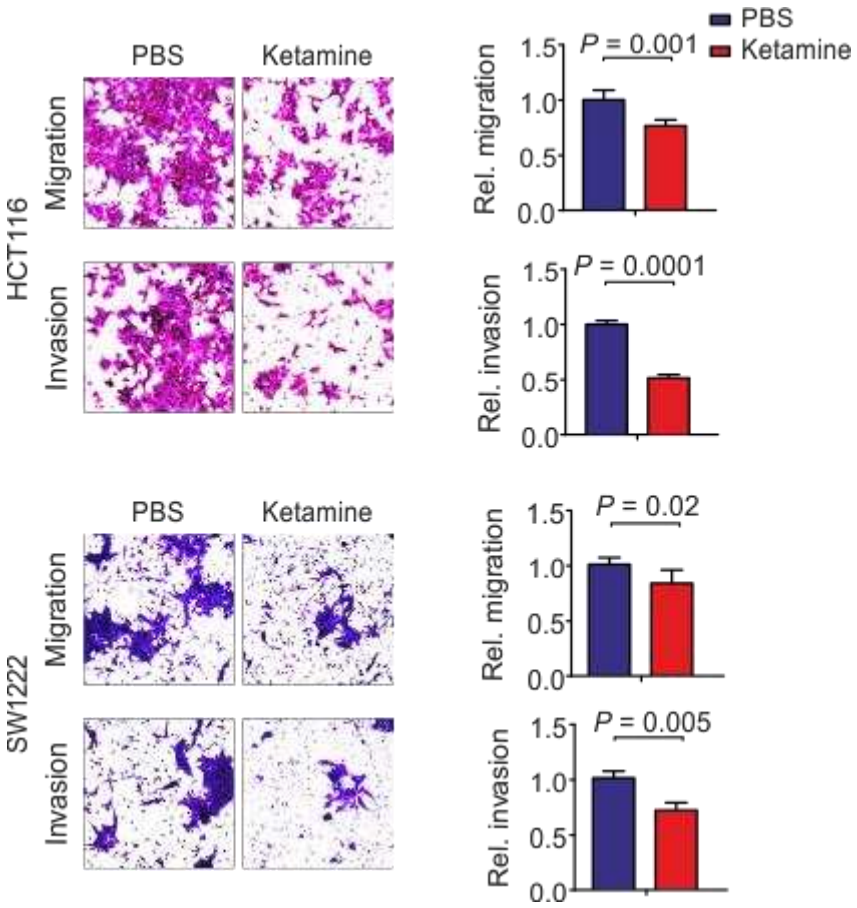

Figure 18. Ketamine reduced migration and invasion of colon cancer cells *in vitro*. Representative micrographs (left panels) and quantification (right panels) of migrated or invaded HCT116 or SW1222 tumor cells in transwell assays, treated with PBS or 200 µM ketamine for 24 h, as indicated. Data are mean ± SD, P values are t test results, $n \geq 3$.

Next, we treated NOD/SCID mice bearing colon cancer cell line or primary colon cancer xenografts with sub-narcotic doses of ketamine and observed tumor growth over time. Ketamine treatment significantly slowed tumor growth (Figure 19 A) and prolonged tumor survival (Figure 19 B). These findings implicate that, through induction of ADNP and WNT repression, sub-narcotic doses of ketamine can inhibit colorectal cancer growth and tumor progression *in vivo*.

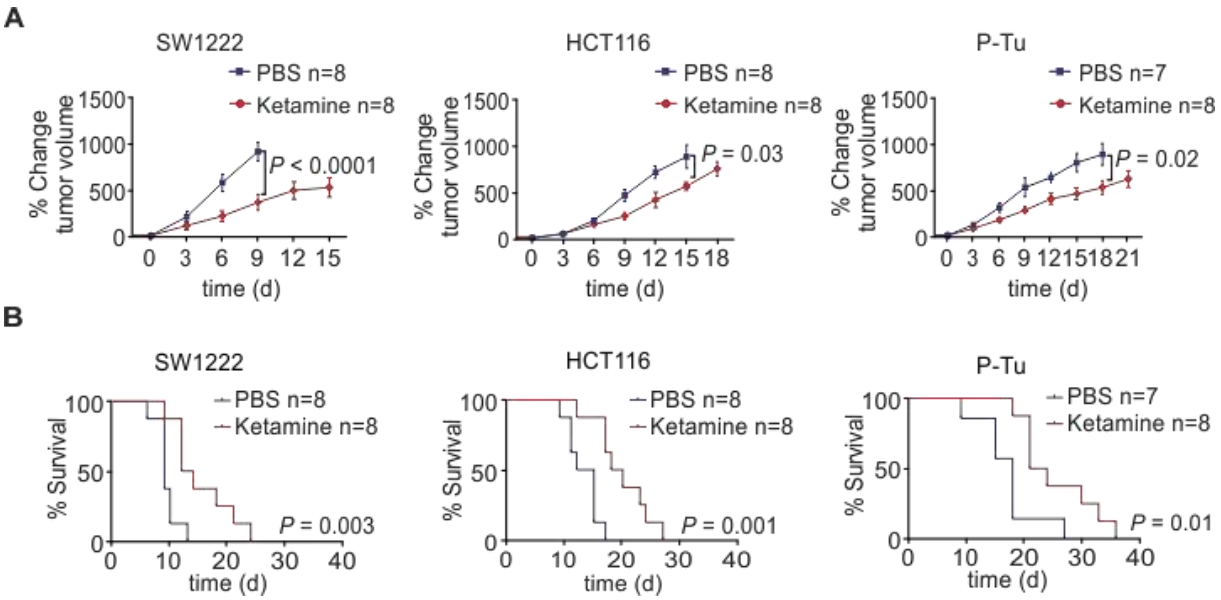

Figure 19. Low dose ketamine slows tumor growth of colon cancer xenografts. (A, B) Impact of daily treatment with ketamine (20 mg/kg) or PBS as control on xenograft growth of indicated colon cancer cells or primary colon cancer (P-Tu), shown as growth curves (A) and tumor specific survival in Kaplan-Meier plots (B). *P* values are t test results and data are mean ± SE in (A) or log-rank test results in (B).

4.1.5. High ADNP expression predicts good outcome of colorectal cancer patients

Finally we tested for ADNP expression and disease outcome of colorectal cancer patients. Using immunohistochemistry, we scored overall ADNP expression in a collection of 221 stage I and II human colorectal cancers with recorded clinical follow-up data. ADNP expression varied substantially between cases, ranging from negative or barely detectable (score 0) to strong expression (score 3, Figure 20 A, Table 10). Using Kaplan-Meier statistics, we found that differential ADNP expression was strongly linked to cancer specific survival. All patients with strong ADNP expression completely survived their follow-up period (score 3, five-year survival rate 100 %). In contrast, moderate (score 2, five-year survival rate 88.7 %), weak (score 1, five-year survival rate 78.2 %), and barely detectable or negative ADNP expression (score 0, five-year survival rate 60.4 %) were significantly linked to cancer specific deaths at increasing frequencies (Figure 21 A). Testing for disease free survival yielded comparable, yet slightly less stark results (Figure 21 A). We then categorized ADNP expression into low (scores 0 and 1) and high (scores 2 and 3), and tested for an overall association with β-catenin expression levels. Although not significant, high ADNP expression tended to be more frequent in cases with high nuclear β-catenin (Table 10).

Interestingly however, high and low ADNP expression separated survival probabilities particularly well in the subset of colorectal cancer cases with high nuclear β-catenin expression (Figure 21B). We then evaluated co-occurrences of ADNP expression and other clinical/pathological variables and found that T-stages were significantly associated with different ADNP expression scores, with a tendency of lower T-stages linked to higher ADNP expression. Also low tumor grade tended to associate with low ADNP expression, while the other core clinical variables age and sex were not linked to ADNP (Table 10). Including these variables and β-catenin expression levels into proportional hazards regression analyses revealed that ADNP expression was an independent predictor of favorable outcome (Table 11). Collectively, high ADNP expression was a marker of good prognosis in colorectal cancer patients which is in agreement with its tumor suppressive function in this malignancy.

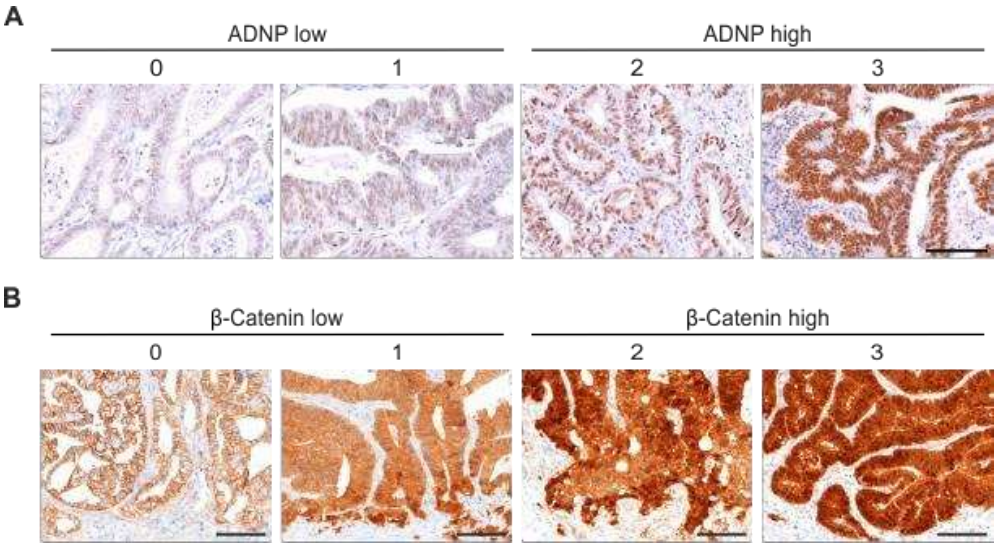

Figure 20. Assessment of ADNP (A) and nuclear β-catenin (B) immunostaining in a collection of 221 primary human colorectal cancers. (A) Tumors were assigned semi-quantitative expression scores from 0 (no or barely detetable ADNP staining) to 3 (strong ADNP staining). (B) Tumors were assigned scores from 0 (no nuclear β-Catenin) to 3 (most tumor cells with strong nuclear β-Catenin) and accordingly categorized as β-catenin low (score 0-1) and β-catenin high (score 2-3). Scale bars, 100 µm.

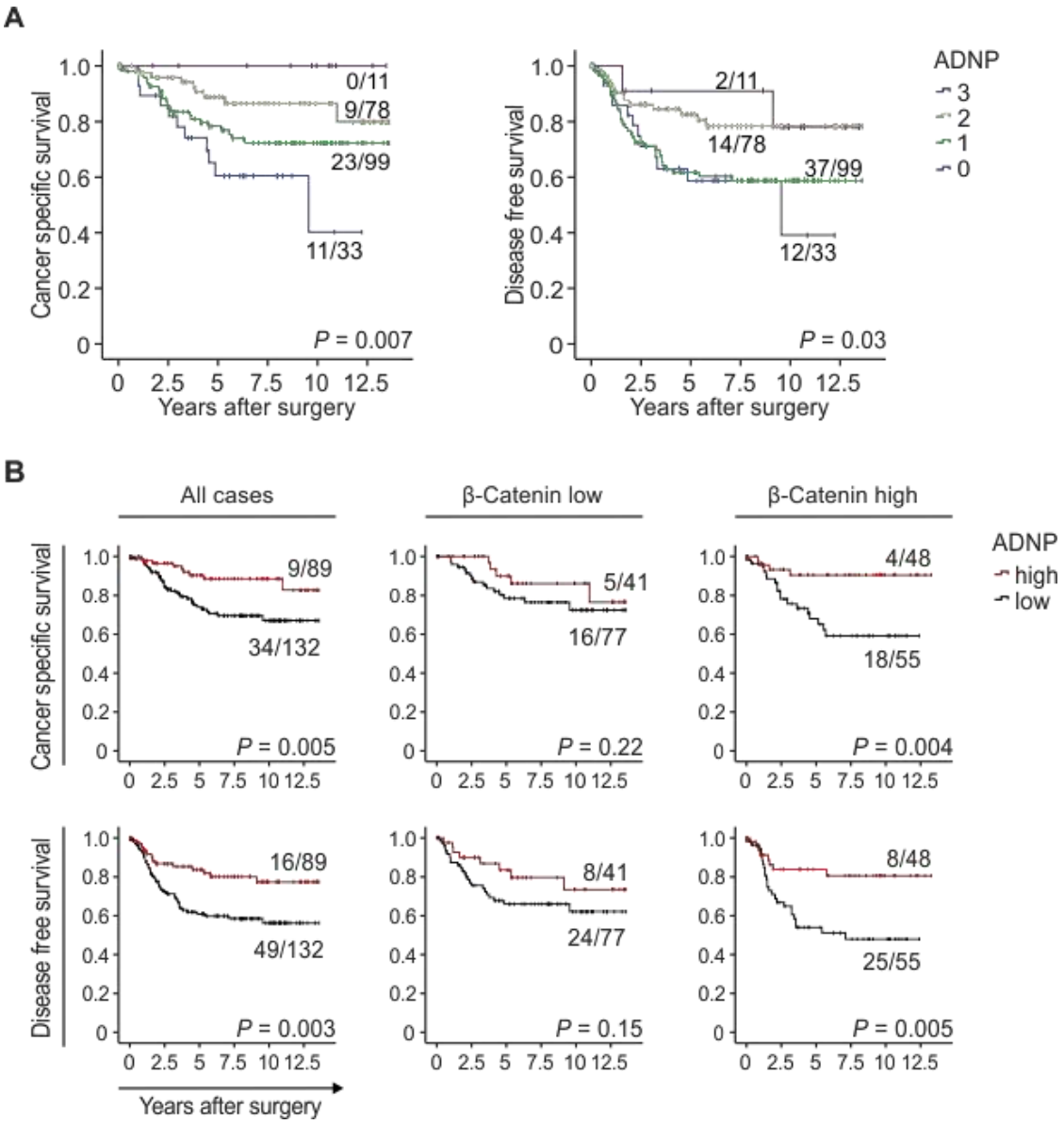

Figure 21. Loss of ADNP expression indicates poor prognosis in colorectal cancer. (A) Kaplan-Meier plots for different ADNP expression scores for tumor specific survival and disease free survival indicate significant poorer outcomes with decreasing ADNP expression. (B) Kaplan-Meier plots for low and high ADNP expression in all cases, and in colon cancer subsets with low or high expression of nuclear β-catenin. P values indicate log-rank test results. Ratios on curves indicate the number of events over the number of patients per group.

Table 10. Clinical/pathological data and ADNP expression in colorectal cancer.

Characteristics	Total	ADNP expression score				*P*
		0	1	2	3	
All patients	221 (100)	33 (14.9)	99 (44.8)	78 (35.3)	11 (5.0)	
Age (y, median 69)						
≤ 68	110 (49.8)	16 (14.8)	45 (41.7)	41 (38.0)	6 (5.6)	0.794
≥ 69	111 (50.2)	17 (15.0)	54 (47.8)	37 (32.7)	5 (4.4)	
Gender						
Male	121 (54.8)	14 (11.5)	59 (48.4)	42 (34.4)	7 (5.7)	0.344
Female	100 (45.2)	19 (19.2)	40 (40.4)	36 (36.4)	4 (4.0)	
T-stage (UICC)						
T1	1 (0.5)	0 (0)	1 (100)	0 (0)	0 (0)	0.01
T2	36 (16.3)	1 (2.7)	18 (48.6)	15 (40.5)	3 (8.1)	
T3	176 (79.6)	27 (15.4)	77 (44.0)	63 (36.0)	8 (4.6)	
T4	8 (3.6)	5 (62.5)	3 (37.5)	0 (0)	0 (0)	
Tumor grade (WHO)						
low grade	200 (90.5)	29 (14.6)	86 (43.2)	73 (36.7)	3 (5.5)	0.308
high grade	21 (9.5)	4 (18.2)	13 (59.1)	5 (22.7)	0 (0)	

Row percent values are given in parentheses

Table 11. Multivariate analysis of cancer specific survival.

Variables	Cancer specific survival		
	HR	(95% confidence interval)	*P*
Age (≥ vs < median)	2.0	(1.05-3.86)	0.034
Gender (F vs M)	0.8	(0.44-1.59)	0.598
T-stage	2.5	(1.1-5.8)	0.028
Tumor grade	1.2	(0.53-2.82)	0.637
ADNP expression score	0.6	(0.37-0.87)	0.01

4.2. Analysis of differential MAPK signaling in colorectal cancer

The results presented in this section are part of the following publication:

Blaj, C., Schmidt, E.M., Lamprecht, S., Hermeking, H., Jung, A., Kirchner, T., Horst, D. Oncogenic Effects of High MAPK Activity in Colorectal Cancer Mark Progenitor Cells and Persist Irrespective of RAS Mutations. *Cancer Research,* 2017 Apr 1;77(7)

4.2.1. MAPK activity is heterogeneous in colorectal cancer

To characterize MAPK activity in colorectal cancer, we stained a collection of 160 cases, half of which were *KRAS* wild-type and half of which had activating *KRAS* mutations (Table 1), for phosphorylated ERK (p-ERK). Cases with detectable p-ERK (59.4 %) generally showed a heterogeneous staining pattern and were composed of p-ERK positive and negative tumor cell subpopulations. In specific, p-ERK strongly marked colon cancer cells at the infiltrative tumor edge, including tumor cells that invaded the stroma by apparently detaching from the gland forming tumor mass (Figure 22 A). This staining pattern was observed in *KRAS* wild-type and mutant colon cancer cases (Figure 22 B). To exclude that heterogeneous p-ERK expression in *KRAS* mutant cancers was caused by a mixture of *KRAS* mutant and wild-type tumor cell subclones, we then microdissected p-ERK positive and negative colon cancer cells in 3 of these cases, and generally found an identical *KRAS* mutation status in both subpopulations. Next, we assessed MAPK activity through staining for FRA1, a component of the AP1 transcription factor complex. Similar to p-ERK, all cases with detectable FRA1 expression (75.0 %) showed a heterogeneous distribution with clearly predominant expression in infiltrative tumor cells at the leading tumor edge that again was irrespective of the tumors' *KRAS* mutation status (Figure 22 A-B). Furthermore, we injected cells of a *KRAS* wild-type primary colon cancer (P-Tu) or *KRAS* mutant T84 colon cancer cells into NOD/SCID mice for xenograft formation. In both cases adenocarcinomas formed that showed heterogeneous expression of p-ERK and FRA1 with predominant staining at the tumor edge (Figure 22 C). We then constructed a lentiviral MAPK reporter with GFP expression under control of multimerized serum response elements (pLenti SRE-GFP), expanded single cell clones of transduced P-Tu$^{SRE\text{-}GFP}$ and T84$^{SRE\text{-}GFP}$ colon cancer cells, and s.c. injected them into NOD/SCID mice. In the resulting xenograft tumors, GFP expression was strongly heterogeneous and again predominantly localized at the tumor edge (Figure 22 D). These

findings demonstrated that MAPK signaling is strongly regulated in colon cancers with and without activating *KRAS* mutations by locoregional cues, with colon cancer cells at the infiltrative tumor edge displaying the highest MAPK activity levels.

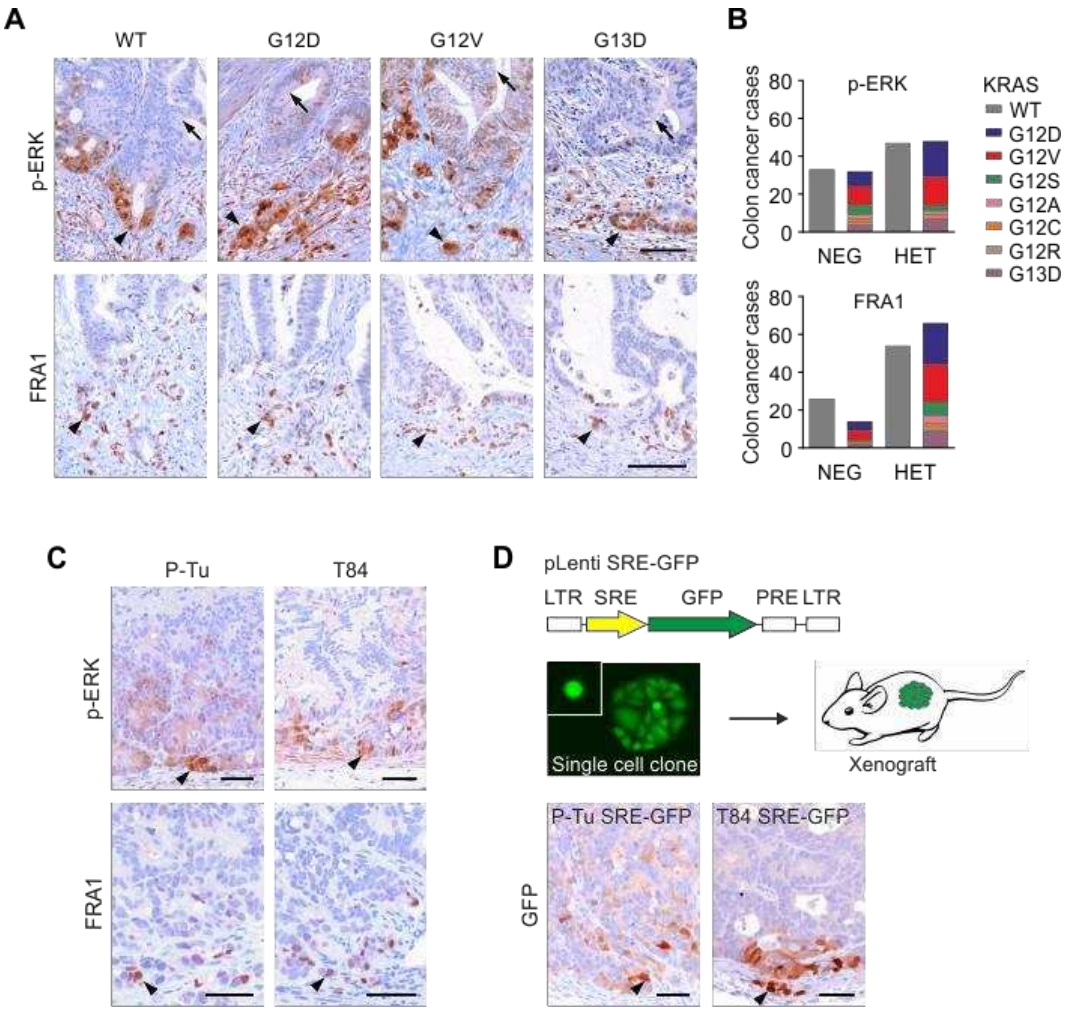

Figure 22. Heterogeneous MAPK activity in colorectal cancer. (A) Representative immunostainings for p-ERK and FRA1 in human colorectal cancer specimens with indicated *KRAS* mutation status. WT, *KRAS* wild-type. Arrowheads indicate positive staining of tumor cells at the leading tumor edge. Arrows indicate tumor cells without staining. *Scale bars* 100 µm. (B) Frequencies of colorectal cancers (n = 160) without detectable staining (NEG) or heterogeneous staining (HET) for p-ERK and FRA1. *KRAS* mutation status is indicated by distinct colors. WT, *KRAS* wild-type. (C) Immunostainings of primary (P-Tu) or T84 colon cancer xenografts (n ≥ 3) for p-ERK and FRA1. Arrowheads indicate positive staining. *Scale bars* 50 µm. (D) *Upper panel*: Lentiviral MAPK reporter pLenti SRE-GFP. LTR, long terminal repeat; SRE, serum response element; PRE, posttranscriptional regulatory element. *Mid panel*: Expansion of single transduced colon cancer cells and injection into NOD/SCID mice for xenograft formation. *Lower panel*: Immunostainings of pLenti SRE-GFP transduced P-Tu or T84 single cell derived xenografts (n ≥ 3) for GFP. Arrowheads indicate positive staining. *Scale bars* 50 µm.

4.2.2. MAPK signaling is regulated through wild-type RAS isoforms in colorectal cancer

To determine the underlying regulations, we next analyzed MAPK signaling upon stimulation by growth factor receptors in colon cancer cells with and without *KRAS* mutations *in vitro*. Within the MAPK pathway, stimulation of EGFR is transduced through the RAS-RAF-MEK-ERK signaling cascade. Expectedly, stimulation of *KRAS* wild-type colon cancer cells with EGF caused strong phosphorylation of ERK, indicating pathway activation, while blocking EGFR with cetuximab prevented this effect (Figure 23 A). Surprisingly, we observed exactly the same response upon EGF treatment of *KRAS* mutant colon cancer cell lines that also was abolished by cetuximab (Figure 23B). Moreover, in both *KRAS* wild-type and mutant colon cancer cells, stimulation by EGF led to phosphorylation of EGFR and MEK in addition to ERK, indicating full pathway response (Figure 23 C). These findings suggested that MAPK signaling remains responsive to external stimulation of EGFR in *KRAS* wild-type and mutant colon cancer cells. To shed light on the underlying mechanism, we then used GTP pulldown assays that expectedly showed predominant GTP loading of KRAS and NRAS in *KRAS* wild-type colon cancer cells (Figure 23 D). In contrast, *KRAS* mutated colon cancer cells showed constitutively GTP bound KRAS, while EGF stimulation caused additional GTP loading of either wild-type NRAS or HRAS or both (Figure 23 D). Collectively, these findings demonstrate that remaining wild-type RAS isoforms contribute to sustained regulation of MAPK signaling in *KRAS* mutant colon cancers.

4.2.3. Colorectal cancer cells with high MAPK activity have a distinct phenotype

To learn about the relevance of regulated MAPK signaling in colon cancer, we further characterized the phenotype of colon cancer cell subpopulations with low and high pathway activity. We examined colon cancer specimens with and without *KRAS* mutations by double immune-fluorescence. Tumor cells with high p-ERK expression at the leading tumor edge showed concomitant overexpression of nuclear β-catenin (Figure 24 A-B), indicating coincident activation of MAPK and WNT signaling. Furthermore, as indicated by Ki67 staining, proliferation was strongly reduced in colon cancer cells with high p-ERK staining when compared to gland forming tumor cells with lower or absent p-ERK staining (Figure 24 C-D).

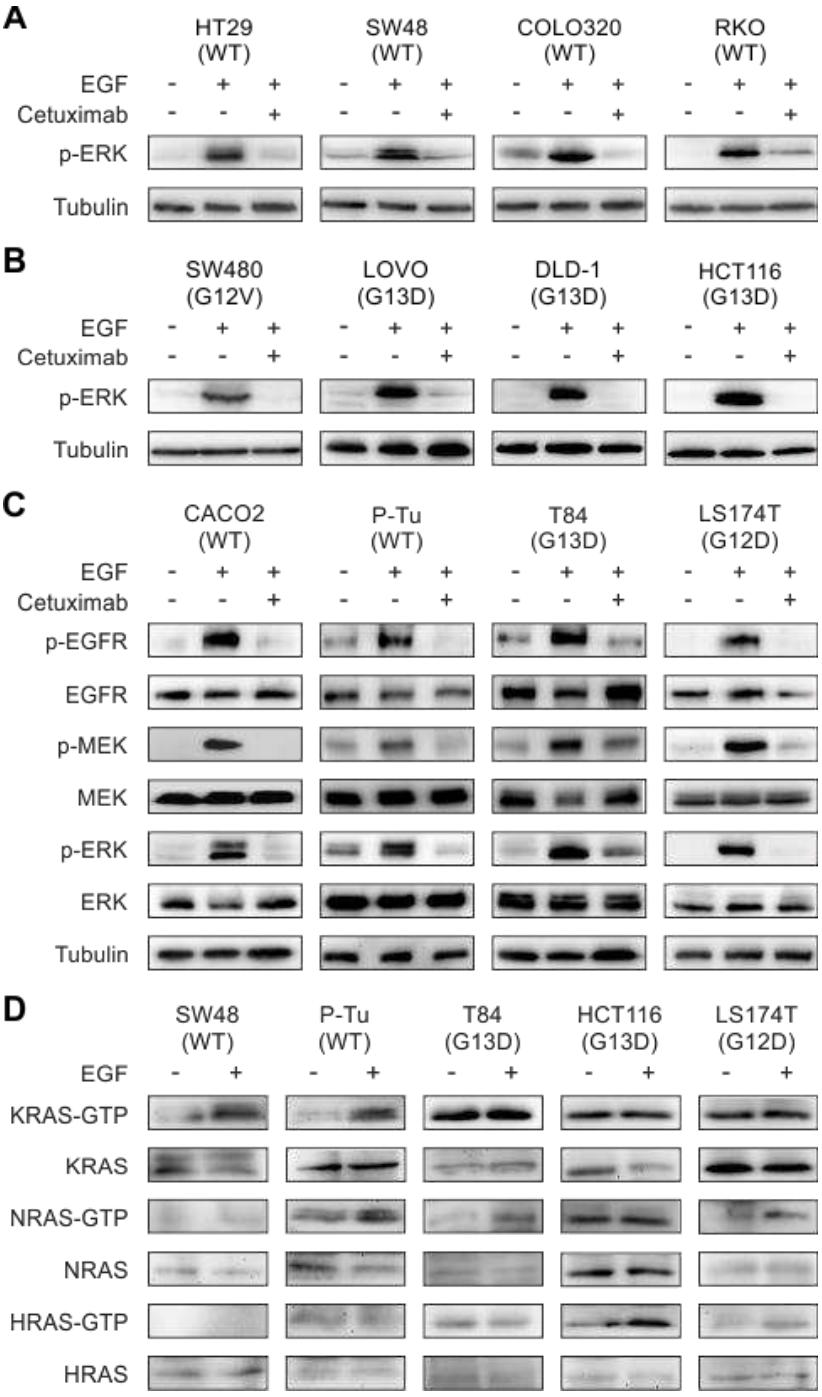

Figure 23. RAS mediated MAPK pathway regulation in colorectal cancer cells. (A-C) Colon cancer cell lines were serum starved, treated with 10 µg/ml cetuximab or PBS for two hours, and then stimulated with 40 ng/ml EGF, or not stimulated. Immunoblotting on whole cell lysates for indicated proteins 10 minutes after stimulation in (A) KRAS wild-type (WT) cell lines, (B) KRAS mutated cell lines, and (C) KRAS WT or mutated cell lines. (D) RAS activity in cell lines with indicated KRAS mutation status was determined by RAS-GTP pulldown assays and immunoblotting for indicated proteins. $n \geq 3$

At the same time, highly p-ERK positive tumor cells exhibited a significantly reduced expression of the epithelial cell adhesion molecule E-cadherin (Figure 24 E-F) and increased expression of LAMC2 (Figure 24 G-H), both indicating epithelial-mesenchymal transition (EMT) in CRC. Taken together, tumor cells with high MAPK activity at the infiltrative tumor edge of CRC displayed increased WNT signaling, decreased proliferation, and had undergone an EMT.

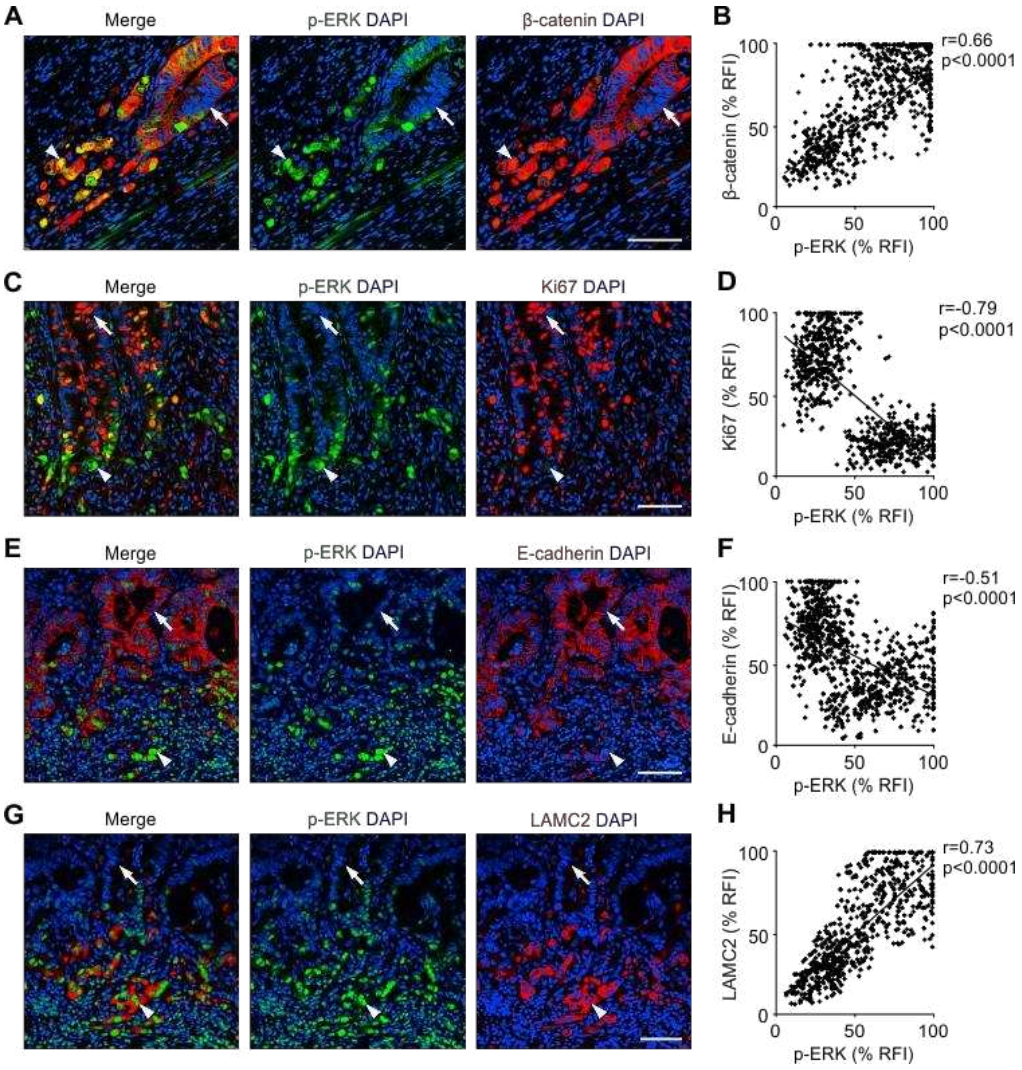

Figure 24. Phenotype of colorectal cancer cells with differential MAPK activity. (A, C, E, G) Representative immune fluorescence for indicated proteins in human colorectal cancer specimens. *Arrowheads* indicate p-ERK positive tumor cells at the leading tumor edge. *Arrows* indicate p-ERK negative gland forming tumor cells. *Scale bars* 100 μm. (B, D, F, H) Quantification of co-immune fluorescence signals for indicated proteins. Percentage values of relative fluorescence intensity (% RFI) for individual tumor cells ($n \geq 700$) of different colorectal cancer samples ($n \geq 7$) are shown. *P* values are results of linear regression analyses.

4.2.4. MAPK signaling regulates EMT in colorectal cancer

In order to determine the impact of MAPK signaling on the observed tumor cell phenotype, we transduced *KRAS* wild-type and mutant colon cancer cells with two lentiviral vectors encoding a doxycycline inducible constitutively active MEK1 (caMEK-Tet-On, Figure 25 A). Treatment of P-Tu$^{caMEK\text{-}Tet\text{-}On}$ and T84$^{caMEK\text{-}Tet\text{-}On}$ colon cancer cells with doxycycline caused strong up-regulation of p-ERK and FRA1, indicating the expected activation of downstream MAPK signaling (Figure 25B).

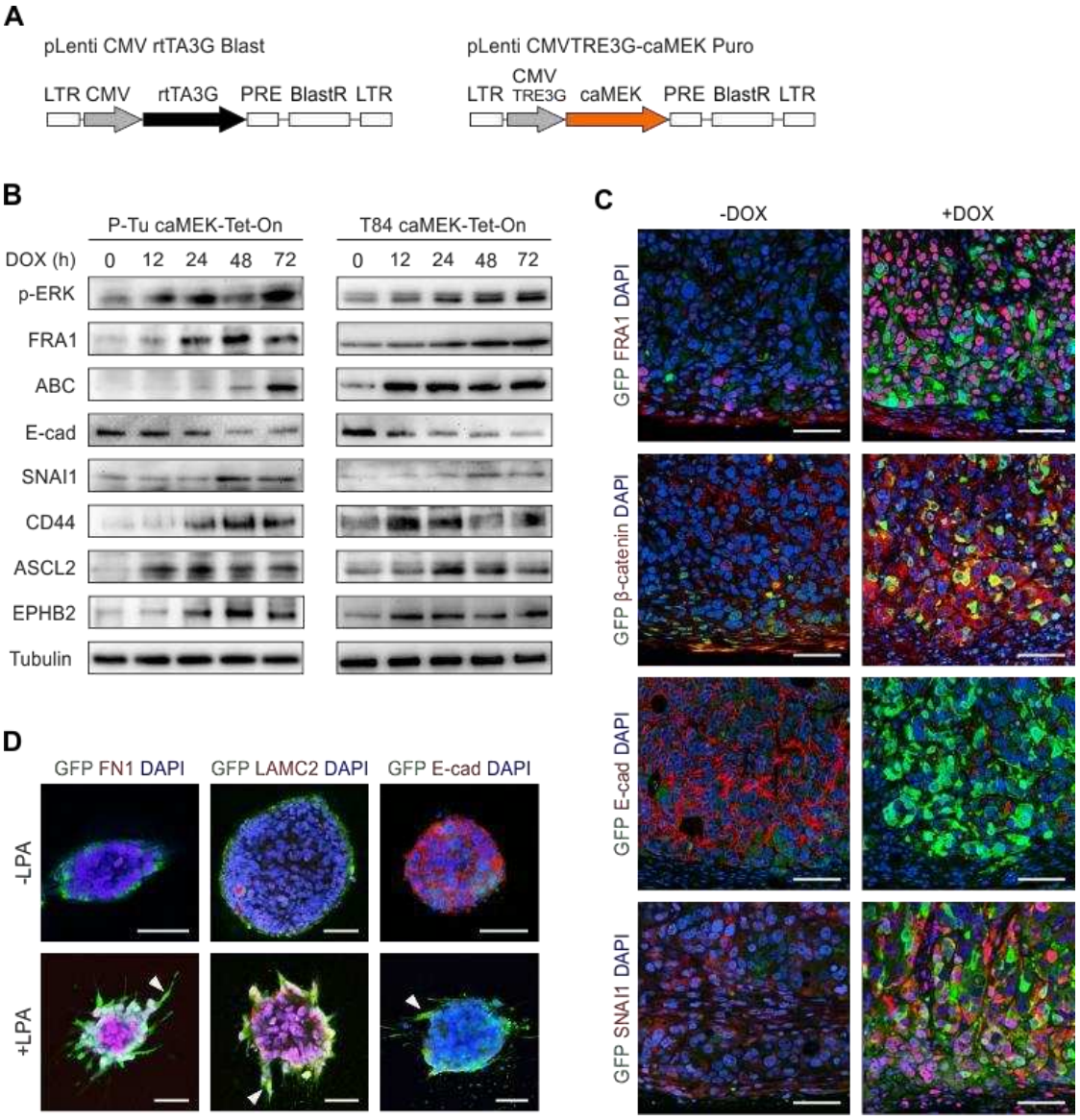

Figure 25. Effects of MAPK overactivation in colorectal cancer cells. (A) Lentiviral vectors for doxycycline inducible overexpression (TET-On) of constitutively active MEK (caMEK). CMV, cytomegalovirus promoter; BlastR, blasticidin resistance; PuroR, puromycine resistance; LTR, long terminal repeat; PRE,

posttranscriptional regulatory element. (B) Immunoblotting of indicated proteins on whole cell lysates of pLenti CMV rtTA3G Blast and pLenti CMVTRE3G-caMEK Puro primary (P-TucaMEK-Tet-On) and T84caMEK-Tet-On colon cancer cells at indicated time points after doxycycline (DOX) stimulation. n ≥ 3. (C) Immune fluorescence for indicated proteins in T84SRE-GFP/caMEK-Tet-On xenografts (n ≥ 3), 4 days after treatment with doxycycline (+DOX) or without doxycycline treatment (-DOX). *Scale bars* 50 μm. (D) Immune fluorescence for indicated proteins in 3D spheroids of P-TuSRE-GFP colon cancer cells (n ≥ 3) with or without LPA stimulation for 4 days. *Arrowheads* indicate radial cytoplasmic extensions upon LPA stimulation. *Scale bars* 50 μm. E-cad, E-cadherin; ABC, active β-catenin.

Importantly, caMEK induction also caused elevated expression of active β-catenin (ABC), indicating increased WNT activity, as well as induction of SNAI1 and a decrease of E-cadherin, both indicating an EMT phenotype. Furthermore, induction of caMEK caused pronounced expression of the putative colon cancer stem cell antigens CD44, ASCL2, and EPHB2. We then additionally transduced $T84^{caMEK\text{-}Tet\text{-}On}$ colon cancer cells with a pLenti SRE-GFP reporter (Figure 22 D), yielding $T84^{SRE\text{-}GFP/caMEK\text{-}Tet\text{-}On}$, expanded single cell clones, injected them into NOD/SCID mice for xenograft formation, and examined the effects of caMEK induction by doxycycline *in vivo*. Similar to our results in cell culture, doxycycline treatment induced the expression of FRA1 and GFP, indicating MAPK activation, increased β-catenin and SNAI1 expression, and repressed expression of E-cadherin (Figure 25 C). To further evaluate effects of MAPK on EMT, we then stimulated *in vitro* spheroids of $P\text{-}Tu^{SRE\text{-}GFP}$ colon cancer cells with the MAPK activator LPA. While tumor spheroids without stimulation formed rounded edges, LPA stimulation caused tumor cells to form radial cytoplasmic extensions with spindle cell morphology (Figure 25 D). Moreover, we found an upregulation of FN1 and LAMC2 with concomitant downregulation of E-cadherin upon LPA stimulation (Figure 25 D). Collectively, these findings demonstrated induction of EMT and expression of putative cancer stem cell antigens upon MAPK stimulation in *KRAS* wild-type and mutant colon cancer cells.

4.2.5. Lineage tracing reveals a progenitor cell phenotype of colon cancer cells with high MAPK activity

Ectopic activation of MAPK signaling caused increased WNT signaling and expression of markers that had been previously related to tumor-initiating colon cancer stem cells (Hanahan & Weinberg, 2011; Herbst et al., 2014; Lustig et al., 2002). To test if colon cancer cells with high MAPK activity represent a progenitor cell compartment within growing tumors *in vivo*, we developed a Cre-lox based lineage tracing system that allowed to genetically label and follow tumor cells and their progeny over time. We designed two lentiviral vectors that either expressed GFP and CreERT2 under control of the MAPK sensitive serum response element (pLenti SRE-GFP-CreERT2) or of a ubiquitously active PGK promoter (pLenti PGK-GFP-CreERT2) (Figure 26 A). We then created a second lentiviral vector that upon Cre activation irreversible recombined with a switch from mCherry to LacZ expression (pLenti lox-mCh-LacZ) (Figure 26 B). Next, we transduced primary colon cancer cells with pLenti lox-mCh-LacZ and either pLenti SRE-GFP-CreERT2 (P-Tu$^{SRE\text{-}lin}$) or pLenti PGK-GFP-CreERT2 (P-Tu$^{PGK\text{-}lin}$), expanded single cell clones, and injected them into NOD/SCID mice (Figure 26 C).

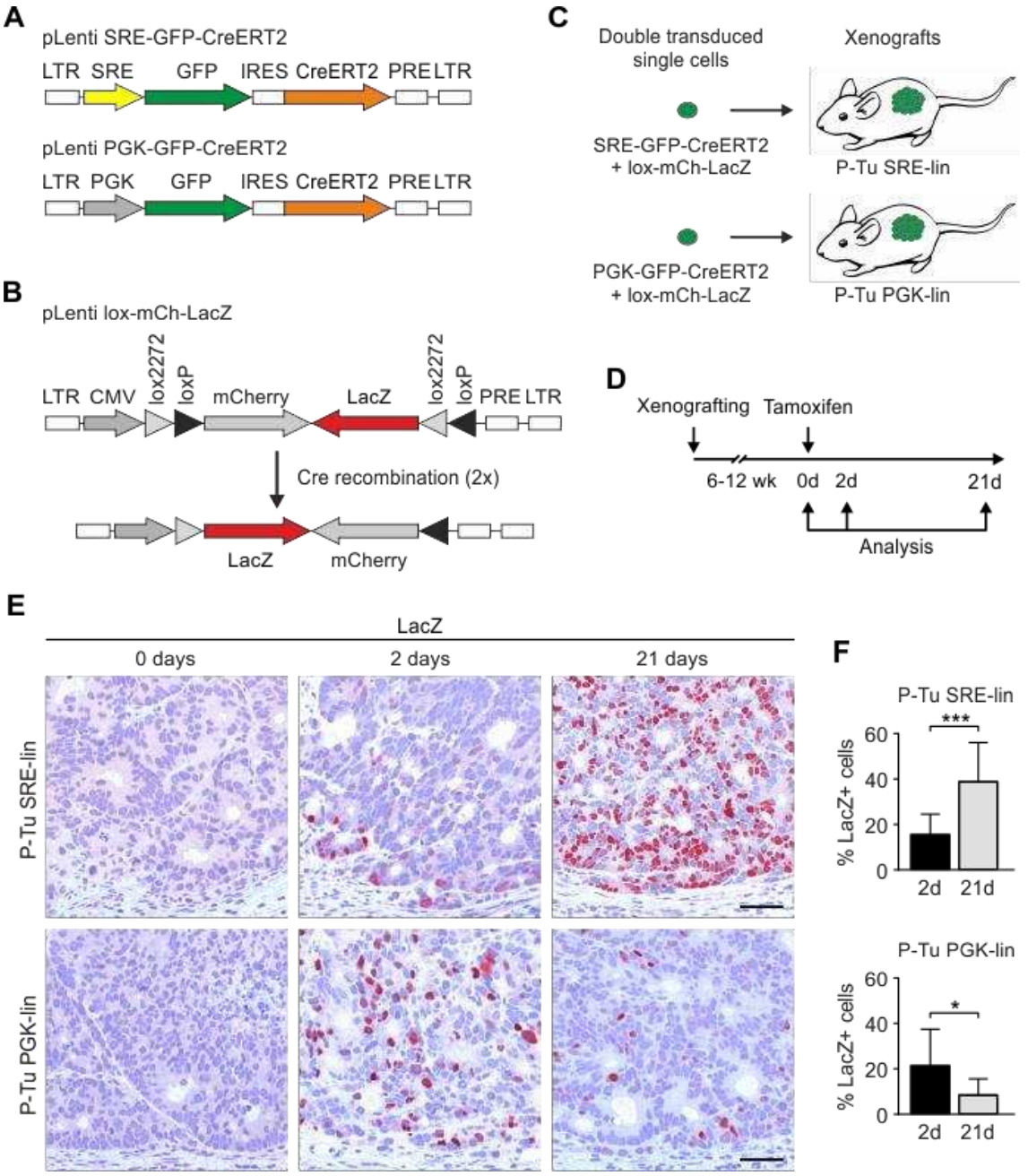

Figure 26. Lineage tracing of colon cancer cells with high MAPK activity. (A) Lentiviral vectors for GFP and CreERT2 expression under control of a MAPK responsive promoter (pLenti SRE-GFP-CreERT2) or a ubiquitously active promoter (pLenti PGK-GFP-CreERT2). (B) Cre-responsive lentiviral vector with a double-floxed inverted *LacZ* gene. Upon Cre activation, the *LacZ* gene will be irreversibly inverted and expressed under control of the CMV promoter. mCherry expression can be used as a transduction marker. LTR, long terminal repeat; SRE, serum response element; PRE posttranscriptional regulatory element. (C) P-TuSRE-lin and control P-TuPGK-lin xenografts ($n \geq 3$) were derived from single cells that were double transduced with pLenti lox-mCh-LacZ and pLenti pLenti SRE-GFP-CreERT2 or pLenti PGK-GFP-CreERT2, respectively.

(D) Experimental schedule for lineage tracing. (E) Immunostaining for LacZ and (F) quantification of LacZ positive (LacZ+) tumor cells in PTuSRE-lin and P-TuPGK-lin xenografts ($n \geq 3$) at indicated time points after tamoxifen induced recombination. *Scale bars* 50 μm. *** $P < 0.001$; * $P < 0.05$ by t test.

After xenograft growth, a single tamoxifen pulse was given to induce recombination (Figure 26 D) that after 2 days caused labelling of individual tumor cells by LacZ in P-Tu$^{SRE\text{-}lin}$ and P-Tu$^{PGK\text{-}lin}$ xenografts (Figure 26 E). Importantly, at this early time point, recombined LacZ positive tumor cells were located towards the leading tumor edge in P-Tu$^{SRE\text{-}lin}$ xenografts, whereas in P-Tu$^{PGK\text{-}lin}$ xenografts they were randomly distributed throughout the tumor (Figure 26 E). Moreover, when examining tumors 21 days after tamoxifen induction, the number of recombined LacZ positive tumor cells had significantly increased throughout the tumor in P-Tu$^{SRE\text{-}lin}$ xenografts, whereas in contrast, P-Tu$^{PGK\text{-}lin}$ xenografts showed a loss of LacZ labelled tumor cells (Figure 26 F). These findings demonstrated a higher potential of initially labelled tumor cells in P-Tu$^{SRE\text{-}lin}$ than in P-Tu$^{PGK\text{-}lin}$ xenografts for maintaining tumor cell lineages in colon cancer.

To further characterize recombined colon cancer cells in P-Tu$^{SRE\text{-}lin}$ xenografts, we analyzed them for co-localization with GFP, indicating high MAPK activity. As expected, 2 days after tamoxifen induction most recombined LacZ positive tumor cells showed high GFP expression, indicating predominant labeling of tumor cells with high MAPK activity (Figure 27 A-B). Importantly, when examining tumors 21 days after recombination, the LacZ label had extended into tumor cell subpopulations with low GFP expression, and thus, lower MAPK activity (Figure 27 A-B). We then tested for co-localization of recombined cells and nuclear β-catenin as a marker for high WNT activity. 2 days after recombination, LacZ labeled tumor cells had significantly higher levels of nuclear β-catenin than LacZ negative tumor cells (Figure 27 C-D). Similar to our findings for GFP, the label had extended into tumor cell subpopulations without nuclear β-catenin staining 21 days after recombination (Figure 27 C-D). Collectively, these data demonstrated a significant contribution of colon cancer cell subsets with high MAPK activity and concomitantly high WNT activity to lineage persistence *in vivo*.

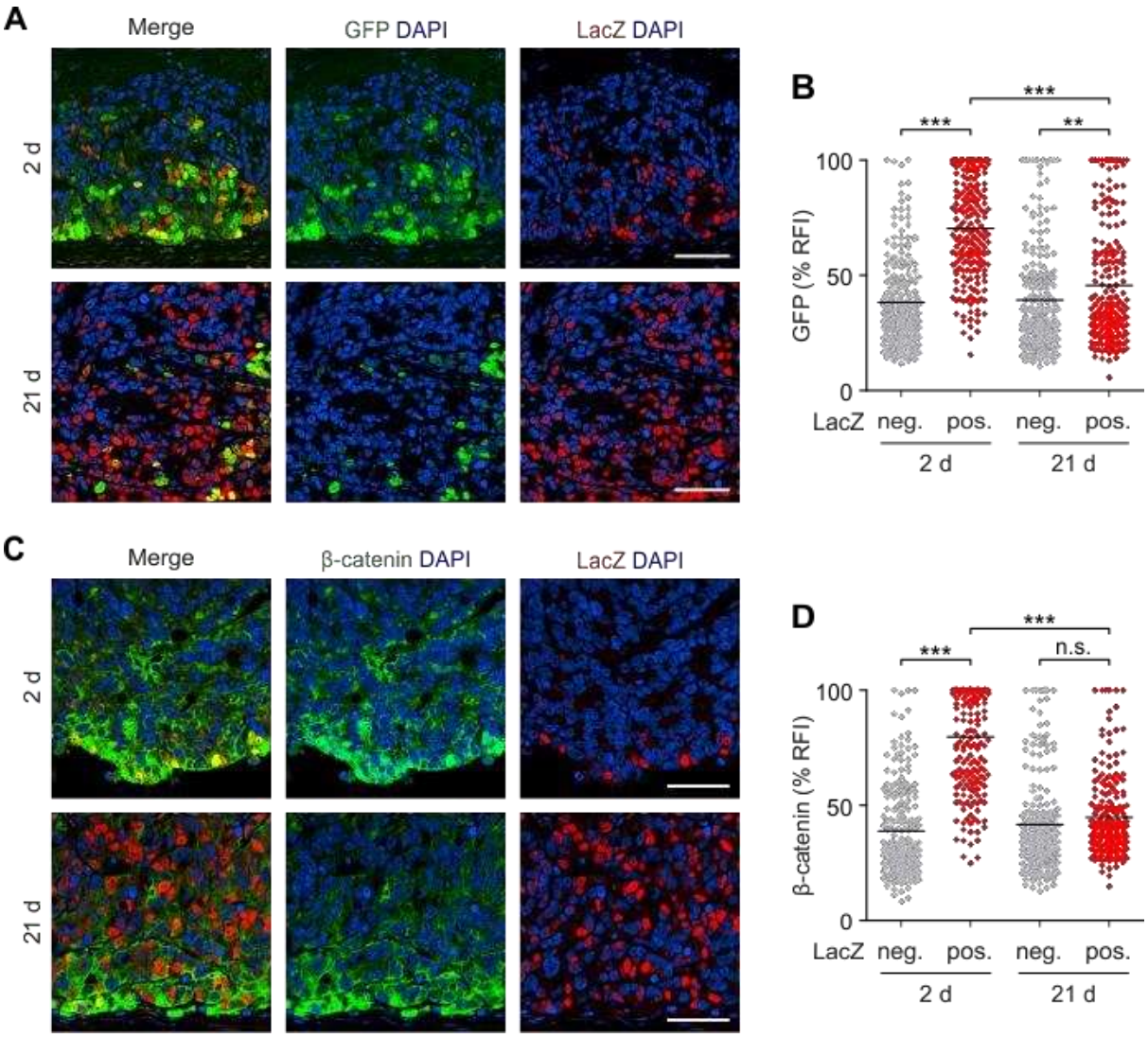

Figure 27. Phenotypic switch of tumor cells during lineage outgrowth. (A, C) Immune fluorescence for indicated proteins in P-TuSRE-lin xenografts (n ≥ 3) at indicated time points after tamoxifen induced recombination. *Scale bars* 50 μm. (B, D) Quantification of GFP and β-catenin immune fluorescence in LacZ positive (LacZ+) or negative (LacZ-) tumor cells at indicated time points after tamoxifen induced recombination. Percentage values of relative fluorescence intensity (% RFI) of individual tumor cells (n ≥ 200) in ≥ 3 biological replicates are shown. *** $P < 0.0001$; ** $P < 0.01$; n.s., non-significant by ttest.

5. Discussion

5.1. ADNP is a therapeutically inducible repressor of WNT signaling in colorectal cancer

Constitutive activation of WNT signaling by inactivating mutations in APC is hallmark of most colorectal cancers and drives tumor progression via target genes that promote cell proliferation, invasion, and spawn putative cancer stem cell traits (Brabletz et al., 2005; The Cancer Genome Atlas Network, 2012; Vermeulen et al., 2010). Therefore, identifying effectors or regulators of WNT signaling which are involved in governing these malignant traits may hold keys for a deeper understanding of colon cancer biology, and the development of more effective therapies (Anastas & Moon, 2013). In this context, we here identified upregulation of the transcription factor ADNP in colon cancer cells with high WNT signaling activity. Although differential expression of ADNP in colon cancer cell subpopulations with high and low WNT activity was relatively small, we demonstrate high consistency of this finding on mRNA and protein levels. However, a direct regulation of ADNP through WNT remained unclear, since modulation of WNT signaling in colon cancer and other cells yielded no measurable effects on ADNP expression. How ADNP expression itself is regulated in colon cancer cells therefore still needs to be determined, keeping in mind that ADNP is known to engage in auto-regulatory feedback loops, as others report (Aboonq et al., 2012).

Consistent upregulation of ADNP in colon cancer cells with high WNT activity prompted us to further investigate its functional relevance. Unexpectedly, ADNP depletion caused significant upregulation of WNT target genes, as assessed on multiple levels of the transcriptome, proteome, for individual factors, and in reporter assays, while, in line with these findings, overexpression of ADNP in colon cancer cells showed opposite effects. ADNP therefore exhibited a previously unknown function in suppressing WNT activity in colon cancer. In specific, ADNP knockdown caused overexpression of WNT targets such as DNMT1 and the recently identified WNT signaling node Talin-1, which are reported drivers of tumor cell proliferation, invasion and migration, respectively (Bayerlová et al., 2015; Bostanci et al., 2014). Indeed, we found that these attributes of malignancy were strongly unleashed in colorectal cancer cells under ADNP knockdown or knockout *in vitro*, and that ADNP depletion strongly enhanced tumor growth *in vivo*. ADNP therefore acted as a

tumor suppressor gene in colorectal cancer and our data suggest that this may mainly be transduced through WNT repression. Due to strongest ADNP expression in tumor cells with high WNT activity, its function may thus partially mirror that of WNT feedback inhibitors such as AXIN2 (Lustig et al., 2002). However, although these effects may be mediated through chromatin remodeling, since ADNP has been shown to interact with SWI/SNF complexes that also are known to impact on WNT signaling (Mandel & Gozes, 2007; Wang, Haswell, & Roberts, 2014), the exact mechanism of ADNP function, and the detailed dynamics of its WNT and tumor suppressive effects in colon cancer yet remain to be determined. Moreover, since ADNP knockdown also upregulated genes of other pathways driving colon cancer progression, such as angiogenesis and EGFR signaling (Hanahan & Weinberg, 2011; Normanno et al., 2006), we hypothesize that tumor suppressor effects of ADNP may additionally transduce through other pathways than WNT.

ADNP can be pharmacologically induced in neurons by ketamine (Brown et al., 2015; Turner et al., 2012) and our data demonstrate how this aspect may translate into a therapeutic approach for colorectal cancer. Treatment with sub-narcotic ketamine induced ADNP, suppressed WNT signaling, inhibited migration and invasion of colon cancer cells, and significantly slowed tumor growth of colon cancer xenografts *in vivo*. Although the mechanism of ADNP induction by ketamine is currently unknown (Brown et al., 2015), we demonstrate that the effects of ketamine treatment were similar to those of ADNP overexpression, and decreased in ADNP knockout cells, suggesting that the tumor suppressive effects of ketamine in part depend on ADNP-mediated WNT repression. These findings are of specific interest when considering that transcription factors are usually difficult drug targets due to their binding promiscuity and the intrinsically disordered nature of their binding sites (Dunker & Uversky, 2010). Moreover, direct targeting of WNT signaling poses substantial challenges due to complexity of its signaling cascade and cross talk from various other signaling pathways (Kahn, 2014; Niehrs, 2012; Voronkov & Krauss, 2013). The benefit for colorectal cancer patients with advanced disease by repressing WNT through ADNP induction with low dose ketamine may quite easily be tested as an add-on to existing treatment regimens, since this substance and its pharmacological characteristics are well studied (Kurdi et al., 2015). Of course side effects of this treatment are to be carefully evaluated and strictly balanced with potential therapeutic benefits, especially since others reported adverse effects of ketamine for patients with other malignancies, such as breast cancer (He et al., 2013).

Although ADNP was consistently linked to nuclear β-catenin expression within individual colorectal cancers, we were surprised to find only a weak and non-significant overall association of ADNP expression and nuclear β-catenin in our tissue collection. This may be attributed to heterogeneous genetic backgrounds in colorectal cancers with differential influence of other signaling pathways on WNT activity that may not necessarily impact on nuclear β-catenin (Ormanns et al., 2014; The Cancer Genome Atlas Network, 2012). However, in support of the idea that ADNP functions as a tumor suppressor, we found that high ADNP expression predicted better outcomes for cancer and disease free survival in human colorectal cancer, while this was independent of other core clinical variables. Because ADNP predicted differential outcome particularly well in cases with high nuclear β-catenin expression levels that also have been attributed more aggressive behavior in some studies (Z. Chen et al., 2013), ADNP may predominantly exhibit its protective role in this subset of colorectal cancer cases. Since more than 50 % of colorectal cancers progress and/or develop metastases during the course of the disease, markers predicting prognosis and individual risk may guide personalized therapy regimens (Langan et al., 2013). In this context, patients with low stage colorectal cancer but loss of ADNP expression may benefit from increased clinical attention and intensified or adjuvant treatment protocols. In regard to ketamine treatment, since individual colon cancers showed significantly different expression levels of ADNP, it may be a useful biomarker in predicting therapy response, a hypothesis to be addressed in further pre-clinical and eventually clinical trials.

In conclusion, we here identified ADNP as a transcription factor that is overexpressed in colon cancer cells with high WNT signaling activity, counteracts WNT activity in these tumor cells, and exhibits tumor suppressor functions. These characteristics may be therapeutically exploited since ADNP is inducible by low dose ketamine treatment which reduces tumor growth in pre-clinical xenograft models *in vivo*. Moreover, in human colorectal cancer patients ADNP predicts superior clinical outcome. We propose that these potentials of ADNP as a prognostic marker and therapeutic target may be considered in further trials to improve management and treatment options for colorectal cancer patients.

5.2. High MAPK activity induces EMT and marks progenitor cells in colorectal cancer

In this work we demonstrate strong intratumoral heterogeneity and sustained regulation of MAPK signaling in KRAS wild-type but also in KRAS mutant CRC. We show that in human CRC tissues and in primary and cultured colon cancer xenografts with clonal KRAS mutation status, high MAPK activity is consistently restricted to tumor cells at the leading tumor edge, while more centrally and glandular differentiated tumor cell subpopulations have lower MAPK activity. This observation at first is unexpected when considering that oncogenic mutations in KRAS are assumed to constitutively activate MAPK signaling in all clonally derived colon cancer cells (Fearon, Hamilton, & Vogelstein, 1987; Hatzivassiliou et al., 2013; Khambata-Ford et al., 2007). However, our in vitro data demonstrate that in both KRAS wild-type and mutant colon cancers, the inducibility of MAPK signaling is retained at all levels upon growth factor stimulation. Furthermore, we show that in KRAS mutated CRC, regulation of MAPK signaling is maintained through the remaining wild-type RAS isoforms. Our findings thus parallel recent observations in other RAS mutated cancer cells in which the capacity to activate downstream MAPK signaling is not saturated (Young, Lou, & McCormick, 2013). When additionally considering that growth factor secreting stromal cells surround colon cancers at the leading tumor edge (Brabletz et al., 2001; Vermeulen et al., 2010), heterogenous MAPK signaling may likely be caused by differential stimulation of tumor cells by the tumor microenvironment, irrespective of the tumors' KRAS mutation status. Of note, since activating mutations in RAS decrease EGFR sensitivity (Young et al., 2013), this may still explain why despite maintained MAPK regulation, KRAS mutated CRCs respond less to EGFR inhibition therapies by antibody drugs, such as cetuximab (Lievre et al., 2008). However, in light of WNT as another signaling pathway that remains regulated in APC mutated tumors (Horst et al., 2012a), the paradigm of constitutive pathway activation through oncogenic mutations may generally require reconsideration.

Colon cancer cells with high MAPK activity had a distinct phenotype with decreased E-cadherin expression and increased expression of the ZEB1 target LAMC2, indicating loss of epithelial and gain of mesenchymal characteristics (Sánchez-tilló et al., 2011). Moreover, ectopic activation of MAPK signaling caused loss of E-cadherin and upregulation of SNAI1, and inducer of EMT (Peinado, Olmeda, & Cano, 2007). In line with these findings, previous studies demonstrated that ectopic expression of FRA1 or constitutively active MEK1 induced EMT in colon cancer cells and was linked to tumor progression (Bakiri et al., 2015; Diesch et

al., 2014). Because we show similar effects of MAPK activation in colon cancer cells with and without activating KRAS mutations, we propose that MAPK signaling generally regulates EMT in CRC. Moreover, our data may provide a rationale for this sustained MAPK regulation, since we found that colon cancer cells with high MAPK activity undergoing EMT had low proliferation rates. Differentially high and low MAPK activity may thus be required to balance infiltrative tumor cells undergoing EMT, and tumor cell proliferation forming new tumor mass. We therefore suggest that the full malignant potential of CRC may depend on differential MAPK signaling, allowing for phenotypic plasticity that generates tumor cell subpopulations with distinct phenotypes fostering tumor growth and progression, respectively.

In addition to an EMT phenotype, colon cancer cells with high MAPK activity showed strong staining for nuclear β-Catenin, indicating high WNT activity (Fodde & Brabletz, 2007). Moreover, activation of MAPK signaling caused increased expression of CD44, ASCL2, and EPHB2. Because these markers and high WNT activity have previously been linked to putative colon cancer-initiating cells (Dalerba et al., 2007; Merlos-Suárez et al., 2011; Stange et al., 2010; Vermeulen et al., 2010), we hypothesized that high MAPK activity may indicate a progenitor cell phenotype in CRC. Using a lineage tracing strategy, we demonstrate a higher contribution of colon cancer cells with high MAPK activity to persistent tumor cell lineages, when compared to a random tumor cell subpopulation. Moreover, we show lineage outgrowth of colon cancer cells with high MAPK and high WNT activity into cancer cell subpopulations with lower activity for both signaling pathways. Therefore, our findings suggest that high MAPK activity characterizes stem-like tumor cells that continuously give rise to more differentiated tumor cell subpopulations, and might hence be regarded as the cancerous equivalent of an organ based adult tissue stem cell (Barker, Van Oudenaarden, & Clevers, 2012). Our approach differs from previous descriptions of colon cancer stem cells that were operationally defined by tumor-initiating potential in limiting-dilution xenografts, which had the caveat of low reproducibility (Gallinger et al., 2007; Horst et al., 2012; Shmelkov et al., 2008; Vermeulen et al., 2010). Inducing a tumor in mice may rather require robustness of the injected tumor cell but may not directly assess its hierarchical level within the original tumor (Clevers, 2011). In contrast to such tumor-initiating studies that capture an event that yet has to build a new tumor, our approach marks a growth-fueling progenitor cell compartment within the mature tumor architecture. We therefore believe that lineage tracing advances the cancer stem cell field and will improve our understanding on how tumor cell subpopulations contribute to cancer outgrowth and persistence.

Summary

Constitutively active WNT signaling in colorectal cancers is hallmark and driver of malignant progression in these tumors. However, therapeutic targeting of WNT signaling is difficult due to anticipated side effects on WNT dependent normal tissue homeostasis. Using transcriptome, proteome and cell biology approaches, we identified the transcription factor ADNP as a repressor of WNT signaling in colon cancer that can be induced pharmacologically by treatment with sub-narcotic doses of ketamine. Treatment results in significantly slowed tumor growth in pre-clinical xenograft models of colon cancer. Moreover, high ADNP expression in human colorectal cancers predicts improved disease outcome. Our findings indicate ADNP as a tumor suppressor and promising prognostic marker, and ketamine treatment with ADNP induction as a potential therapeutic approach that may add to current treatment protocols with benefits for colorectal cancer patients.

Beside mutational WNT activation, about 40 % of colorectal cancers have mutations in KRAS with downstream activation of MAPK signaling that promotes tumor invasion and progression. We demonstrate that MAPK signaling shows strong intratumoral heterogeneity, and surprisingly remains regulated in colorectal cancer, irrespective of the tumors' KRAS mutation status. Using primary colorectal cancer tissues, xenografts and MAPK reporter constructs, we show that tumor cells with high MAPK activity specifically reside at the leading tumor edge, cease to proliferate, undergo epithelial-mesenchymal transition (EMT), and express markers related to colon cancer stem cells. In KRAS mutant colon cancer cells, regulation of MAPK signaling is preserved through remaining wild-type RAS isoforms. Moreover, using a lineage tracing strategy, we provide evidence that high MAPK activity marks a progenitor cell compartment of growth fueling colon cancer cells in vivo. Our results imply that differential MAPK signaling balances EMT, cancer stem cell potential, and tumor growth in colorectal cancer.

The positive crosstalk between WNT and MAPK signaling in colorectal cancer has strong implications for the development of combination therapies and a better understanding of the underlying mechanisms may lead to improved therapeutic strategies.

Zusammenfassung

In Kolorektalkarzinomen wird die maligne Progression durch eine konstitutive Aktivierung des WNT Signalwegs gekennzeichnet und gefördert. Der gezielte therapeutische Eingriff in den WNT Signalweg, erweist sich jedoch, aufgrund von voraussichtlichen WNT-abhängigen Nebeneffekten auf die Homeostase des gesunden Gewebes, als schwierig. Mittels Transkriptom-, Proteom- und zellbiologischen Analysen, haben wir den Transkriptionsfaktor ADNP als einen WNT-Repressor in Kolorektalkarzinomen identifiziert, der mit subnarkotischen Ketamindosen pharmakologisch induziert werden kann. Die Behandlung führt zu einer signifikanten Verlangsamung des Tumorwachstums in preklinischen Xenograft-Modellen. Ferner, prognostiziert eine hohe ADNP-Expression einen verbesserten Krankheitsverlauf. Unsere Ergebnisse deuten darauf hin, dass ADNP ein Tumorsuppressor und vielversprechender prognostischer Marker ist. Eine ADNP-Induktion durch Ketaminbehandlung ist eine mögliche therapeutische Strategie zur Verbesserung aktueller klinischer Protokolle.

Zusätzlich zu einer mutationsbedingten Aktivierung des WNT Signalwegs, weisen ungefähr 40% der Kolorektalkarzinomen KRAS-Mutationen und eine nachgeschaltete MAPK Signalaktivierung auf, die die Tumorinvasion und Tumorprogression fördert. Wir konnten zeigen, dass der MAPK-Signalweg eine starke intratumorale Heterogenität aufweist und, unabhängig vom KRAS-Mutationsstatus, in Kolorektalkarzinomen reguliert bleibt. Mittels Analysen von Primärgeweben aus Kolorektalkarzinomen und dem Einsatz von Xenografts und MAPK Reporterkonstrukten, zeigen wir, dass Tumorzellen mit hoher MAPK-Aktivität am Tumorrand lokalisiert sind. Gleichzeitig hören sie auf zu proliferieren, durchlaufen eine epithelial-mesenchymale Transition und exprimieren Tumorstammzell-assoziierte Marker. Die Regulierung des MAPK-Signalwegs bleibt in KRAS mutierten Kolonkrebszellen durch die anderen Wildtyp-RAS-Isoformen erhalten. Darüber hinaus, konnten wir mittels „lineage tracing“ Experimenten nachweisen, dass eine hohe MAPK-Aktivität eine Population von Vorläuferzellen markiert, die für das Tumorwachstum *in vivo* verantwortlich ist. Unsere Ergebnisse implizieren, dass die differentielle MAPK-Signalaktivität für die Erhaltung des Gleichgewichts zwischen EMT, Tumorstammzellpotential und Tumorwachstum in Kolorektalkarzinomen zuständig ist.

Das Zusammenspiel zwischen der WNT- und MAPK- Signaltransduktion in Kolorektalkarzinomen hat weitreichende Implikationen für die Entwicklung von

Kombinationstherapien. Ein besseres Verständnis der grundlegenden Mechanismen könnte zu effizienteren therapeutischen Strategien führen.

References

Aboonq, M. S., Vasiliou, S. A., Haddley, K., Quinn, J. P., & Bubb, V. J. (2012). Activity- dependent neuroprotective protein modulates its own gene expression. *Journal of Molecular Neuroscience*, *46*(2), 33–39. http://doi.org/10.1007/s12031-011-9562-y

Al-Haji, M., Wicha, M. S., Benito-Hernandez, A., Morrison, S. J., & Clarke, M. F. (2003). Prospective identification of tumorigenic breast cancer cells. *Proc Natl Acad Sci U S A*, *100*(11).

Anastas, J. N., & Moon, R. T. (2013). WNT signalling pathways as therapeutic targets in cancer. *Nat Rev Cancer*, *13*(1), 11–26. http://doi.org/10.1038/nrc3419

Bakiri, L., Macho-Maschler, S., Custic, I., Niemiec, J., Guío-Carrión, A., Hasenfuss, S., … Wagner, E. (2015). Fra-1/AP-1 induces EMT in mammary epithelial cells by modulating Zeb1/2 and TGFβ expression. *Cell Death and Differentiation*, *22*(10), 336–350. http://doi.org/10.1038/cdd.2014.157

Barker, N. (2014). Adult intestinal stem cells: critical drivers of epithelial homeostasis and regeneration. *Nature Reviews. Molecular Cell Biology*, *15*(1), 19–33. http://doi.org/10.1038/nrm3721

Barker, N., van Es, J. H., Kuipers, J., Kujala, P., van den Born, M., Cozijnsen, M., … Clevers, H. (2007). Identification of stem cells in small intestine and colon by marker gene Lgr5. *Nature*, *449*(7165), 1003–1007. http://doi.org/10.1038/nature06196

Barker, N., Van Oudenaarden, A., & Clevers, H. (2012). Identifying the stem cell of the intestinal crypt: Strategies and pitfalls. *Cell Stem Cell*, *11*(4), 452–460. http://doi.org/10.1016/j.stem.2012.09.009

Bassan, M., Zamostiano, R., Davidson, a, Pinhasov, a, Giladi, E., Perl, O., … Gozes, I. (1999). Complete sequence of a novel protein containing a femtomolar-activity-dependent neuroprotective peptide. *Journal of Neurochemistry*, *72*, 1283–1293. http://doi.org/10.1046/j.1471-4159.1999.0721283.x

Bayerlová, M., Klemm, F., Kramer, F., Pukrop, T., Beißbarth, T., & Bleckmann, A. (2015). Newly constructed network models of different WNT signaling cascades applied to breast cancer expression data. *PLoS ONE*, *10*(12), 1–19. http://doi.org/10.1371/journal.pone.0144014

Baylin, S. B., & Jones, P. A. (2011). A decade of exploring the cancer epigenome - biological and translational implications. *Nature Reviews. Cancer*, *11*(10), 726–34. http://doi.org/10.1038/nrc3130.A

Bonnet, D., & Dick, J. E. (1997). Human acute myeloid leukemia is organized as a hierarchy that originates from a primitive hematopoietic cell. *Nat Med*, *3*(7), 303–308. http://doi.org/10.1038/nm0798-822

Bostanci, O., Kemik, O., Kemik, A., Battal, M., Demir, U., Purisa, S., & Mihmanli, M. (2014). A novel screening test for colon cancer: Talin-1. *European Review for Medical and Pharmacological Sciences*, *18*(17), 2533–2537.

Brabletz, T., Jung, A., Spaderna, S., Hlubek, F., & Kirchner, T. (2005). Opinion:

Migrating cancer stem cells - an integrated concept of malignant tumour progression. *Nat Rev Cancer*, *5*(9), 744–749. http://doi.org/10.1038/nrc1694

Brabletz, T., Jung, a, Reu, S., Porzner, M., Hlubek, F., Kunz-Schughart, L. a, … Kirchner, T. (2001). Variable beta-catenin expression in colorectal cancers indicates tumor progression driven by the tumor environment. *Proceedings of the National Academy of Sciences of the United States of America*, *98*(18), 10356–10361. http://doi.org/10.1073/pnas.171610498

Brown, B. P., Kang, S. C., Gawelek, K., Zacharias, R. A., Anderson, S. R., Turner, C. P., & Morris, J. K. (2015). In vivo and in vitro ketamine exposure exhibits a dose-dependent induction of activity-dependent neuroprotective protein in rat neurons. *Neuroscience*, *290*, 31–40. http://doi.org/10.1016/j.neuroscience.2014.12.076

Calabrese, C., Poppleton, H., Kocak, M., Hogg, T. L., Fuller, C., Hamner, B., … Gilbertson, R. J. (2007). A Perivascular Niche for Brain Tumor Stem Cells. *Cancer Cell*, *11*(1), 69– 82. http://doi.org/10.1016/j.ccr.2006.11.020

Cernat, L., Blaj, C., Jackstadt, R., Brandl, L., Engel, J., Hermeking, H., … Horst, D. (2014). Colorectal cancers mimic structural organization of normal colonic crypts. *PLoS ONE*, *9*(8), 4–11. http://doi.org/10.1371/journal.pone.0104284

Chen, K., Huang, Y., & Chen, J. (2013). Understanding and targeting cancer stem cells: therapeutic implications and challenges. *Acta Pharmacologica Sinica*, *34*(6), 732–740. http://doi.org/10.1038/aps.2013.27

Chen, Z., He, X., Jia, M., Liu, Y., Qu, D., Wu, D., … Huang, J. (2013). β-catenin overexpression in the Nucleus Predicts Progress Disease and Unfavourable Survival in Colorectal Cancer: A Meta-Analysis. *PLoS ONE*, *8*(5), 1–9. http://doi.org/10.1371/journal.pone.0063854

Cheng, H., & Leblond, C. (1974). Origin, differentiation and renewal of the four main epithelial cell types in the mouse small intestine. I. Columnar cell, II. mucous cell, III. entero-endocrine cells, IV. Paneth cells. *Am J Anat*, *141*, 461–536.

Cheruku, H. R., Mohamedali, A., Cantor, D. I., Tan, S. H., Nice, E. C., & Baker, M. S. (2015). Transforming growth factor-β, MAPK and Wnt signaling interactions in colorectal cancer. *EuPA Open Proteomics*, *8*, 104–115. http://doi.org/10.1016/j.euprot.2015.06.004

Clevers, H. (2006). Wnt/??-Catenin Signaling in Development and Disease. *Cell*, *127*(3), 469–480. http://doi.org/10.1016/j.cell.2006.10.018

Clevers, H. (2011). The cancer stem cell: premises, promises and challenges. *Nature Medicine*, *17*(3), 313–9. http://doi.org/10.1038/nm.2304

Clevers, H., & Nusse, R. (2012). Wnt/??-catenin signaling and disease. *Cell*, *149*(6), 1192–1205. http://doi.org/10.1016/j.cell.2012.05.012

Cojoc, M., Mäbert, K., Muders, M. H., & Dubrovska, A. (2015). A role for cancer stem cells in therapy resistance: Cellular and molecular mechanisms. *Seminars in Cancer Biology*, *31*, 16–27. http://doi.org/10.1016/j.semcancer.2014.06.004

Covassin, L. D., Siekmann, A. F., Kacergis, M. C., Laver, E., Moore, J. C., Villefranc, J. A., … Lawson, N. D. (2009). A genetic screen for vascular mutants in zebrafish reveals dynamic roles for Vegf/Plcg1 signaling during artery development. *Developmental Biology*, *329*(2), 212–226. http://doi.org/10.1016/j.ydbio.2009.02.031

Dalerba, P., Dylla, S. J., Park, I. K., Liu, R., Wang, X., Cho, R. W., … Clarke, M. F. (2007). Phenotypic characterization of human colorectal cancer stem cells, *104*(24), 10158–10163. http://doi.org/10.1073/pnas.0703478104

De Ferrari, G. V, & Moon, R. T. (2006). The ups and downs of Wnt signaling in prevalent neurological disorders. *Oncogene*, *25*(57), 7545–7553. http://doi.org/10.1038/sj.onc.1210064

Diaz, L. a., Williams, R. T., Wu, J., Kinde, I., Hecht, J. R., Berlin, J., … Vogelstein, B. (2012). The molecular evolution of acquired resistance to targeted EGFR blockade in colorectal cancers. *Nature*, *486*(7404), 4–7. http://doi.org/10.1038/nature11219

Diesch, J., Sanij, E., Gilan, O., Love, C., Tran, H., Fleming, N. I., … Dhillon, A. S. (2014). Widespread FRA1-Dependent Control of Mesenchymal Transdifferentiation Programs in Colorectal Cancer Cells. *PLoS ONE*, *9*(3), 1–11. http://doi.org/10.1371/journal.pone.0088950

Dieter, S. M., Ball, C. R., Hoffmann, C. M., Nowrouzi, A., Herbst, F., Zavidij, O., … Glimm, H. (2011). Distinct types of tumor-initiating cells form human colon cancer tumors and metastases. *Cell Stem Cell*, *9*(4), 357–365. http://doi.org/10.1016/j.stem.2011.08.010

Dunker, A. K., & Uversky, V. N. (2010). Drugs for "protein clouds": Targeting intrinsically disordered transcription factors. *Current Opinion in Pharmacology*, *10*(6), 782–788. http://doi.org/10.1016/j.coph.2010.09.005

Fearon, E. R., Hamilton, S. R., & Vogelstein, B. (1987). Clonal analysis of human colorectal tumors. *Science*, *238*(4824), 193–197. Retrieved from http://www.ncbi.nlm.nih.gov/pubmed/2889267

Fodde, R., & Brabletz, T. (2007). Wnt/β-catenin signaling in cancer stemness and malignant behavior. *Current Opinion in Cell Biology*, *19*(2), 150–158. http://doi.org/10.1016/j.ceb.2007.02.007

Gammons, M. V., Renko, M., Johnson, C. M., Rutherford, T. J., & Bienz, M. (2016). Wnt Signalosome Assembly by DEP Domain Swapping of Dishevelled. *Molecular Cell*, 92– 104. http://doi.org/10.1016/j.molcel.2016.08.026

Golebiewska, A. et al., 2011. Critical appraisal of the side population assay in stem cell and cancer stem cell research. *Cell Stem Cell*, 8(2), pp.136–147. Available at: http://dx.doi.org/10.1016/j.stem.2011.01.007.

Marcato, P. et al., 2011. Aldehyde dehydrogenase its role as a cancer stem cell marker comes down to the specific isoform. *Cell Cycle*, 10(9), pp.1378–1384.

Peitzsch, C. et al., 2013. Discovery of the cancer stem cell related determinants of radioresistance. *Radiotherapy and Oncology*, 108(3), pp.378–387. Available at: http://dx.doi.org/10.1016/j.radonc.2013.06.003.

Rausch, V. et al., 2012. Autophagy mediates survival of pancreatic tumour-initiating cells in a hypoxic microenvironment. *Journal of Pathology*, 227(3), pp.325–335.

Gonzalez, D. M., & Medici, D. (2014). Signaling mechanisms of the epithelial-mesenchymal transition. *Science Signaling*, *7*(344), re8-re8. http://doi.org/10.1126/scisignal.2005189

Hanahan, D., & Weinberg, R. A. (2011). Hallmarks of cancer: The next generation. *Cell*, *144*(5), 646–674. http://doi.org/10.1016/j.cell.2011.02.013

Hatzivassiliou, G., Haling, J. R., Chen, H., Song, K., Price, S., Heald, R., … Belvin, M. (2013). Mechanism of MEK inhibition determines efficacy in mutant KRAS- versus BRAF-driven cancers. *Nature*, *501*(7466), 232–6.http://doi.org/10.1038/nature12441

Hayes, T. E., Sengupta, P., & Cochran, B. H. (1988). The human c-fos serum response factor and the yeast factors GRM/PRTF have related DNA-binding specificities. *Genes & Development*, *2*(12 B), 1713–1722. http://doi.org/10.1101/gad.2.12b.1713

He, H., Chen, J., Xie, W. P., Cao, S., Hu, H. Y., Yang, L. Q., & Gong, B. (2013). Ketamine used as an acesodyne in human breast cancer therapy causes an undesirable side effect, upregulating anti-apoptosis protein Bcl-2 expression. *Genetics and Molecular Research*, *12*(2), 1907–1915. http://doi.org/10.4238/2013.January.4.7

Heppner, G. (1984). Tumor Heterogeneity, (June), 2259–2265.

Heppner Goss, K., & Groden, J. (2000). Biology of the adenomatous polyposis coli tumor suppressor. *Journal of Clinical Oncology*, *18*(9), 1967–1979.

Herbst, A., Jurinovic, V., Krebs, S., Thieme, S. E., Blum, H., Göke, B., & Kolligs, F. T. (2014). Comprehensive analysis of β-catenin target genes in colorectal carcinoma cell lines with deregulated Wnt/β-catenin signaling. *BMC Genomics*, *15*, 74. http://doi.org/10.1186/1471-2164-15-74

Herrero, A., Pinto, A., Colón-Bolea, P., Casar, B., Jones, M., Agudo-Ibáñez, L., … Crespo, P. (2015). Small Molecule Inhibition of ERK Dimerization Prevents Tumorigenesis by RAS-ERK Pathway Oncogenes. *Cancer Cell*, *28*(2), 170–182. http://doi.org/10.1016/j.ccell.2015.07.001

Hobor, S., Van Emburgh, B. O., Crowley, E., Misale, S., Di Nicolantonio, F., & Bardelli, A. (2014). TGFα and amphiregulin paracrine network promotes resistance to EGFR blockade in colorectal cancer cells. *Clinical Cancer Research*, *20*(24), 6429–6438. http://doi.org/10.1158/1078-0432.CCR-14-0774

Hoey, T., Yen, W. C., Axelrod, F., Basi, J., Donigian, L., Dylla, S., … Gurney, A. (2009). DLL4 Blockade Inhibits Tumor Growth and Reduces Tumor-Initiating Cell Frequency. *Cell Stem Cell*, *5*(2), 168–177. http://doi.org/10.1016/j.stem.2009.05.019

Horst, D., Chen, J., Morikawa, T., Ogino, S., Kirchner, T., & Shivdasani, R. A. (2012). Differential WNT activity in colorectal cancer confers limited tumorigenic potential and is regulated by MAPK signaling. *Cancer Research*, *72*(6), 1547–1556. http://doi.org/10.1158/0008-5472.CAN-11-3222

Humphries, A., & Wright, N. a. (2008). Colonic crypt organization and tumorigenesis. *Nature Reviews. Cancer*, *8*(6), 415–24. http://doi.org/10.1038/nrc2392

Itzkovitz, S., Lyubimova, A., Blat, I., Maynard, M., Es, J. Van, Lees, J., … Oudenaarden, A. Van. (2012). Single molecule transcript counting of stem cell markers in the mouse intestine. *Nat Cell Biol.*, *14*(1), 106–114. http://doi.org/10.1038/ncb2384.Single

Jemal, A., Siegel, R., Ward, E., Hao, Y., Xu, J., & Thun, M. J. (2009). Cancer Statistics , 2009 BOTH SEXES FEMALE BOTH SEXES ESTIMATED DEATHS. *CA Cancer J Clin*, *59*(4), 1–25. http://doi.org/10.1002/caac.20073.Available

Junttila, M. R., & de Sauvage, F. J. (2013). Influence of tumour micro-environment heterogeneity on therapeutic response. *Nature*, *501*(7467), 346–354.

http://doi.org/10.1038/nature12626

Kahn, M. (2014). Can we safely target the WNT pathway? *Nature Reviews. Drug Discovery*, *13*(7), 513–32. http://doi.org/10.1038/nrd4233

Kalluri, R., & Weinberg, R. a. (2009). Review series The basics of epithelial-mesenchymal transition. *Journal of Clinical Investigation*, *119*(6), 1420–1428. http://doi.org/10.1172/JCI39104.1420

Khambata-Ford, S., Garrett, C. R., Meropol, N. J., Basik, M., Harbison, C. T., Wu, S., … Mauro, D. J. (2007). Expression of epiregulin and amphiregulin and K-ras mutation status predict disease control in metastatic colorectal cancer patients treated with cetuximab. *Journal of Clinical Oncology*, *25*(22), 3230–3237. http://doi.org/10.1200/JCO.2006.10.5437

Kirchner, T., & Brabletz, T. (2000). Patterning and nuclear beta-catenin expression in the colonic adenoma-carcinoma sequence. Analogies with embryonic gastrulation. *The American Journal of Pathology*, *157*(4), 1113–1121. http://doi.org/10.1016/S0002-9440(10)64626-3

Kita-Matsuo, H., Barcova, M., Prigozhina, N., Salomonis, N., Wei, K., Jacot, J. G., … Mercola, M. (2009). Lentiviral vectors and protocols for creation of stable hESC lines for fluorescent tracking and drug resistance selection of cardiomyocytes. *PLoS ONE*, *4*(4). http://doi.org/10.1371/journal.pone.0005046

Kreso, A., & Dick, J. E. (2014). Evolution of the cancer stem cell model. *Cell Stem Cell*, *14*(3), 275–291. http://doi.org/10.1016/j.stem.2014.02.006

Kreso, A., O'Brien, C. A., van Galen, P., Gan, O. I., Notta, F., Brown, A. M., … Dick, J. E. (2013). Variable clonal repopulation dynamics influence chemotherapy response in colorectal cancer. *Science*, *339*(6119), 543–548. http://doi.org/science.1227670 [pii]\r10.1126/science.1227670

Kretzschmar, K., & Watt, F. M. (2012). Lineage tracing. *Cell*, *148*(1–2), 33–45. http://doi.org/10.1016/j.cell.2012.01.002

Krishnamurthy, S., Dong, Z., Vodopyanov, D., Imai, A., Joseph, I., Prince, M. E., … Nör, J. E. (2011). NIH Public Access, *70*(23), 9969–9978. http://doi.org/10.1158/0008-5472.CAN-10-1712.Endothelial

Kurdi, M. S., Theerth, K. A., & Deva, R. S. (2015). Ketamine: Current applications in anesthesia, pain, and critical care. *Anesthesia, Essays and Researches*, *8*(3), 283–90. http://doi.org/10.4103/0259-1162.143110

Langan, R. C., Mullinax, J. E., Raiji, M. T., Upham, T., Summers, T., Stojadinovic, A., & Avital, I. (2013). Colorectal cancer biomarkers and the potential role of cancer stem cells. *Journal of Cancer*, *4*(3), 241–250. http://doi.org/10.7150/jca.5832

Lee, E., Salic, A., Krüger, R., Heinrich, R., & Kirschner, M. W. (2003). The roles of APC and axin derived from experimental and theoretical analysis of the Wnt pathway. *PLoS Biology*, *1*(1), 116–132. http://doi.org/10.1371/journal.pbio.0000010

Li, C., Heidt, D. G., Dalerba, P., Burant, C. F., Zhang, L., Adsay, V., … Simeone, D. M. (2007). Identification of pancreatic cancer stem cells. *Cancer Research*, *67*(3), 1030– 1037. http://doi.org/10.1158/0008-5472.CAN-06-2030

Li, V. S. W., Ng, S. S., Boersema, P. J., Low, T. Y., Karthaus, W. R., Gerlach, J. P., … Clevers, H. (2012). Wnt Signaling through Inhibition of β-catenin Degradation in an Intact Axin1 Complex. *Cell*, *149*(6), 1245–1256.

http://doi.org/10.1016/j.cell.2012.05.002

Lievre, A., Bachet, J.-B., Boige, V., Cayre, A., Le Corre, D., Buc, E., … Laurent-Puig, P. (2008). KRAS Mutations As an Independent Prognostic Factor in Patients With Advanced Colorectal Cancer Treated With Cetuximab. *Journal of Clinical Oncology : Official Journal of the American Society of Clinical Oncology*, *26*(3), 374–379. http://doi.org/10.1200/JCO.2007.12.5906

Lim, J., & Thiery, J. P. (2012). Epithelial-mesenchymal transitions: insights from development. *Development*, *139*(19), 3471–3486. http://doi.org/10.1242/dev.071209

Linnekamp, J. F., Wang, X., Medema, J. P., & Vermeulen, L. (2015). Colorectal cancer heterogeneity and targeted therapy: A case for molecular disease subtypes. *Cancer Research*, *75*(2), 245–249. http://doi.org/10.1158/0008-5472.CAN-14-2240

Lu, J., Ye, X., Fan, F., Xia, L., Bhattacharya, R., Bellister, S., … Ellis, L. M. (2013).

Endothelial Cells Promote the Colorectal Cancer Stem Cell Phenotype through a Soluble Form of Jagged-1. *Cancer Cell*, *23*(2), 171–185. http://doi.org/10.1016/j.ccr.2012.12.021

Lustig, B., Jerchow, B., Sachs, M., Weiler, S., Pietsch, T., Karsten, U., … Behrens, J. (2002).

Negative feedback loop of Wnt signaling through upregulation of conductin/axin2 in colorectal and liver tumors. *Molecular and Cellular Biology*, *22*(4), 1184–93. http://doi.org/10.1128/MCB.22.4.1184

Mandel, S., & Gozes, I. (2007). Activity-dependent neuroprotective protein constitutes a novel element in the SWI/SNF chromatin remodeling complex. *Journal of Biological Chemistry*, *282*(47), 34448–34456. http://doi.org/10.1074/jbc.M704756200

Mani, S. A., Guo, W., Liao, M. J., Eaton, E. N., Ayyanan, A., Zhou, A. Y., … Weinberg, R.

(2008). The Epithelial-Mesenchymal Transition Generates Cells with Properties of Stem Cells. *Cell*, *133*(4), 704–715. http://doi.org/10.1016/j.cell.2008.03.027Golebiewska, A. et al., 2011. Critical appraisal of the side population assay in stem cell and cancer stem cell research. *Cell Stem Cell*, 8(2), pp.136–147. Available at: http://dx.doi.org/10.1016/j.stem.2011.01.007.

Marcato, P. et al., 2011. Aldehyde dehydrogenase its role as a cancer stem cell marker comes down to the specific isoform. *Cell Cycle*, 10(9), pp.1378–1384.

Marusyk, a., & Polyak, K. (2013). Cancer Cell Phenotypes, in Fifty Shades of Grey. *Science*, *339*(6119), 528–529. http://doi.org/10.1126/science.1234415

Matsuda, T., & Cepko, C. L. (2007). Controlled expression of transgenes introduced by in vivo electroporation. *Proceedings of the National Academy of Sciences of the United States of America*, *104*(3), 1027–1032. http://doi.org/10.1073/pnas.0610155104

McGranahan, N., & Swanton, C. (2015). Biological and therapeutic impact of intratumor heterogeneity in cancer evolution. *Cancer Cell*, *27*(1), 15–26. http://doi.org/10.1016/j.ccell.2014.12.001

Merlos-Suárez, A., Barriga, F. M., Jung, P., Iglesias, M., Céspedes, M. V., Rossell, D., … Batlle, E. (2011). The intestinal stem cell signature identifies colorectal cancer stem

cells and predicts disease relapse. *Cell Stem Cell*, *8*(5), 511–524. http://doi.org/10.1016/j.stem.2011.02.020

Miller, J. R. (2001). Protein family review. The Wnts Gene organization and evolutionary history. *Genome Biology* 2001, 3(1):reviews3001.1–3001.15

Misale, S., Yaeger, R., Hobor, S., Scala, E., Liska, D., Valtorta, E., … Siena, S. (2014). Emergence of KRAS mutations and acquired resistance to anti EGFR therapy in colorectal cancer. *Nature*, *486*(7404), 532–536. http://doi.org/10.1038/nature11156.Emergence

Muñoz, J., Stange, D. E., Schepers, A. G., van de Wetering, M., Koo, B.-K., Itzkovitz, S., … Clevers, H. (2012). The Lgr5 intestinal stem cell signature: robust expression of proposed quiescent "+4" cell markers. *The EMBO Journal*, *31*(14), 3079–91. http://doi.org/10.1038/emboj.2012.166

Niehrs, C. (2012). The complex world of WNT receptor signalling. *Nature Reviews. Molecular Cell Biology*, *13*(12), 767–779. http://doi.org/10.1038/nrm3470

Nieto, M. A., Huang, R. Y. Y. J., Jackson, R. A. A., & Thiery, J. P. P. (2016). Emt: 2016. *Cell*, *166*(1), 21–45. http://doi.org/10.1016/j.cell.2016.06.028

Nishisho, I., Nakamura, Y., Miyoshi, Y., Miki, Y., Baba, S., Hedge, P., … Vogelstein, B. (1991). Mutations of Chromosome 5q21 Genes in FAP and Colorectal Cancer Patients, *371*(1988).

Normanno, N., De Luca, A., Bianco, C., Strizzi, L., Mancino, M., Maiello, M. R., … Salomon, D. S. (2006). Epidermal growth factor receptor (EGFR) signaling in cancer. *Gene*, *366*(1), 2–16. http://doi.org/10.1016/j.gene.2005.10.018

O'Brien, C. A., Gallinger, S., Pollett, A., & Dick, J. E. (2007). A human colon cancer cell capable of initiating tumour growth in immunodeficient mice. *Nature*, *445*(7123), 106– 10. http://doi.org/10.1038/nature05372

O'Brien, C. A., Kreso, A., & Jamieson, C. H. M. (2010). Cancer stem cells and self-renewal. *Clinical Cancer Research*, *16*(12), 3113–3120. http://doi.org/10.1158/1078-0432.CCR-09-2824

Ormanns, S., Neumann, J., Horst, D., Kirchner, T., & Jung, A. (2014). WNT signaling and distant metastasis in colon cancer through transcriptional activity of nuclear β-catenin depend on active PI3K signaling. *Oncotarget*, *5*(10), 2999–3011. Retrieved from http://www.pubmedcentral.nih.gov/articlerender.fcgi?artid=4102786&tool=pmcentrez&rendertype=abstract

Pang, R., Law, W. L., Chu, A. C. Y., Poon, J. T., Lam, C. S. C., Chow, A. K. M., … Wong, A. C. Y. (2010). A subpopulation of CD26 + cancer stem cells with metastatic capacity in human colorectal cancer. *Cell Stem Cell*, *6*(6), 603–615. http://doi.org/10.1016/j.stem.2010.04.001

Peinado, H., Olmeda, D., & Cano, A. (2007). Snail, Zeb and bHLH factors in tumour progression: an alliance against the epithelial phenotype? *Nature Reviews Cancer*, *7*(6), 415–428. http://doi.org/10.1038/nrc2131

Peitzsch, C. et al., 2013. Discovery of the cancer stem cell related determinants of radioresistance. *Radiotherapy and Oncology*, 108(3), pp.378–387. Available at: http://dx.doi.org/10.1016/j.radonc.2013.06.003.

Pfeifer, A., Brandon, E. P., Kootstra, N., Gage, F. H., & Verma, I. M. (2001). Delivery of the Cre recombinase by a self-deleting lentiviral vector: efficient gene targeting in vivo. *Proceedings of the National Academy of Sciences of the United States of America*, *98*(20), 11450–5. http://doi.org/10.1073/pnas.201415498

Pinhasov, A., Mandel, S., Torchinsky, A., Giladi, E., Pittel, Z., Goldsweig, A. M., … Gozes, I. (2003). Activity-dependent neuroprotective protein: A novel gene essential for brain formation. *Developmental Brain Research*, *144*(1), 83–90. http://doi.org/10.1016/S0165- 3806(03)00162-7

Prince, M. E., Sivanandan, R., Kaczorowski, A., Wolf, G. T., Kaplan, M. J., Dalerba, P., … Ailles, L. E. (2007). Identification of a subpopulation of cells with cancer stem cell properties in head and neck squamous cell carcinoma, *104*(3), 973–978. http://doi.org/10.1073/pnas.0610117104

Quail, D., & Joyce, J. (2013). Microenvironmental regulation of tumor progression and metastasis. *Nature Medicine*, *19*(11), 1423–1437. http://doi.org/10.1038/nm.3394.Microenvironmental

Quante, M., Varga, J., Wang, T. C., & Greten, F. R. (2013). The Gastrointestinal Tumor Microenvironment. *Gastroenterology*, *145*(1), 63–78. http://doi.org/10.1053/j.gastro.2013.03.052.The

Quintana, E., Shackleton, M., Sabel, M. S., Fullen, D. R., Johnson, T. M., & Morrison, S. J. (2008). Efficient tumour formation by single human melanoma cells. *Nature*, *456*(7222), 593–598. http://doi.org/nature07567 [pii]10.1038/nature07567

Rausch, V. et al., 2012. Autophagy mediates survival of pancreatic tumour-initiating cells in a hypoxic microenvironment. *Journal of Pathology*, 227(3), pp.325–335.

Ricci-Vitiani, L., Lombardi, D. G., Pilozzi, E., Biffoni, M., Todaro, M., Peschle, C., & De Maria, R. (2007). Identification and expansion of human colon-cancer-initiating cells. *Nature*, *445*(7123), 111–115. http://doi.org/10.1038/nature05384

Roberts, P. J., & Der, C. J. (2007). Targeting the Raf-MEK-ERK mitogen-activated protein kinase cascade for the treatment of cancer. *Oncogene*, *26*(22), 3291–3310. http://doi.org/10.1038/sj.onc.1210422

Sánchez-tilló, E., Barrios, O. De, Siles, L., Cuatrecasas, M., Castells, A., & Postigo, A. (2011). ZEB1 to regulate tumor invasiveness. http://doi.org/10.1073/pnas.1108977108/-/DCSupplemental.www.pnas.org/cgi/doi/10.1073/pnas.1108977108

Scheffzek, K., Ahmadian, M. R., Kabsch, W., Wiesmüller, L., Lautwein, a, Schmitz, F., & Wittinghofer, a. (1997). The Ras-RasGAP Complex: Structural Basis for GTPase Activation and Its Loss in Oncogenic Ras Mutants. *Science*, *277*(5324), 333–338. http://doi.org/10.1126/science.277.5324.333

Schubbert, S., Shannon, K., & Bollag, G. (2007). Hyperactive Ras in developmental disorders and cancer. *Nature Reviews. Cancer*, *7*(4), 295–308. http://doi.org/10.1038/nrc2109

Sergey V. Shmelkov, Jason M. Butler, Andrea T. Hooper, Adilia Hormigo, Jared Kushner,

Till Milde, Ryan St. Clair, Muhamed Baljevic, Ian White, David K. Jin, Amy Chadburn, Andrew J. Murphy, David M. Valenzuela, Nicholas W. Gale, Gavin Thurston, George D. Y, S. R. (2008). CD133 expression is not restricted to metastatic colon cancer cells initiate tumors. *The Journal of Clinical Investigation*, *118*(6), 2111–2120. http://doi.org/10.1172/JCI34401DS1

Sharma, S. V., Lee, D. Y., Li, B., Quinlan, M. P., Takahashi, F., Maheswaran, S., … Settleman, J. (2010). A Chromatin-Mediated Reversible Drug-Tolerant State in Cancer Cell Subpopulations. *Cell*, *141*(1), 69–80. http://doi.org/10.1016/j.cell.2010.02.027

Singh SK, Hawkins C, Clarke ID, Squire JA, Bayani J, Hide T, Henkelman RM, Cusimano MD, D. P. (2004). Identification of human brain tumour initiating cells. *Nature*, *432*(November), 396–401. http://doi.org/10.1038/nature03031.1.

Smith, K. J., Johnson, K. a, Bryan, T. M., Hill, D. E., Markowitz, S., Willson, J. K., … Vogelstein, B. (1993). The APC gene product in normal and tumor cells. *Proceedings of the National Academy of Sciences of the United States of America*, *90*(April), 2846–2850.

Snuderl, M., Fazlollahi, L., Le, L. P., Nitta, M., Zhelyazkova, B. H., Davidson, C. J., … Iafrate, A. J. (2011). Mosaic amplification of multiple receptor tyrosine kinase genes in glioblastoma. *Cancer Cell*, *20*(6), 810–817. http://doi.org/10.1016/j.ccr.2011.11.005

Stange, D. E., Engel, F., Longerich, T., Koo, B. K., Koch, M., Delhomme, N., … Radlwimmer, B. (2010). Expression of an ASCL2 related stem cell signature and IGF2 in colorectal cancer liver metastases with 11p15.5 gain. *Gut*, *59*(9), 1236–1244. http://doi.org/10.1136/gut.2009.195701

Tam, W. L., & Weinberg, R. A. (2013). The epigenetics of epithelial-mesenchymal plasticity in cancer. *Nature Medicine*, *19*(11), 1438–49. http://doi.org/10.1038/nm.3336

The Cancer Genome Atlas Network. (2012). Comprehensive molecular characterization of human colon and rectal cancer. *Nature*, *487*(7407), 330–337. http://doi.org/10.1038/nature11252.Comprehensive

Thiery, J. P., Acloque, H., Huang, R. Y. J., & Nieto, M. A. (2009). Epithelial-Mesenchymal Transitions in Development and Disease. *Cell*, *139*(5), 871–890. http://doi.org/10.1016/j.cell.2009.11.007

Todaro, M., Gaggianesi, M., Catalano, V., Benfante, A., Iovino, F., Biffoni, M., … Stassi, G. (2014). CD44v6 is a marker of constitutive and reprogrammed cancer stem cells driving colon cancer metastasis. *Cell Stem Cell*, *14*(3), 342–356. http://doi.org/10.1016/j.stem.2014.01.009

Torre, L. A., Bray, F., Siegel, R. L., Ferlay, J., Lortet-tieulent, J., & Jemal, A. (2015). Global Cancer Statistics, 2012. *CA: A Cancer Journal of Clinicians.*, *65*(2), 87–108. http://doi.org/10.3322/caac.21262.

Turner, C. P., Gutierrez, S., Liu, C., Miller, L., Chou, J., Finucane, B., … Phillips, A. (2012). Strategies to defeat ketamine-induced neonatal brain injury. *Neuroscience*, *210*, 384–392. http://doi.org/10.1016/j.neuroscience.2012.02.015

Urosevic, J., Garcia-Albéniz, X., Planet, E., Real, S., Céspedes, M. V., Guiu, M., … Gomis, R. R. (2014). Colon cancer cells colonize the lung from established liver metastases through p38 MAPK signalling and PTHLH. *Nature Cell Biology*, *16*(7), 685–94.

http://doi.org/10.1038/ncb2977

Van Emburgh, B. O., Sartore-Bianchi, A., Di Nicolantonio, F., Siena, S., & Bardelli, A. (2014). Acquired resistance to EGFR-targeted therapies incolorectal cancer. *Molecular Oncology*, *8*(6), 1084–1094. http://doi.org/10.1016/j.molonc.2014.05.003

Varnat, F., Duquet, A., Malerba, M., Zbinden, M., Mas, C., Gervaz, P., & Ruiz I Altaba, A. (2009). Human colon cancer epithelial cells harbour active HEDGEHOG-GLI signalling that is essential for tumour growth, recurrence, metastasis and stem cell survival and expansion. *EMBO Molecular Medicine*, *1*(6–7), 338–351. http://doi.org/10.1002/emmm.200900039

Vermeulen, L., De Sousa E Melo, F., van der Heijden, M., Cameron, K., de Jong, J. H., Borovski, T., … Medema, J. P. (2010). Wnt activity defines colon cancer stem cells and is regulated by the microenvironment. *Nature Cell Biology*, *12*(5), 468–476. http://doi.org/10.1038/ncb2048

Vermeulen, L., & Snippert, H. J. (2014). Stem cell dynamics in homeostasis and cancer of the intestine. *Nature Reviews. Cancer*, *14*(June), 468–80. http://doi.org/10.1038/nrc3744

Vermeulen, L., Sprick, M. R., Kemper, K., Stassi, G., & Medema, J. P. (2008). Cancer stem cells – old concepts, new insights. *Cell Death and Differentiation*, *15*, 947–958. http://doi.org/10.1038/cdd.2008.20

Vogelstein, B., Papadopoulos, N., Velculescu, V. E., Zhou, S., Diaz Jr., L. A., & Kinzler, K. W. (2013). Cancer Genome Landscapes. *Science*, *339*(6127), 1546–1558. http://doi.org/10.1126/science.1235122

Voronkov, A., & Krauss, S. (2013). Wnt/beta-catenin signaling and small molecule inhibitors. *Current Pharmaceutical Design*, *19*(4), 634–64. http://doi.org/10.2174/138161213804581837

Vulih-Shultzman, I., Pinhasov, A., Mandel, S., Grigoriadis, N., Touloumi, O., Pittel, Z., & Gozes, I. (2007). Activity-dependent neuroprotective protein snippet NAP reduces tau hyperphosphorylation and enhances learning in a novel transgenic mouse model. *The Journal of Pharmacology and Experimental Therapeutics*, *323*(2), 438–449. http://doi.org/10.1124/jpet.107.129551.severe

Wang, X., Haswell, J. R., & Roberts, C. W. M. (2014). Molecular pathways: SWI/SNF (BAF) complexes are frequently mutated in cancer-mechanisms and potential therapeutic insights. *Clinical Cancer Research*, *20*(1), 21–27. http://doi.org/10.1158/1078- 0432.CCR-13-0280

Welch, D. R. (2016). Tumor heterogeneity - A “contemporary concept” founded on historical insights and predictions. *Cancer Research*, *76*(1), 4–6. http://doi.org/10.1158/0008- 5472.CAN-15-3024

Yordy, J. S., & Muise-helmericks, R. C. (2000). Signal transduction and the Ets family of transcription factors, 6503–6513.

Young, A., Lou, D., & McCormick, F. (2013). Oncogenic and wild-type Ras play divergent roles in the regulation of mitogen-activated protein kinase signaling. *Cancer Discovery*, *3*(1), 112–123. http://doi.org/10.1158/2159-8290.CD-12-0231

Zamostiano, R., Pinhasov, A., Gelber, E., Steingart, R. A., Seroussi, E., Giladi, E., … Gozes,

I. (2001). Cloning and characterazation of the human activity-dependent neuroprotective protein. *Journal of Biological Chemistry*, *276*(1), 708–714. http://doi.org/10.1074/jbc.M007416200

Zhang, F., Gradinaru, V., Adamantidis, A. R., Durand, R., Airan, R. D., de Lecea, L., & Deisseroth, K. (2010). Optogenetic interrogation of neural circuits: technology for probing mammalian brain structures. *Nature Protocols*, *5*(3), 439–56. http://doi.org/10.1038/nprot.2009.226

Zheng, X., Carstens, J. L., Kim, J., Scheible, M., Kaye, J., Sugimoto, H., … Biology, C. (2016). EMT Program is Dispensable for Metastasis but Induces Chemoresistance in Pancreatic Cancer, *Nature 527*(7579), 525–530. http://doi.org/10.1038/nature16064.

Abreviations

Ab	Antibody
ABC	Active β-catenin
ADNP	Activity-dependent neuroprotector homeobox
ALL	Acute lymphoblastic leukemia
AML	Acute myeloid leukemia
AP-1	Activator protein 1
APC	Adenomatous polyposis coli
Bmi1	B lymphoma Mo-MLV insertion region 1 homolog
BMP	Bone morphogenetic protein
CBC	Crypt base columnar
CK1	Casein kinase 1
CpG	Cytidine-phosphate-guanidin
CRC	Colorectal cancer
CreERT2	Cre – estrogen receptor T2
CRISPR/CAS9	Clustered regularly interspaced short palindromic repeats/ CRISPR associated 9
CSC	Cancer stem cell
DMEM	Dulbecco's modified Eagles medium
DMSO	Dimethyl sulfoxide
DNA	Deoxyribonucleic acid
DNMT1	DNA (cytosine-5)-methyltransferase 1
EGF	Epidermal growth factor
EGFR	Epidermal growth factor receptor
ELK-1	ETS-like gene 1
EMT	Epithelial-mesenchymal transition
ERK	Extracellular signal-regulated kinase
FAP	Familial adenomatous polyposis
FCS	Fetal calf serum
FDR	False discovery rate
FGF	Fibroblast growth factors
FN1	Fibronectin 1
GAPDH	Glyceraldehyde 3-phosphate dehydrogenase
GFP	Green fluorescent protein
GSEA	Gene Set Enrichment Analysis
GSK3	Glycogen synthase kinase 3

GTP	Guanosine triphosphate
HGF	Hepatocyte growth factor
Hopx	Homeodomain-only protein homeobox
HRAS	Harvey rat sarcoma viral oncogene homolog
HRP	Horseradish peroxidase
IHC	Immunohistochemistry
IRES	Internal ribosome entry site
JNK	c-Jun NH2-terminal kinase
KRAS	Kirsten rat sarcoma viral oncogene homolog
LAMC2	Laminin subunit gamma-2
LEF	Lymphoid enhancer-binding factor 1
LGR5	Leucine rich repeat containing G protein coupled receptor 5
LiCl	Lithium chloride
LPA	Lysophosphatidic acid
Lrig1	Leucine-rich repeats and immunoglobulin-like domains 1
LRP	Low-density lipoprotein receptor-related protein
MAPK	Mitogen-activated protein kinase
MEK/MAP2K	Dual specificity mitogen-activated protein kinase kinase
MET	Mesenchymal-epithelial transition
MS	Mass spectrometry
Nod/SCID	Non-obese diabetic/severe combined immunodeficiency
NRAS	Neuroblastoma rat sarcoma viral oncogene homolog
PCP	Planar cell polarity
PBS	Phosphate-buffered saline
(q)PCR	(quantitative) Polymerase chain reaction
PDGF	Platelet-derived growth factor
p-ERK	Phospho-ERK
PFA	Paraformaldehyde
PI3K	phosphoinositide-3-kinase
Prom1	Prominin-1
RAF	Rapidly accelerated fibrosarcoma
RNA	Ribonucleic acid
RT	Room temperature
RTK	Receptor tyrosine kinases
Smoc2	SPARC-related modular calcium binding
Sox9	SRY-box 9
SRE	Serum response element

TCF	T cell transcription factor
TCGA	The Cancer Genome Atlas
Tert	Telomerase reverse transcriptase
TGF-β	Transforming growth factor beta
TMA	Tissue microarrays
TP53	Tumor protein P53
WNT	Wingless-type MMTV integration site family member
βTrCP	β-transducing repeat-containing protein

List of figures

List of tables